Electronic Supplementary Material (ESI) for Dalton Transactions.
This journal is © The Royal Society of Chemistry 2024

Electronic Supplementary Information

1,2,3-triazol-5-ylidene- *vs* 1,2,3-triazole-based tricarbonylrhenium(I) complexes: Influence of a mesoionic carbene ligand on the electronic and biological properties

Corinne Vanucci-Bacqué, Mariusz Wolff, Béatrice Delavaux-Nicot, Abanoub Mosaad Abdallah, Sonia Mallet-Ladeira, Charles-Louis Serpentini, Florence Bedos-Belval, Kar Wai Fong, Xiao Ying Ng, May Lee Low, Eric Benoist* and Suzanne Fery-Forgues*

Synthesis and chemical characterization

Crystallographic data

Calculations

Electrochemistry

Spectroscopy

Microbiology

Calculations (Annex)

Synthesis and chemical characterization

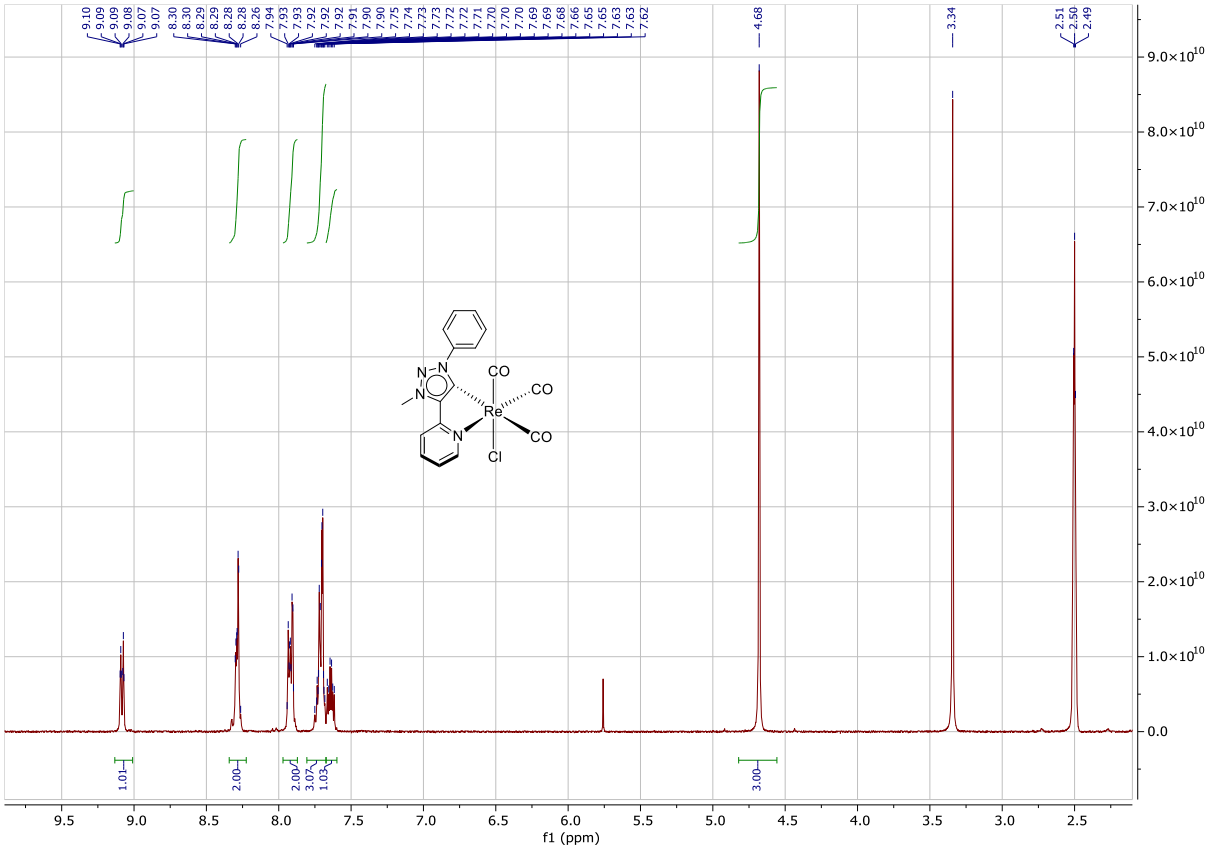

Figure S1. ^{1}H NMR spectrum of complex **Re-T-Phe** in DMSO-d_6.

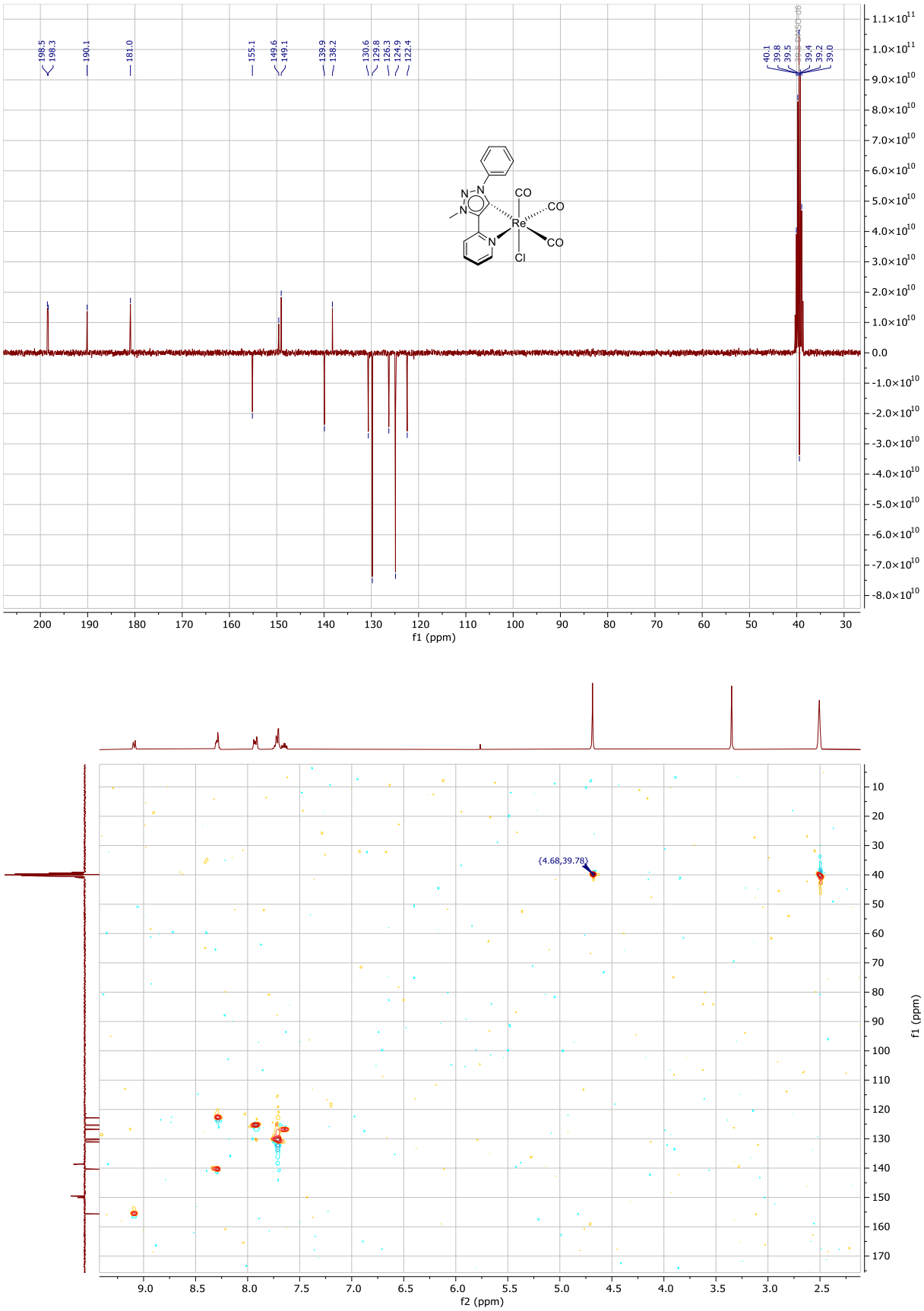

Figure S2. ^{13}C Jmod NMR (top) and HSQC (bottom) spectra of complex **Re-T-Phe** in DMSO-d_6.

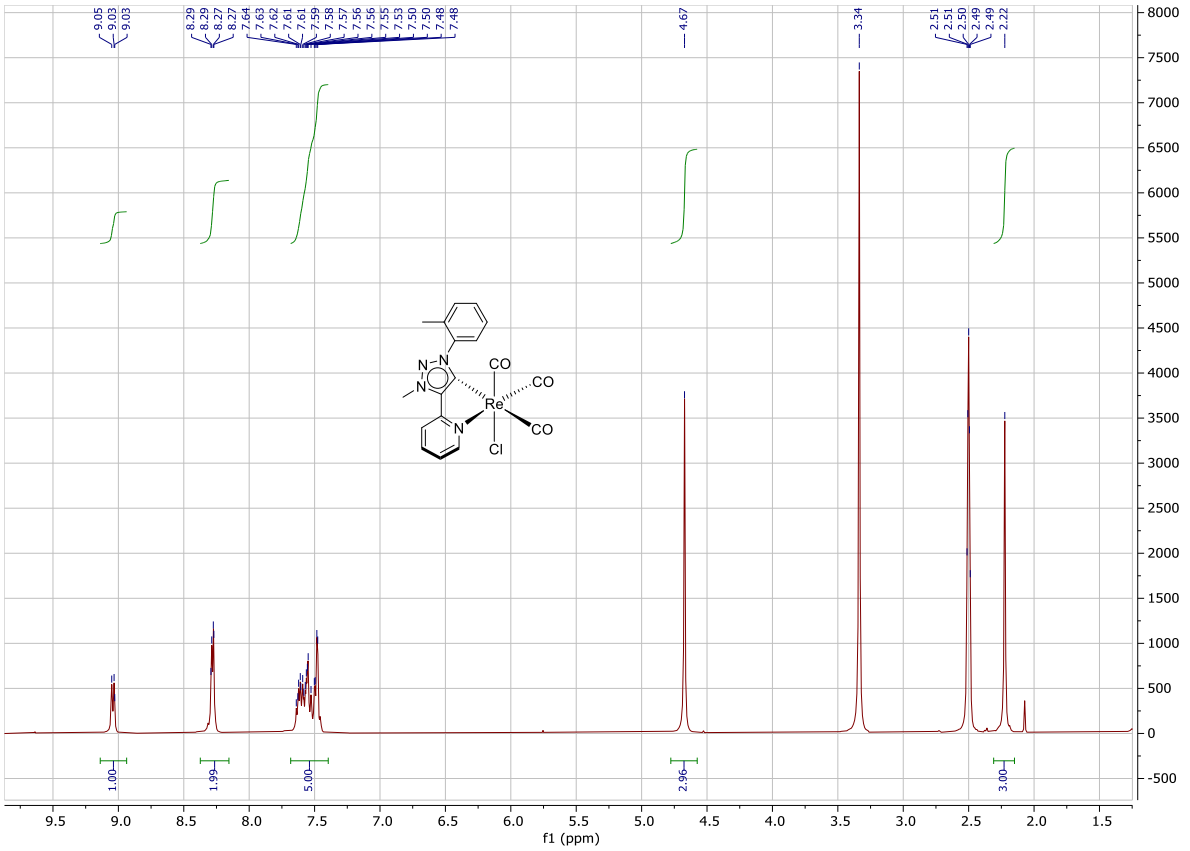

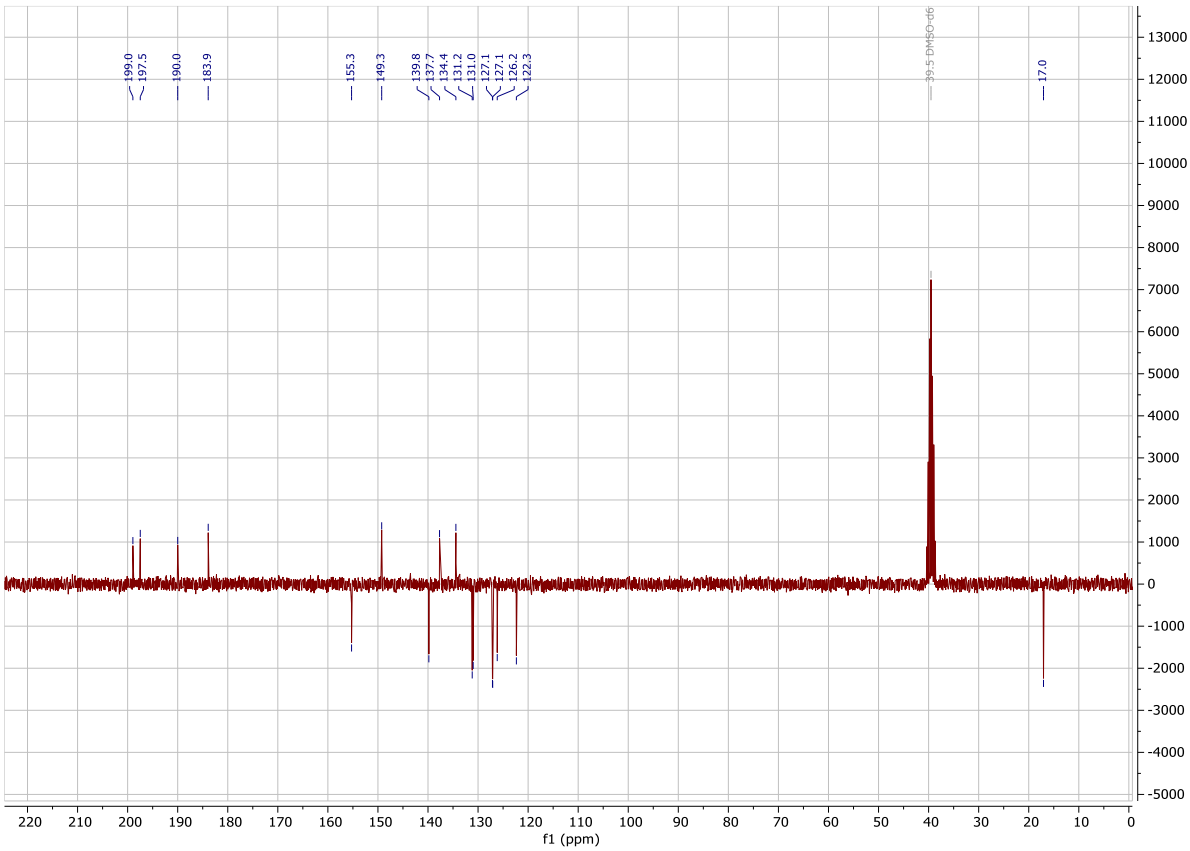

Figure S3. ^{1}H NMR (top) and ^{13}C Jmod NMR (bottom) spectra of complex **Re-T-Tol** in DMSO-d_6.

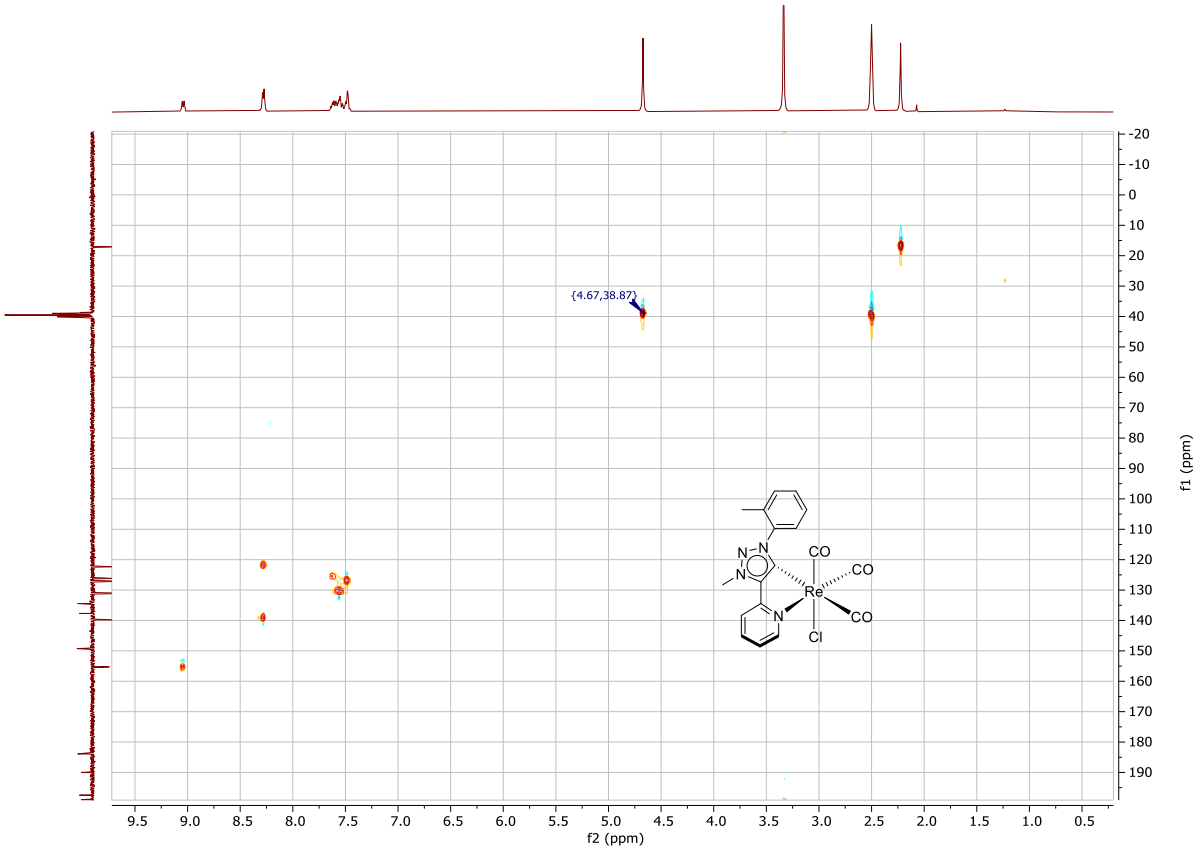

Figure S4. HSQC spectrum of complex **Re-T-Tol** in DMSO-d_6.

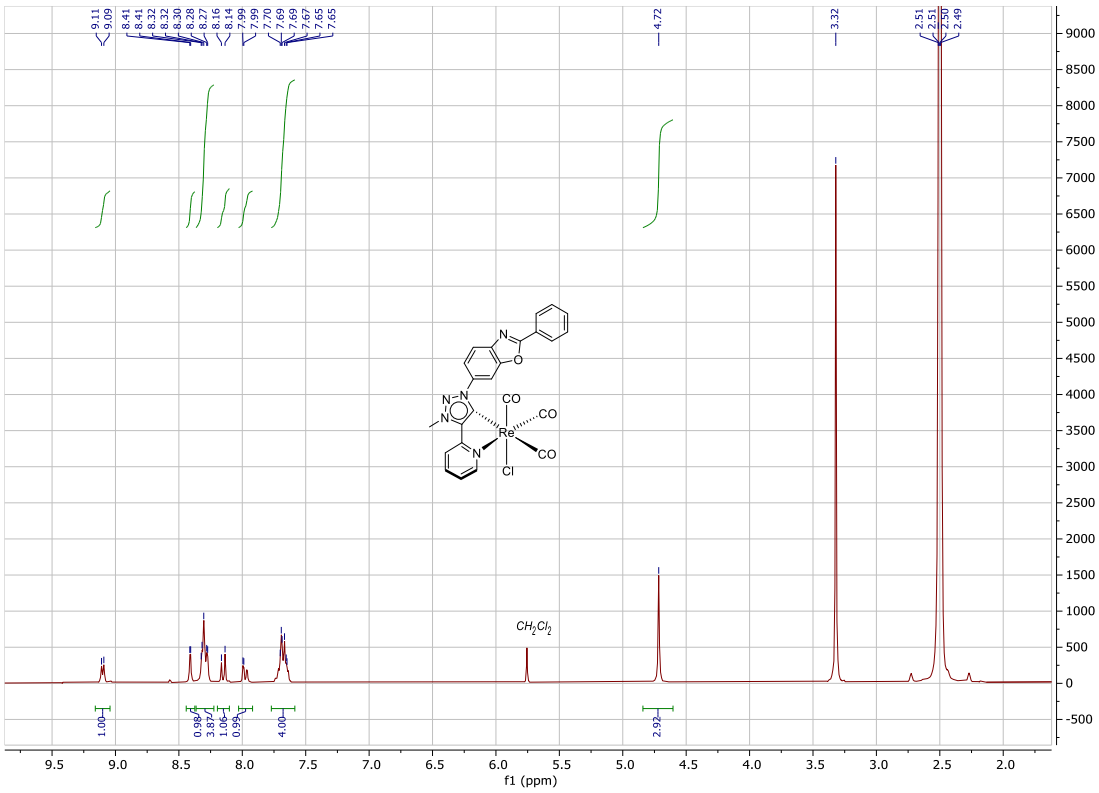

Figure S5. ^{1}H NMR spectrum of complex **Re-T-BOP** in DMSO-d_6.

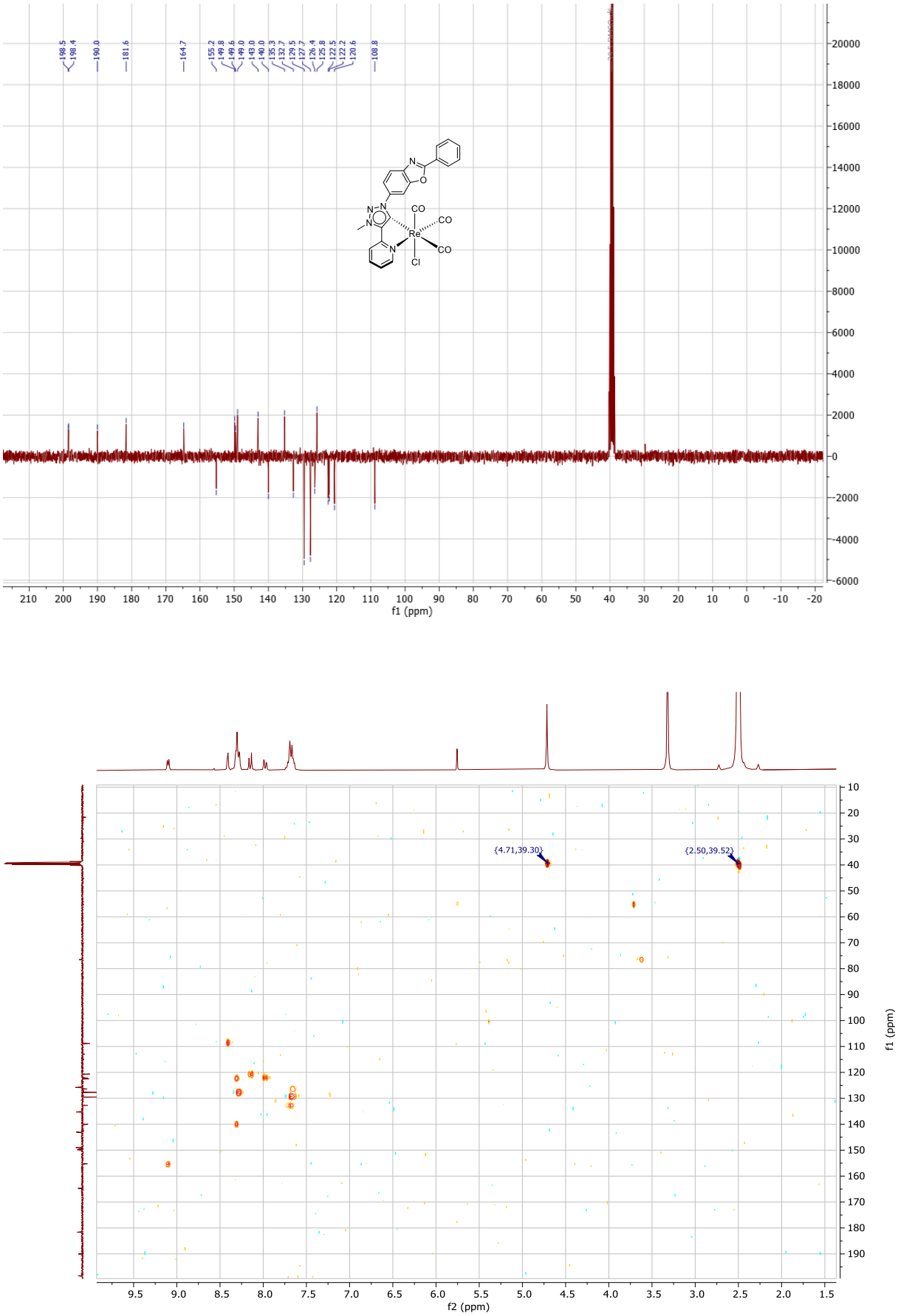

Figure S6. ^{13}C Jmod NMR (top) and HSQC (bottom) spectra of complex **Re-T-BOP** in DMSO-d_6.

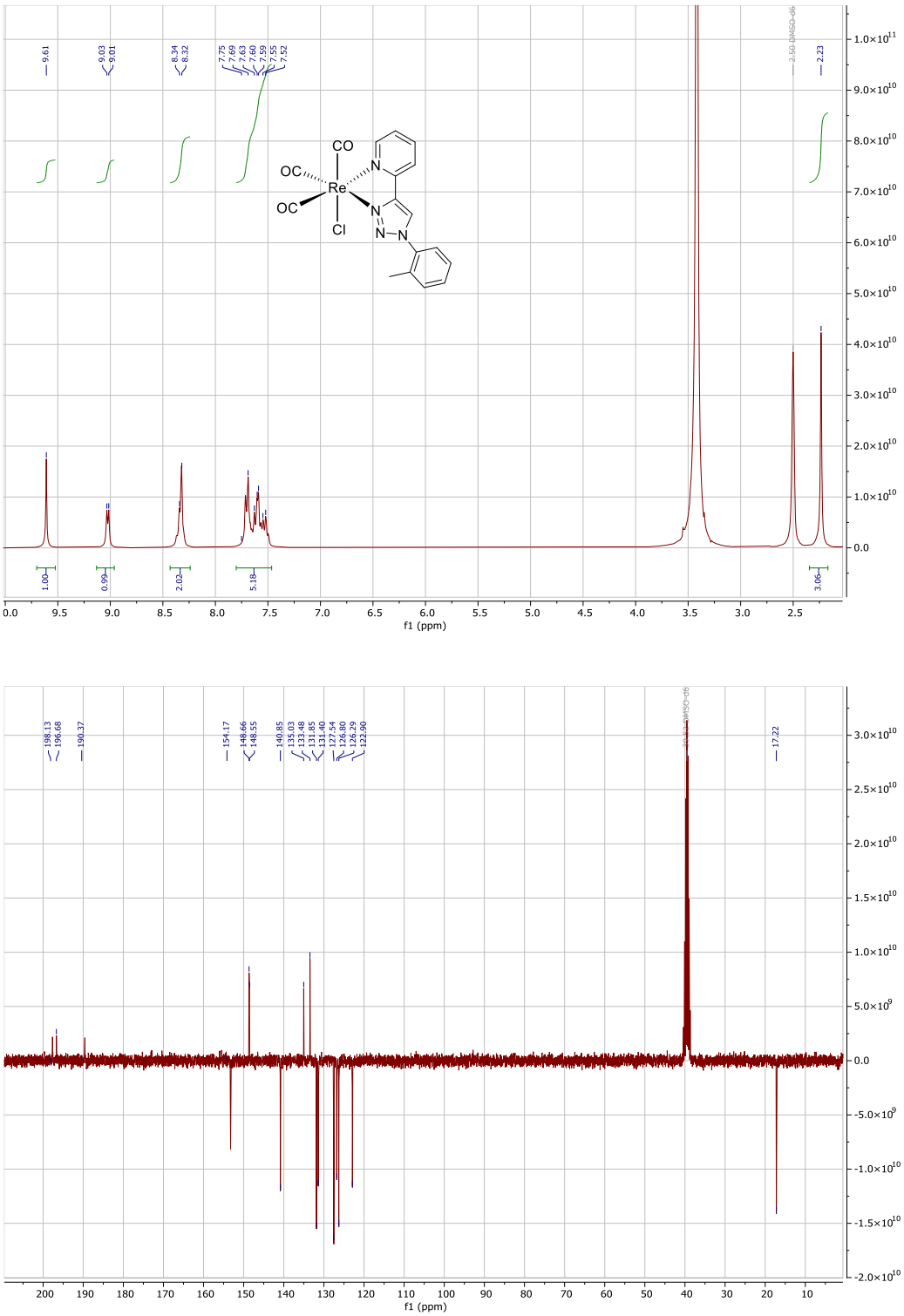

Figure S7. ^{1}H NMR (top) and ^{13}C Jmod NMR (bottom) spectra of complex **Re-Tol** in DMSO-d_6.

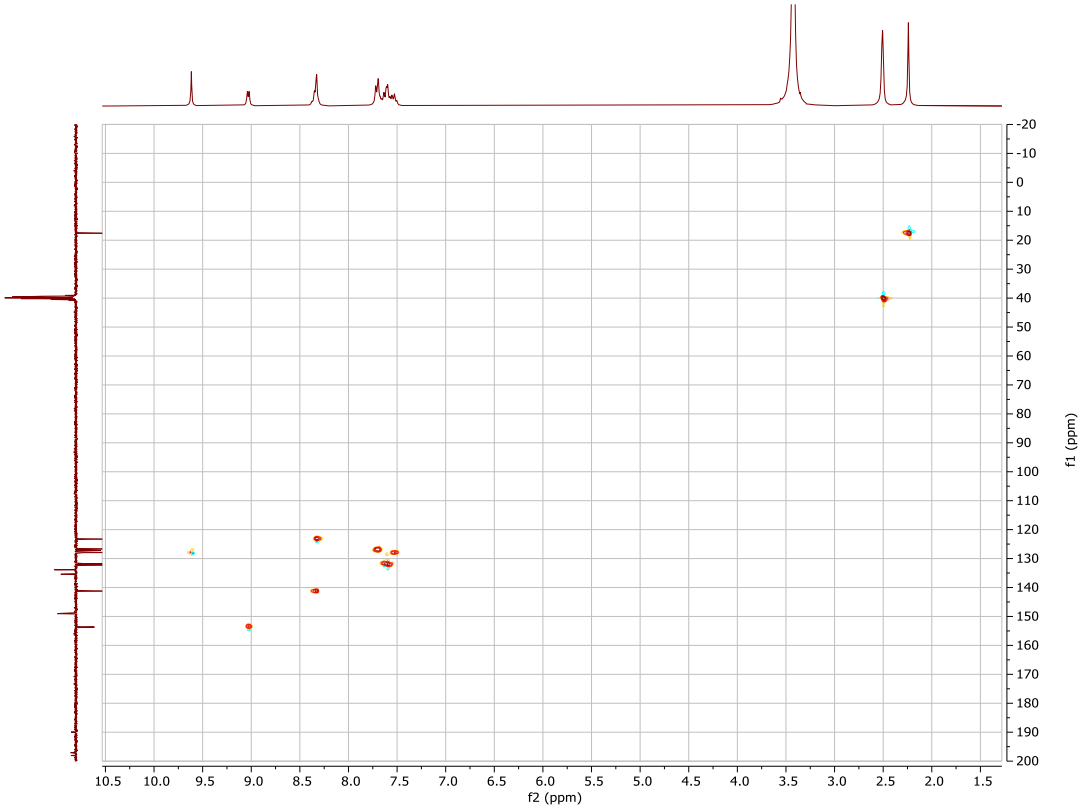

Figure S8. HSQC (bottom) spectrum of complex **Re-Tol** in DMSO-d_6.

Elemental Composition Report

Single Mass Analysis
Tolerance = 3.0 PPM / DBE: min = -5.0, max = 70.0
Element prediction: Off
Number of isotope peaks used for i-FIT = 3

Monoisotopic Mass, Odd and Even Electron Ions
879 formula(e) evaluated with 6 results within limits (up to 50 closest results for each mass)
Elements Used:
C: 0-100 H: 0-150 N: 0-5 O: 0-5 Cl: 0-1 185Re: 0-1

Cone voltage =30V
cvb6-107-2 89 (0.559) AM2 (Ar,20000.0,0.00,0.00); Cm (89:94-53:62x2.000)
Xevo G2 QTOF #YCA210
11-Apr-2023 10:32:18
1: TOF MS ES+
1.27e+006

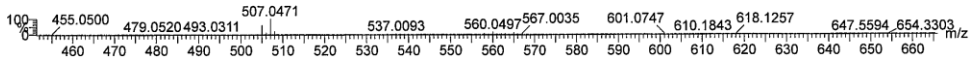

Mass	Calc. Mass	mDa	PPM	DBE	i-FIT	Norm	Conf(%)	Formula
Minimum:				-5.0				
Maximum:		5.0	3.0	70.0				
558.0479	558.0480	-0.1	-0.2	16.0	158.4	1.984	13.75	C22 H15 N O5 185Re
	558.0485	-0.6	-1.1	11.5	158.0	1.561	21.00	C19 H18 N2 O4 Cl 185Re
	558.0471	0.8	1.4	12.0	158.1	1.732	17.69	C17 H16 N5 O3 Cl 185Re
	558.0470	0.9	1.6	44.0	158.9	2.453	8.60	C46 H6
	558.0466	1.3	2.3	16.5	157.6	1.186	30.55	C20 H13 N4 O4 185Re
	558.0493	-1.4	-2.5	21.0	158.9	2.478	8.39	C23 H11 N5 O 185Re

$[M + NH_4]^+$

Cone voltage =30V
cvb6-107-2 89 (0.559) AM2 (Ar,20000.0,0.00,0.00); Cm (89:94-53:62x2.000)
Xevo G2 QTOF #YCA210
11-Apr-2023 10:32:18
1: TOF MS ES+
1.27e+006

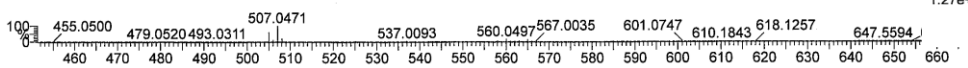

Mass	Calc. Mass	mDa	PPM	DBE	i-FIT	Norm	Conf(%)	Formula
Minimum:				-5.0				
Maximum:		5.0	3.0	70.0				
505.0443	505.0447	-0.4	-0.8	29.0	291.6	1.383	25.09	C29 H7 N5 O5
	505.0439	0.4	0.8	14.0	290.8	0.543	58.11	C17 H12 N4 O3 185Re
	505.0452	-0.9	-1.8	13.5	292.0	1.783	16.81	C19 H14 N O4 185Re

$[M - Cl]^+$

Figure S9. HRMS data for **Re-T-Phe**

Elemental Composition Report

Single Mass Analysis
Tolerance = 3.0 PPM / DBE: min = -5.0, max = 100.0
Element prediction: Off
Number of isotope peaks used for i-FIT = 3

Monoisotopic Mass, Odd and Even Electron Ions
1772 formula(e) evaluated with 11 results within limits (up to 50 closest results for each mass)
Elements Used:
C: 0-100 H: 0-120 N: 0-5 O: 0-5 Na: 0-1 Cl: 0-1 185Re: 0-1

Cone voltage = 30 V
CVB5-155 81 (0.503) AM2 (Ar,20000.0,0.00,0.00); Cm (80:85-59:63x2.000)
XEVO G2 QTOF
08-Jun-2021 14:18:01
1: TOF MS ES+
3.93e+004

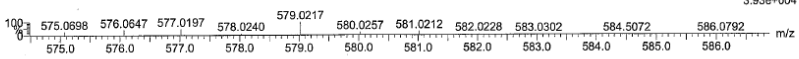

	Mass	Calc. Mass	mDa	PPM	DBE	i-FIT	Norm	Conf(%)	Formula
Minimum:					-5.0				
Maximum:			1.0	3.0	100.0				
	577.0197	577.0195	0.2	0.3	12.5	212.6	2.357	9.47	C20 H16 N O4 Na Cl 185Re
		577.0201	-0.4	-0.7	20.5	213.9	3.636	2.64	C23 H10 N3 O4 185Re
		577.0204	-0.7	-1.2	22.0	214.1	3.886	2.05	C24 H9 N4 O Na 185Re
		577.0190	0.7	1.2	28.0	212.3	2.006	13.45	C30 H9 N5 O5 Na Cl
		577.0190	0.7	1.2	17.0	213.9	3.617	2.69	C23 H13 O5 Na 185Re
		577.0206	-0.9	-1.6	16.0	212.2	1.985	13.73	C20 H13 N4 O3 Cl 185Re
		577.0208	-1.1	-1.9	17.5	212.3	2.055	12.81	C21 H12 N5 Na Cl 185Re
		577.0182	1.5	2.6	13.0	213.4	3.138	4.34	C18 H14 N4 O3 Na Cl 185Re
		577.0212	-1.5	-2.6	37.0	214.4	4.203	1.49	C36 H4 N5 O3 Na
		577.0214	-1.7	-2.9	31.0	211.3	1.021	36.01	C32 H8 N5 O5 Cl
		577.0214	-1.7	-2.9	20.0	214.6	4.324	1.32	C25 H12 O5 185Re

$[M + Na]^+$

Cone voltage = 30 V
CVB5-155 81 (0.503) AM2 (Ar,20000.0,0.00,0.00); Cm (80:85-59:63x2.000)
XEVO G2 QTOF
08-Jun-2021 14:18:01
1: TOF MS ES+
3.99e+005

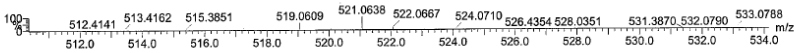

	Mass	Calc. Mass	mDa	PPM	DBE	i-FIT	Norm	Conf(%)	Formula
Minimum:					-5.0				
Maximum:			1.0	3.0	100.0				
	519.0609	519.0609	0.0	0.0	13.5	348.7	1.557	21.07	C20 H16 N O4 185Re
		519.0604	0.5	1.0	29.0	348.5	1.292	27.47	C30 H9 N5 O5
		519.0622	-1.3	-2.5	18.5	349.4	2.212	10.95	C21 H12 N5 185Re
		519.0595	1.4	2.7	14.0	348.1	0.904	40.50	C18 H14 N4 O3 185Re

$[M - Cl]^+$

Figure S10. HRMS data for **Re-T-Tol**.

Elemental Composition Report

Single Mass Analysis
Tolerance = 3.0 PPM / DBE: min = -1.5, max = 50.0
Element prediction: Off
Number of isotope peaks used for i-FIT = 3

Monoisotopic Mass, Odd and Even Electron Ions
2910 formula(e) evaluated with 16 results within limits (up to 50 closest results for each mass)
Elements Used:
C: 0-60 H: 0-100 N: 0-8 O: 0-5 Na: 0-1 Cl: 0-1 185Re: 0-1

	Mass	Calc. Mass	mDa	PPM	DBE	i-FIT	Norm	Conf(%)	Formula
Minimum:					-1.5				
Maximum:			5.0	3.0	50.0				
	680.0256	680.0253	0.3	0.4	18.5	403.1	3.423	3.26	C26 H17 N2 O5 Na Cl 185Re
		680.0259	-0.3	-0.4	26.5	404.3	4.580	1.03	C29 H11 N4 O5 185Re
		680.0250	0.6	0.9	22.5	403.3	3.591	2.76	C24 H12 N8 O3 Cl 185Re
		680.0262	-0.6	-0.9	28.0	404.5	4.776	0.84	C30 H10 N5 O2 Na 185Re
		680.0248	0.8	1.2	28.5	403.9	4.182	1.53	C28 H8 N8 O Na 185Re
		680.0264	-0.8	-1.2	22.0	402.8	3.081	4.59	C26 H14 N5 O4 Cl 185Re
		680.0246	1.0	1.5	27.0	403.8	4.052	1.74	C27 H9 N7 O4 185Re
		680.0267	-1.1	-1.6	23.5	402.8	3.117	4.43	C27 H13 N6 O Na Cl 185Re
		680.0267	-1.1	-1.6	49.5	400.5	0.835	43.38	C52 H7 N Cl
		680.0243	1.3	1.9	46.5	401.8	2.075	12.56	C50 H8 N Na Cl
		680.0270	-1.4	-2.1	43.0	404.9	5.166	0.57	C42 H5 N6 O4 Na
		680.0272	-1.6	-2.4	31.5	404.7	4.986	0.68	C30 H7 N8 O 185Re
		680.0240	1.6	2.4	45.0	402.1	2.375	9.30	C49 H9 O3 Cl
		680.0240	1.6	2.4	19.0	403.8	4.102	1.65	C24 H15 N5 O4 Na Cl 185Re
		680.0275	-1.9	-2.8	38.5	401.9	2.181	11.29	C39 H8 N7 O3 Na Cl
		680.0275	-1.9	-2.8	27.5	405.3	5.581	0.38	C32 H12 N2 O3 Na 185Re

$[M + Na]^+$

Cone voltage = 30 V
CVB5-196-2 98 (0.608) AM2 (Ar,20000.0,0.00,0.00); Cm (92:103-65:73x2.000)
XEVO G2 QTOF
30-Nov-2021 11:37:54
1: TOF MS ES+
3.83e+006

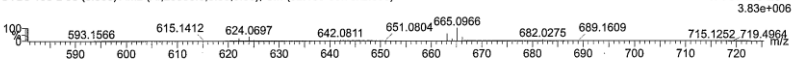

	Mass	Calc. Mass	mDa	PPM	DBE	i-FIT	Norm	Conf(%)	Formula
Minimum:					-5.0				
Maximum:			1.0	3.0	100.0				
	622.0667	622.0667	0.0	0.0	19.5	445.0	1.713	18.03	C26 H17 N2 O5 185Re
		622.0662	0.5	0.8	35.0	444.7	1.462	23.18	C36 H10 N6 O6
		622.0675	-0.8	-1.3	34.5	445.5	2.215	10.92	C38 H12 N3 O7
		622.0657	1.0	1.6	47.5	445.6	2.339	9.65	C50 H8 N
		622.0654	1.3	2.1	20.0	444.6	1.284	27.70	C24 H15 N5 O4 185Re
		622.0680	-1.3	-2.1	24.5	445.5	2.251	10.52	C27 H13 N6 O 185Re

$[M - Cl]^+$

Figure S11. HRMS data for **Re-T-BOP**.

Elemental Composition Report

Single Mass Analysis
Tolerance = 3.0 PPM / DBE: min = -5.0, max = 70.0
Element prediction: Off
Number of isotope peaks used for i-FIT = 3

Monoisotopic Mass, Odd and Even Electron Ions
1550 formula(e) evaluated with 10 results within limits (up to 50 closest results for each mass)
Elements Used:
C: 0-100 H: 0-100 N: 0-10 O: 0-5 Cl: 0-1 187Re: 0-1

Cone voltage =15V
CVB6-90 83 (0.529) AM2 (Ar,20000.0,0.00,0.00); Cm (74:90-48:62x2.000)
Xevo G2 QTOF #YCA210
02-Feb-2023 10:57:48
2: TOF MS ES+
4.04e+005

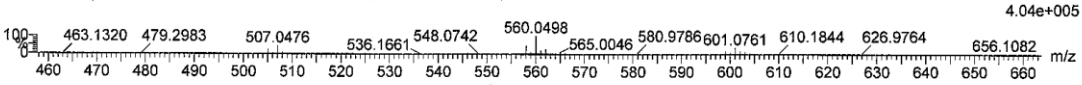

Mass	Calc. Mass	mDa	PPM	DBE	i-FIT	Norm	Conf(%)	Formula
Minimum:				-5.0				
Maximum:		1.0	3.0	70.0				
560.0498	560.0497	0.1	0.2	27.0	309.4	2.927	5.35	C26 H9 N10 O4 Cl
	560.0499	-0.1	-0.2	12.0	306.7	0.252	77.71	C17 H16 N5 O3 Cl 187Re
	560.0500	-0.2	-0.4	43.5	321.6	15.163	0.00	C45 H6 N
	560.0494	0.4	0.7	16.5	319.8	13.369	0.00	C20 H13 N4 O4 187Re
	560.0492	0.6	1.1	31.5	320.2	13.735	0.00	C29 H6 N9 O5
	560.0508	-1.0	-1.8	21.5	320.1	13.680	0.00	C21 H9 N8 187Re
	560.0508	-1.0	-1.8	16.0	320.2	13.759	0.00	C22 H15 N O5 187Re
	560.0510	-1.2	-2.1	26.5	311.0	4.509	1.10	C28 H11 N7 O5 Cl
	560.0486	1.2	2.1	12.5	309.2	2.735	6.49	C15 H14 N8 O2 Cl 187Re
	560.0513	-1.5	-2.7	11.5	308.8	2.370	9.35	C19 H18 N2 O4 Cl 187Re

$[M + NH_4]^+$

Elemental Composition Report

Single Mass Analysis
Tolerance = 3.0 PPM / DBE: min = -5.0, max = 70.0
Element prediction: Off
Number of isotope peaks used for i-FIT = 3

Monoisotopic Mass, Odd and Even Electron Ions
1214 formula(e) evaluated with 7 results within limits (up to 50 closest results for each mass)
Elements Used:
C: 0-100 H: 0-100 N: 0-10 O: 0-10 187Re: 0-1

Cone voltage =15V
CVB6-90 83 (0.529) AM2 (Ar,20000.0,0.00,0.00); Cm (74:90-48:62x2.000)
Xevo G2 QTOF #YCA210
02-Feb-2023 10:57:48
2: TOF MS ES+
4.04e+005

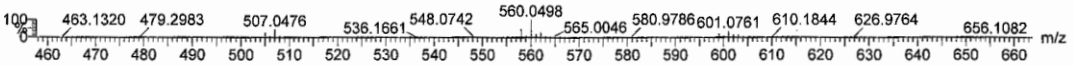

Mass	Calc. Mass	mDa	PPM	DBE	i-FIT	Norm	Conf(%)	Formula
Minimum:				-5.0				
Maximum:		1.0	3.0	70.0				
507.0476	507.0478	-0.2	-0.4	28.5	276.9	6.257	0.19	C28 H7 N6 O5
	507.0480	-0.4	-0.8	13.5	273.6	2.965	5.16	C19 H14 N O4 187Re
	507.0472	0.4	0.8	1.5	278.5	7.865	0.04	C3 H14 N9 O9 187Re
	507.0467	0.9	1.8	14.0	270.7	0.077	92.62	C17 H12 N4 O3 187Re
	507.0485	-0.9	-1.8	1.0	274.7	4.076	1.70	C5 H16 N6 O10 187Re
	507.0465	1.1	2.2	23.5	277.3	6.643	0.13	C27 H11 N2 O9
	507.0464	1.2	2.4	29.0	277.0	6.418	0.16	C26 H5 N9 O4

$[M - Cl]^+$

Figure S12. HRMS data for **Re-Tol**.

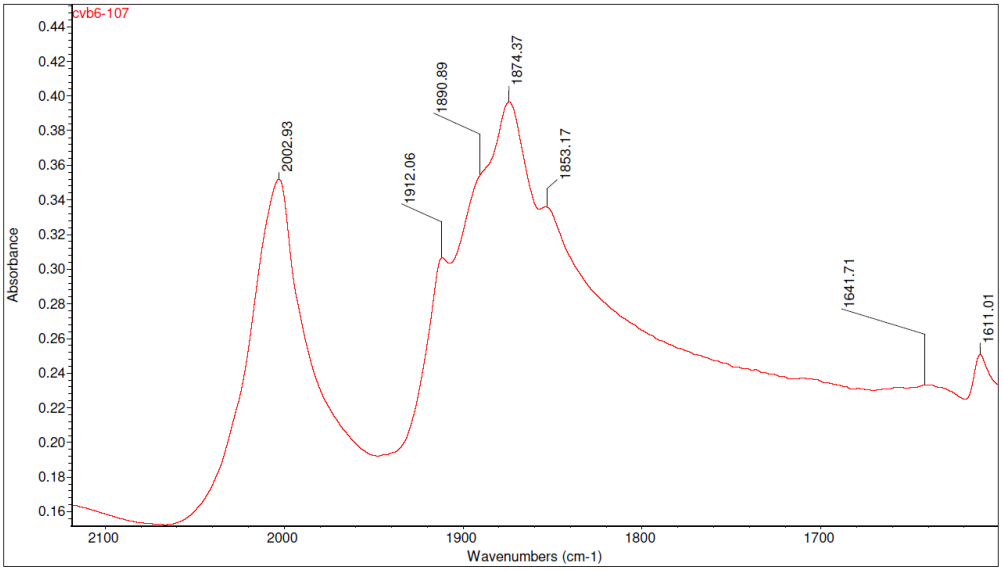

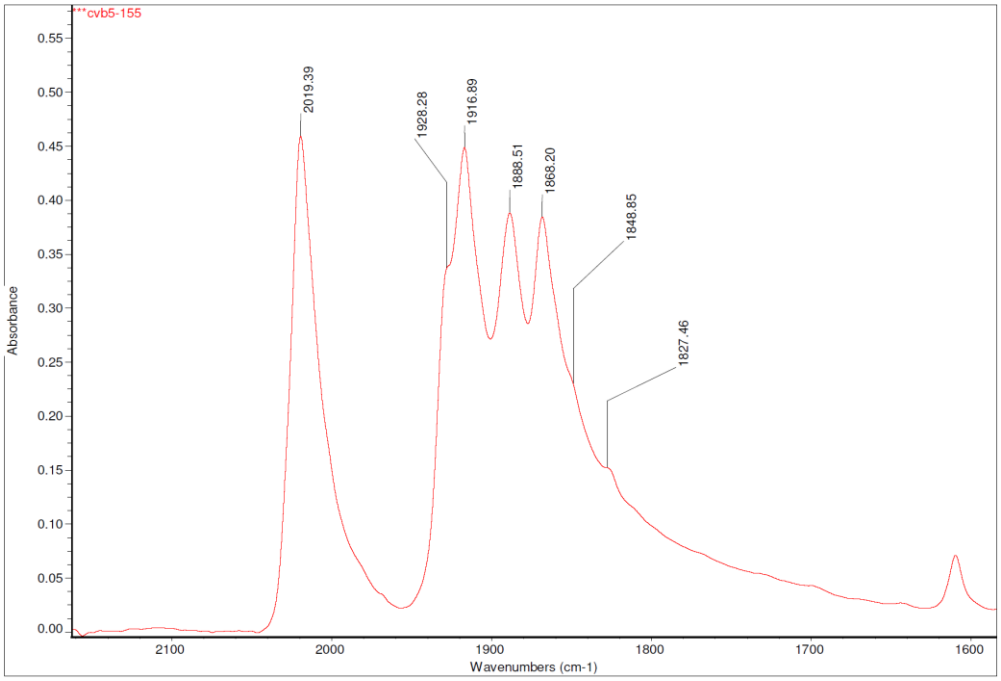

Figure S13. ATR FTIR spectra of the microcrystalline powder of **Re-T-Phe** (top) and **Re-T-Tol** (bottom).

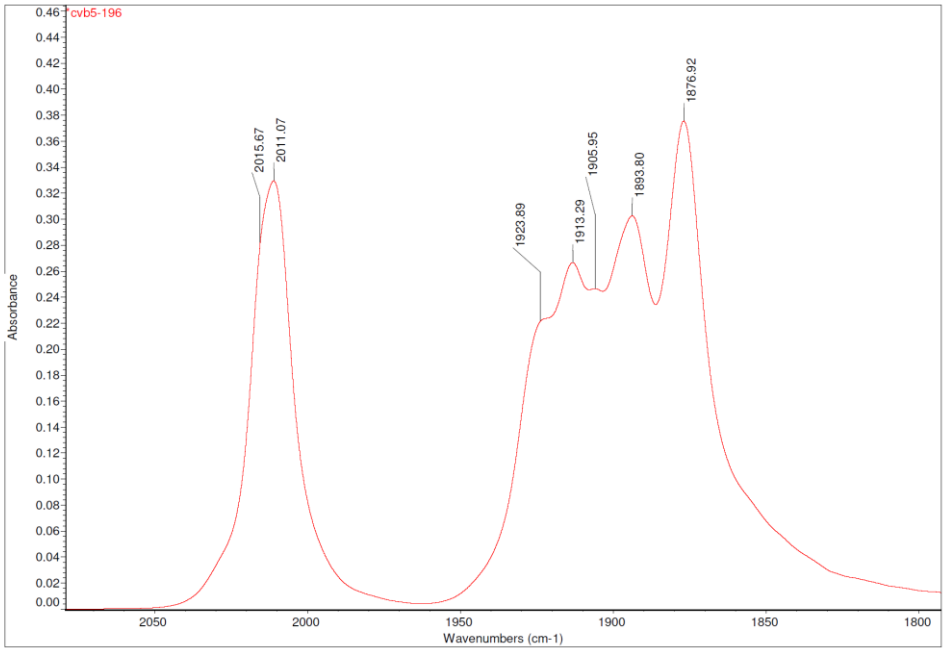

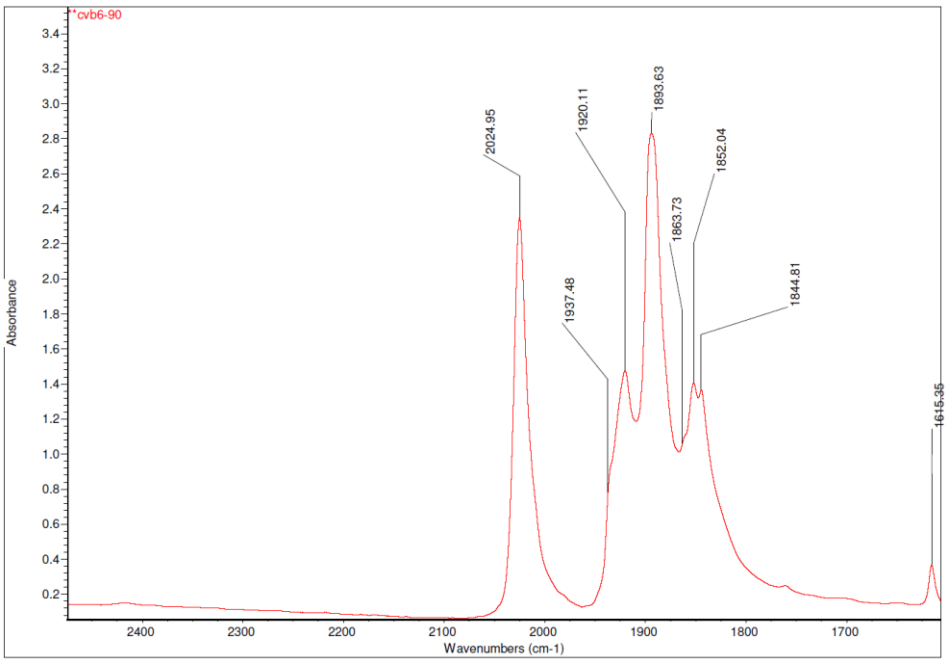

Figure S14. ATR FTIR spectrum of microcrystalline powders of **Re-T-BOP** (top) and **Re-Tol** (bottom)

Table S1. FTIR data for all complexes as microcrystalline powders (ATR) and in CH_2Cl_2 solution.

Complex	$\nu_{C=O}$ (ATR) (cm^{-1})	$\nu_{C=O}$ (CH_2Cl_2) (cm^{-1})	$<\nu_{C=O}$ (CH_2Cl_2)$>$ (cm^{-1})
Re-T-Phe	2003, 1912, 1891, 1874, 1853	2016, 1915, 1885	1939
Re-T-Tol	2019, 1917, 1888, 1868	2016, 1916, 1884	1939
Re-T-BOP	2011, 1913, 1894, 1877	2016, 1916, 1887	1940
Re-Phe	2024, 1930, 1894, 1879, 1848 [a]	2028, 1927, 1900	1952
Re-Tol	2025, 1920, 1894, 1852, 1845	2028, 1927, 1899	1951
Re-BOP	2030, 1920, 1903 [b]	2028, 1943[c], 1921, 1889	1946

[a] From Poirot *et al*. *Dalton Trans.* 2021, **50**, 13686–13698.
[b] From Wang *et al*. *Dalton Trans.* 2018, **47**, 8087–8099.
[c] not considered for calculation.

Crystallographic data

	Re-T-Phe	**Re-T-Tol**	**Re-Phe**	**Re-Tol**
Empirical formula	$C_{17}H_{12}N_4O_3ClRe$	$C_{18}H_{14}ClN_4O_3Re$	$C_{16}H_{10}N_4O_3ClRe$	$C_{17}H_{12}N_4O_3ClRe$
Formula weight	541.97	555.98	527.93	541.97
Crystal system	Monoclinic	Monoclinic	Orthorhombic	Monoclinic
Space group	P_n	$P2_{1/c}$	P b c a	$P2_{1/c}$
Unit cell dimensions				
a (Å)	7.4855(4)	13.0933(5)	13.1442(10)	17.1110(11)
b (Å)	8.5760(4)	8.7846(4)	6.8213(5)	10.9130(8)
c (Å)	13.7433(7)	15.9309(7)	36.375(3)	9.7176(7)
α (°)	90	90	90	90
β (°)	104.060 (1)	92.1447(17)	90	99.738(3)
γ (°)	90	90	90	90
Volume (Å^3)	855.83(7)	1831.08(14)	3261.4(4)	1788.4(2)
Z	2	4	8	4
Density (calculated) (Mg/m^3)	2.103	2.017	2.150	2.013
Crystal size (mm^3)	0.160 × 0.120 × 0.060	0.160 × 0.140 × 0.120	0.200 × 0.040 × 0.040	0.200 × 0.080 × 0.060
Reflections collected	27075	57189	115433	71992
Independent reflections	5797 [R(int) = 0.0299]	4531 [R(int) = 0.0281]	6553 [R(int) = 0.0554]	5983 [R(int) = 0.0762]
Restraints/parameters	2 / 237	0 / 246	0 / 226	0 / 236
Final R1 index I>2σ(I)	0.0166	0.0145	0.0213	0.0250
wR2 (all data)	0.0377	0.0319	0.0435	0.0524
Largest diff. peak and hole (e Å^{-3})	1.422 and -1.178	0.595 and -0.931	0.844 and -1.325	1.015 and -1.002
CCDC	2327668	2327669	2327670	2327671

Table S2. Selected crystallographic data of pyridyl-triazolylidene-based complexes **Re-T-Phe**, **Re-T-Tol** and **Re-T-BOP**, and pyridyl-triazole-based complexes **Re-Phe** and **Re-Tol**.

Table S3. Selected bond lengths (Å) for triazolylidene-based complexes **Re-T-Phe**, **Re-T-Tol** and **Re-T-BOP**, and for the pyta-based complexes **Re-Phe** and **Re-Tol**. The atoms were numbered like on the molecular views. For the sake of comparison, each line corresponds to the same bond in each complex. For molecular views, the displacement ellipsoids are drawn at the 50% probability level.

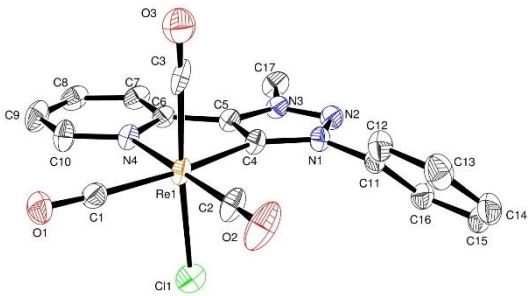

Re-T-Phe

Bond	Re-T-Phe	Bond	Re-T-Tol	Bond	Re-Phe	Re-Tol
Re(1)-C(1)	1.941(4)	Re(1)-C(3)	1.958(2)	Re(1)-C(1)	1.918(2)	1.921(3)
Re(1)-C(2)	1.913(4)	Re(1)-C(2)	1.911(2)	Re(1)-C(2)	1.927(2)	1.916(3)
Re(1)-C(3)	1.994(4)	Re(1)-C(1)	1.897(2)	Re(1)-C(3)	1.906(2)	1.932(3)
Re(1)-C(4)	2.160 (3)	Re(1)-C(4)	2.117(2)	Re(1)-N(1)	2.1589(17)	2.152(2)
Re(1)-N(4)	2.234 (3)	Re(1)-N(4)	2.2341(17)	Re(1)-N(4)	2.2055(19)	2.195(2)
Re(1)-Cl(1)	2.4811(12)	Re(1)-Cl(1)	2.5260(5)	Re(1)-Cl(1)	2.4953(5)	2.4738(8)
O(1)-C(1)	1.144(4)	O(3)-C(3)	1.145(3)	O(1)-C(1)	1.151(3)	1.149(4)
O(2)-C(2)	1.149(5)	O(2)-C(2)	1.151(3)	O(2)-C(2)	1.144(3)	1.146(4)
O(3)-C(3)	1.081(5)	O(1)-C(1)	1.156(3)	O(3)-C(3)	1.147(3)	1.110(4)

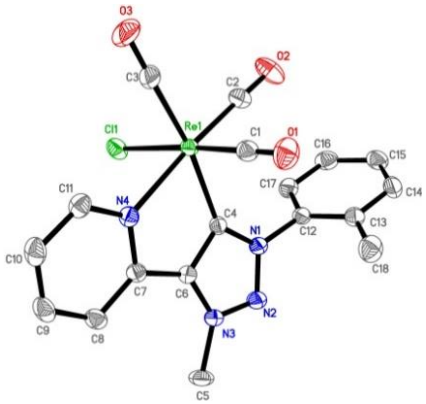

Re-T-Tol

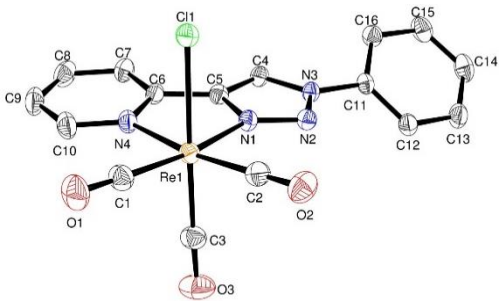

RePhe

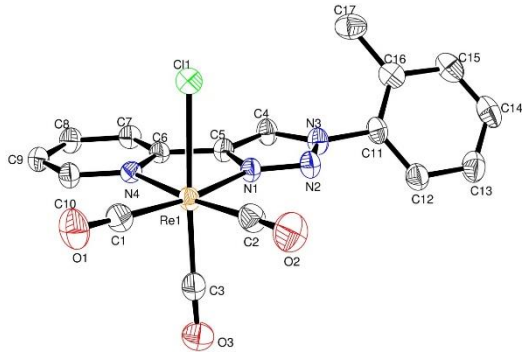

Re-Tol

Table S4. Selected angles (°) for triazolylidene-based complexes **Re-T-Phe**, **Re-T-Tol** and **Re-T-BOP**, and for the pyta-based complexes **Re-Phe** and **Re-Tol**. For the sake of comparison, each line corresponds to the same bond in each complex. The atoms were numbered like on the molecular views.

Angle	**Re-T-Phe**	**Angle**	**Re-T-Tol**	**Angle**	**Re-Phe**	**Re-Tol**
C(1)-Re(1)-C(2)	87.85(16)	C(2)-Re(1)-C(3)	89.54(10)	C(1)-Re(1)-C(2)	90.34(10)	88.08(13)
C(1)-Re(1)-C(3)	91.04(15)	C(1)-Re(1)-C(3)	91.76(9)	C(1)-Re(1)-C(3)	90.56(10)	91.46(13)
C(2)-Re(1)-C(3)	88.38(16)	C(1)-Re(1)-C(2)	88.42(9)	C(2)-Re(1)-C(3)	89.48(10)	88.47(13)
C(1)-Re(1)-C(4)	167.30(15)	C(3)-Re(1)-C(4)	171.19(8)	C(1)-Re(1)-N(1)	171.03(9)	170.94(11)
C(2)-Re(1)-C(4)	104.78(15)	C(2)-Re(1)-C(4)	98.69(8)	C(2)-Re(1)-N(1)	98.14(8)	99.97(11)
C(3)-Re(1)-C(4)	90.61(14)	C(1)-Re(1)-C(4)	91.62(8)	C(3)-Re(1)-N(1)	92.40(8)	92.87(11)
C(1)-Re(1)-N(4)	92.80(13)	C(3)-Re(1)-N(4)	96.92(8)	C(1)-Re(1)-N(4)	96.63(8)	97.47(11)
C(2)-Re(1)-N(4)	179.11(13)	C(2)-Re(1)-N(4)	172.88(8)	C(2)-Re(1)-N(4)	171.87(8)	173.79(11)
C(3)-Re(1)-N(4)	92.22(13)	C(1)-Re(1)-N(4)	94.35(8)	C(3)-Re(1)-N(4)	94.61(9)	94.13(10)
C(4)-Re(1)-N(4)	74.56(12)	C(4)-Re(1)-N(4)	74.71(7)	N(1)-Re(1)-N(4)	74.70(7)	74.29(8)
C(1)-Re(1)-Cl(1)	94.16(12)	C(3)-Re(1)-Cl(1)	89.29(7)	C(1)-Re(1)-Cl(1)	92.75(7)	92.92(9)
C(2)-Re(1)-Cl(1)	91.84(13)	C(2)-Re(1)-Cl(1)	95.39(7)	C(2)-Re(1)-Cl(1)	91.91(7)	92.39(10)
C(3)-Re(1)-Cl(1)	174.80(10)	C(1)-Re(1)-Cl(1)	176.06(6)	C(3)-Re(1)-Cl(1)	176.40(7)	175.55(9)
C(4)-Re(1)-Cl(1)	84.31(10)	C(4)-Re(1)-Cl(1)	86.81(5)	N(1)-Re(1)-Cl(1)	84.11(5)	82.68(7)
N(4)-Re(1)-Cl(1)	87.49(9)	N(4)-Re(1)-Cl(1)	81.75(4)	N(4)-Re(1)-Cl(1)	83.60(5)	84.59(6)
O(1)-C(1)-Re(1)	174.2(4)	O(3)-(C3)-Re(1)	178.5(3)	O(1)-C(1)-Re(1)	177.8(2)	177.3(3)
O(2)-C(2)-Re(1)	177.7(3)	O(2)-C(2)-Re(1)	177.7(3)	O(2)-C(2)-Re(1)	177.9(2)	175.4(3)
O(3)-C(3)-Re(1)	177.3(3)	O(1)-C(1)-Re(1)	177.9(3)	O(3)-C(3)-Re(1)	178.4(2)	174.2(4)

Table S5. Octahedral distortion parameters[a] for complexes **Re-Phe**, **Re-Tol**, **Re-T-Phe** and **Re-T-Tol**.

Complex	Octahedral distortion parameters		
	ζ (Å)	Σ (°)	Θ (°)
Re-Phe	1.11	55.5	151
Re-Tol	1.05	63.1	168
Re-T-Phe	1.03	54.9	186
Re-T-Tol	1.11	58.2	170

[a] Octahedral distortion parameters are composed of three parameters: one bond-length distortion parameter ζ and two bond-angle distortion parameters Σ and Θ. ζ is the average of the sum of the deviation of 6 unique metal–ligand bond lengths around the central metal atom (d_i) from the average value (d_{mean}). Σ can be defined as the sum of the deviation of the 12 *cis* L–Re–L angles ϕ_i from 90°. Σ is a general measure of the deviation of a metal ion from an ideal octahedral geometry. Θ can be defined as the sum of the deviation of the 24 torsional angles between the ligand atoms on opposite triangular faces of the octahedron viewed along the pseudo-threefold axis (θ_i) from 60°. Θ represents the distortion of the MX_6 geometry from perfectly octahedral (O_h) to trigonal prismatic (D_{3h}). Distortion parameters ζ, Σ and Θ were calculated using the OctaDist software [R. Ketkaew, Y. Tantirungrotechai, P. Harding, G. Chastanet, P. Guionneau, M. Marchivie, D. J. Harding, *Dalton Trans.*, **2021**, 50, 1086–1096]. All values lie in the expected range observed for distorted quasi-octahedral Re(I) complexes. In fact, a perfectly octahedral complex would give ζ = Σ = Θ = 0.

Table S6. Short contacts detected in structures of **Re-Phe**, **Re-Tol**, **Re-T-Phe** and **Re-T-Tol**.

D—H···A	D—H (Å)	H···A (Å)	D···A (Å)	D—H···A (°)	Symmetry codes
Re-Phe					
C4—H4···Cl1$^{\#1}$	0.95	2.47	3.377(2)	159	3/2–*x*, 1/2+*y*, *z*
C9—H9···Cl1$^{\#2}$	0.95	2.65	3.577(3)	164	1–*x*, 1–*y*, 1–*z*
Re-Tol					
C4—H4···Cl1$^{\#3}$	0.95	2.61	3.487(3)	154	*x*, 3/2–*y*, –1/2+*z*
C7—H7···Cl1$^{\#3}$	0.95	2.79	3.713(3)	163	*x*, 3/2–*y*, –1/2+*z*
C10—H10···O3$^{\#4}$	0.95	2.57	3.460(4)	157	2–*x*, 2–*y*, 2–*z*
C12—H12···O2$^{\#5}$	0.95	2.47	3.389(4)	164	*x*, 5/2–*y*, –1/2+*z*
Re-T-Phe					
C13—H13···O1$^{\#6}$	0.95	2.52	3.330(6)	143	1/2+*x*, –*y*, –1/2+*z*
Re-T-Tol					
C10—H10···Cl1$^{\#7}$	0.95	2.74	3.570(2)	146	*x*, 1/2–*y*, 1/2+z

Table S7. Geometrical parameters for C–H···π interactions detected in **Re-Phe**, **Re-T-Phe** and **Re-T-Tol**.

X—H(i)···Cg(i)	H···Cg (Å)	X···Cg (Å)	X–H···Cg (°)	H-Perp	Gamma
Re-Phe					
C4—H4···Cg2$^{\#1}$	2.81	3.203(2)	106	–2.75	11.26
C12—H12···Cg4$^{\#1}$	2.97	3.478(2)	115	–2.97	1.32
Re-T-Phe					
C17—H17B···Cg4$^{\#2}$	2.65	3.447(5)	138	–2.62	8.34
Re-T-Tol					
C5—H5B···Cg3$^{\#3}$	2.74	3.593(3)	146	–2.73	4.54

Cg(i) = center of gravity of ring i; X···Cg = distance of X to Cg; X–H···Cg = X–H–Cg angle; H–Perp = perpendicular distance of H to ring plane J; γ = angle between Cg–H vector and ring J normal. For **Re-Phe**, Cg2 and Cg4 are the centroids of the rings (N1/N2/N3/C4/C5) and (C11–C16), respectively. For **Re-T-Phe**, Cg4 is the centroid of the ring (C11–C16). For **Re-T-Tol**, Cg3 is the centroid of the ring (N4/C7–C11). Symmetry codes: #1: 3/2–*x*, 1/2+*y*, *z*; #2: 1/2+*x*, 1–*y*, 1/2+*z*; #3: 2–*x*, 1–*y*, 1–*z*.

Table S8. Geometrical parameters for π···π interactions detected in **Re-Tol**, **Re-T-Phe** and **Re-T-Tol**.

Cg(i)···Cg(j)	Cg···Cg (Å)	α (°)	β (°)	γ (°)	Cgi_Perp	Cgj_Perp	Slippage
Re-Tol							
Cg2···Cg3$^{\#1}$	3.7792(17)	5.48(15)	22.1	17.1	3.6118(11)	3.5011(11)	1.423
Re-T-Phe							
Cg3···Cg4$^{\#3}$	3.648(3)	4.8(2)	25.0	20.3	3.4216(18)	3.3054(19)	1.543
Re-T-Tol							
Cg3···Cg4$^{\#5}$	3.6854(14)	4.49(11)	19.4	23.8	3.3710(9)	3.4763(10)	1.224

Cg(i) = plane number i; α = dihedral angle between planes i and j; β = angle Cg(i)→Cg(j) or Cg(i)→Me vector and normal to plane i; γ = angle Cg(i)→Cg(j) vector and normal to plane j; Cg–Cg = distance between ring centroids; Cg(i)_Perp = perpendicular distance of Cg(i) on ring j; Cg(j)_Perp = perpendicular distance of Cg(j) on ring i; Slippage = distance between Cg(i) and perpendicular projection of Cg(j) on ring I. For **Re-Tol**, Cg2 and Cg3 are the centroids of the rings (N1/N2/N3/C4/C5) and (N4/C6–C10), respectively. For **Re-T-Phe**, Cg3 and Cg4 are the centroids of the rings (N4/C6–C10) and (C11–C16), respectively. For **Re-T-Tol**, Cg3 and Cg4 are the centroids of the rings (N4/C7–C11) and (C12–C17), respectively. Symmetry codes: #1: *x*, 3/2–*y*, –1/2+*z*; #2: *x*, 3/2–*y*, 1/2+*z*; #3: –1/2+*x*, 1–*y*, 1/2+*z*; #4: 1/2+*x*, 1–*y*, –1/2+*z*; #5: *x*, 3/2–*y*, 1/2+*z*; #6: *x*, 3/2–*y*, –1/2+*z*.

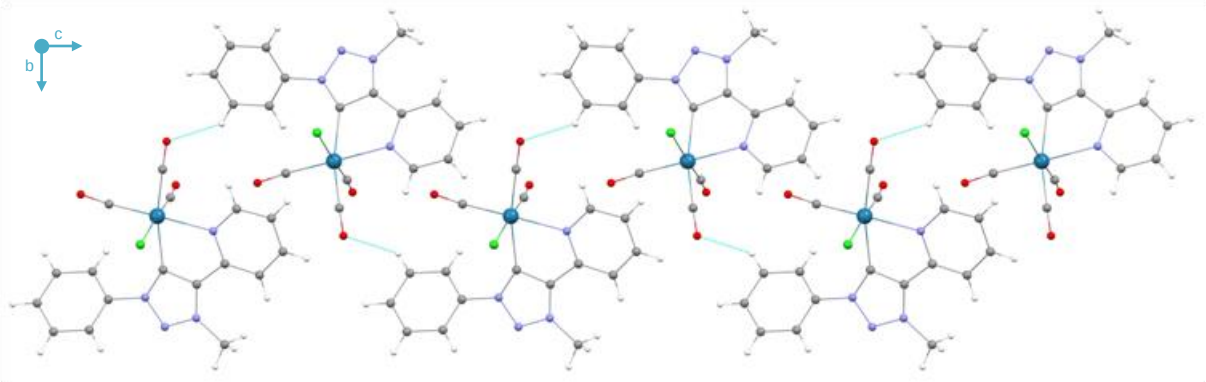

Figure S15. One-dimensional chain of **Re-T-Phe** showing connection of molecules through the intermolecular C–H···O interactions along the *c* axis. Intermolecular C13–H13$_{(Phe)}$···O1$_{(CO)}$ hydrogen bonding takes place between one CH group of the phenyl ring and the oxygen atom of the equatorial carbonyl group.

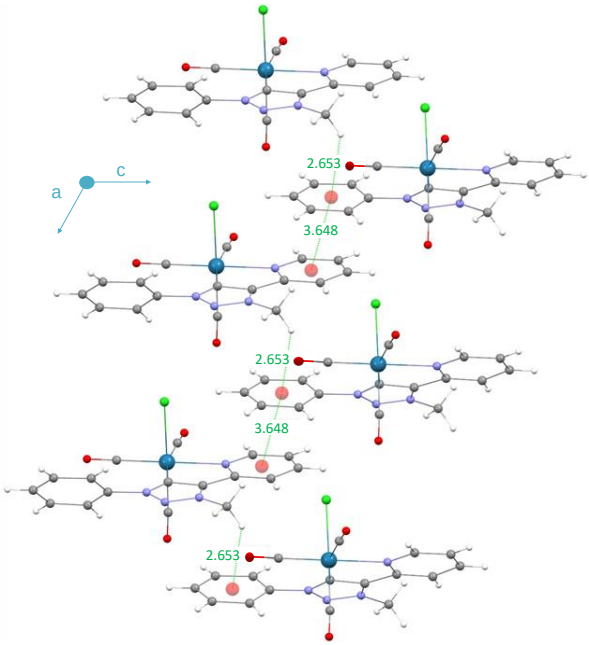

Figure S16. C–H···π and π–π interactions in complexes **Re-T-Phe**, with distances in Å. Intermolecular C17–H17$_{(trz)}$···$\pi_{(Phe)}$ interactions take place between the methyl group of the triazolylidene and the centroid Cg4 of the C11–C16 aromatic ring (C17–H17B···centroid Cg4 distances of 2.653 Å). Intermolecular $\pi_{(py)}$–$\pi_{(Phe)}$ stacking interactions take place between the coordinated N4C6–C10 pyridine ring and the C11–C16 phenyl ring (centroid Cg3···centroid Cg4 distances of 3.648 Å).

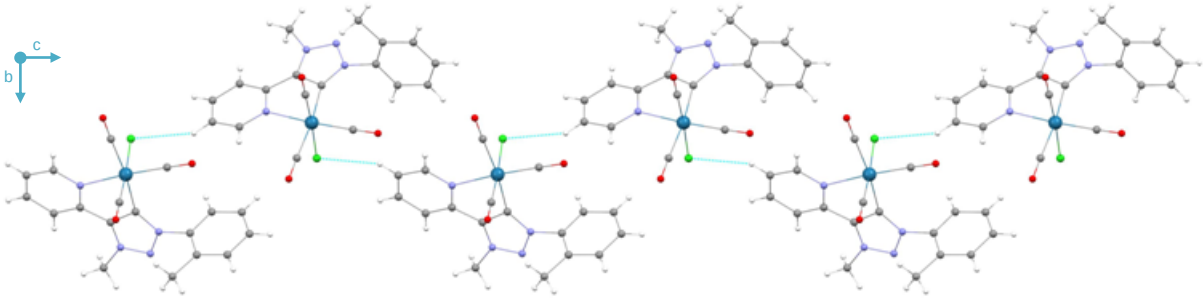

Figure S17. One-dimensional chain of **Re-T-Tol** showing connection of molecules through the intermolecular C–H···Cl interactions along the *c* axis. Adjacent molecules are linked through intermolecular C10–H10(py)···Cl1 hydrogen bonding between the CH group of the coordinated pyridine ring and the chloride ligand.

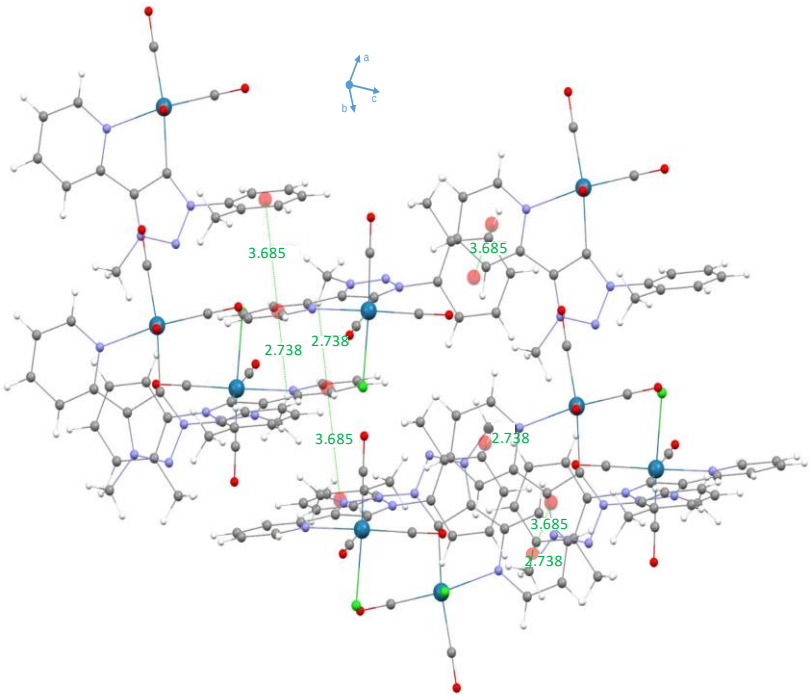

Figure S18. C–H···π and π–π interactions in complex **Re-T-Tol**, with distances in Å. Intermolecular C5–H5B$_{(trz)}$···$\pi_{(py)}$ interactions take place between the methyl group of the triazolylidene and the centroid Cg3 of the N4C7–C11 pyridine ring (C5–H5B···centroid Cg3 distances of 2.738 Å), and the intermolecular $\pi_{(py)}$–$\pi_{(tol)}$ stacking interactions occur between the coordinated pyridine ring N4C7–C11 and the tolyl ring C12–C17 (centroid Cg3···centroid Cg4 distances of 3.685 Å).

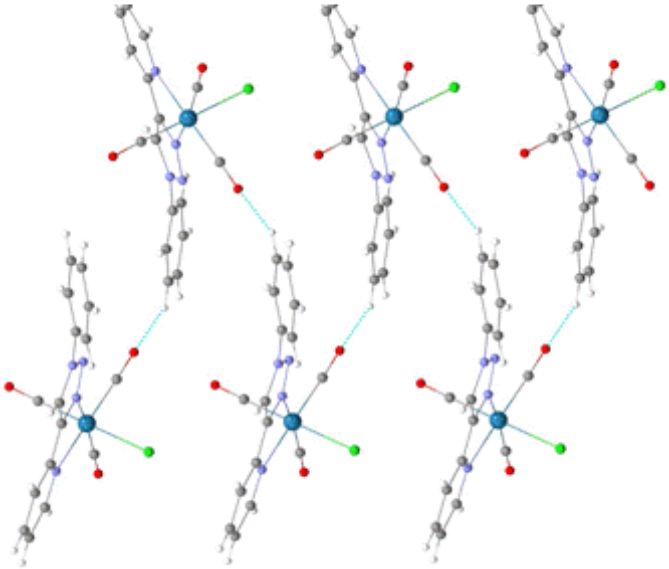

Figure S19. One-dimensional zig-zag chain of **Re-Phe** showing connection of molecules through the intermolecular C13–H13$_{(phe)}$···O2$_{(CO)}$ interactions along the *b* axis.

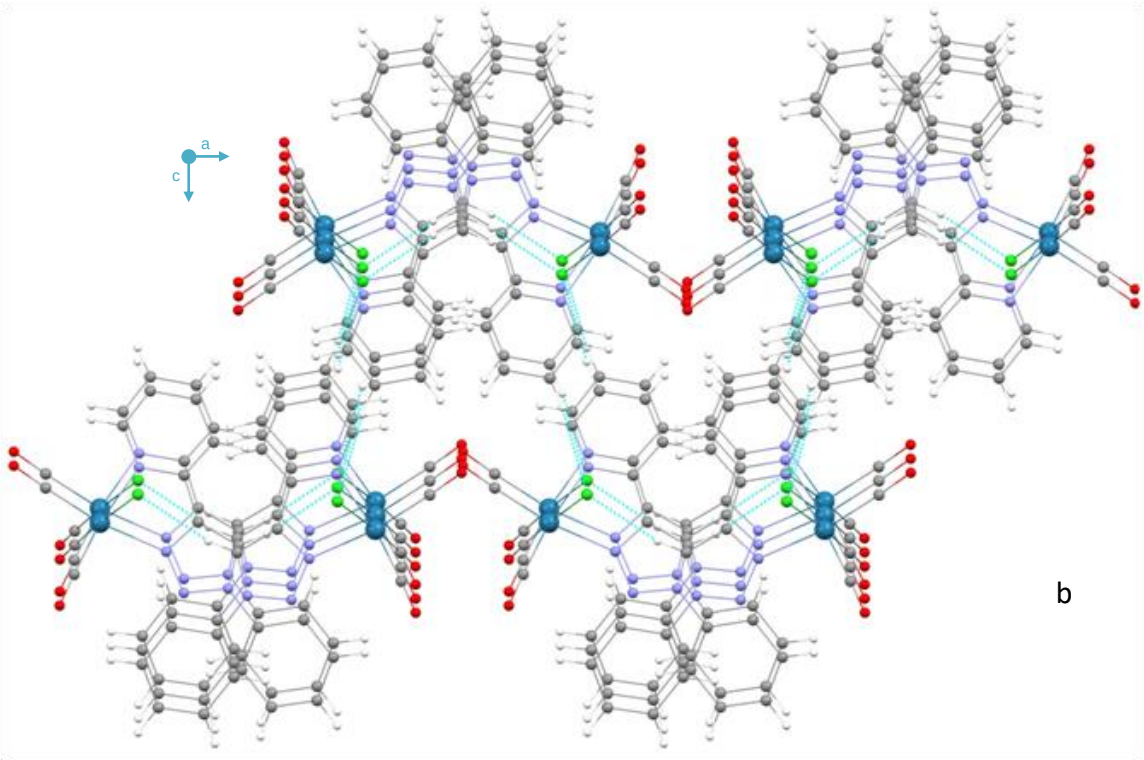

Figure S20. Two dimensional network of **Re-Phe** showing connection of molecules through the intermolecular C–H···Cl interactions in the *ac* plane. The bifurcated hydrogen bond takes place between the chloride ligand and the C–H group of the 1,2,3-triazole ring (C4–H4$_{(trz)}$···Cl1) as well as with the C–H group of the pyridine ring (C9–H9$_{(py)}$···Cl1) of neighboring molecules.

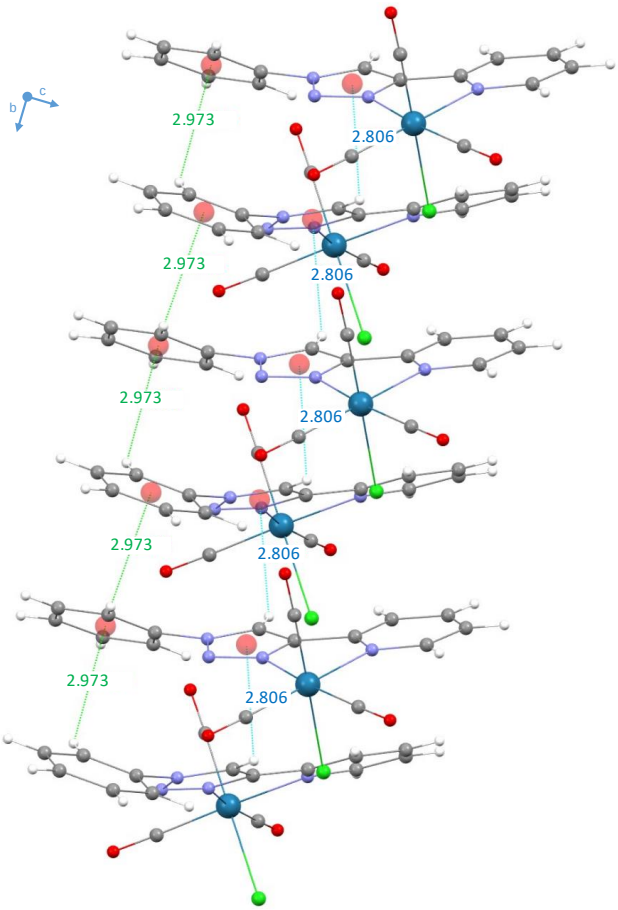

Figure S21. C–H···π interactions in **Re-Phe**, with distances in Å. C4–H4$_{(trz)}$···$\pi_{(trz)}$ and C12–H12$_{(Phe)}$···$\pi_{(Phe)}$ interactions involve respectively the H4 and the Cg2 centroid (N1/N2/N3/C4/C5), with H4···Cg2 distance of 2.806Å, as well as the H12 and the Cg4 centroid (C11–C16), with H12···Cg4 distance of 2.973Å, respectively.

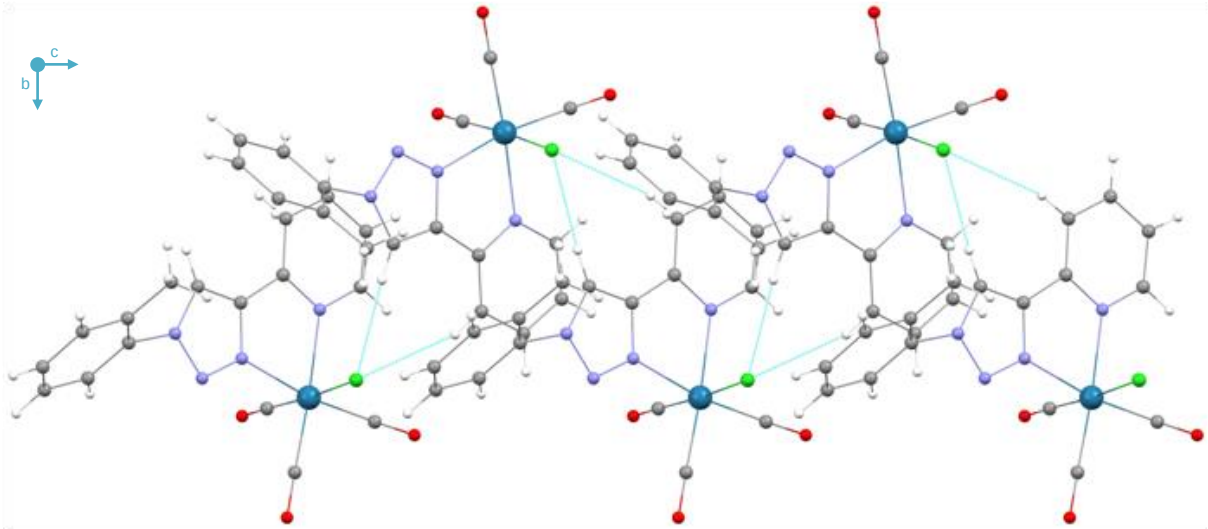

Figure S22. One-dimensional chain of **Re-Tol** showing the connection of molecules through the intermolecular C–H···Cl interactions along the *c* axis. The three-centred hydrogen bonding involves C4–H4$_{(trz)}$···Cl1 and C7–H7$_{(py)}$···Cl1.

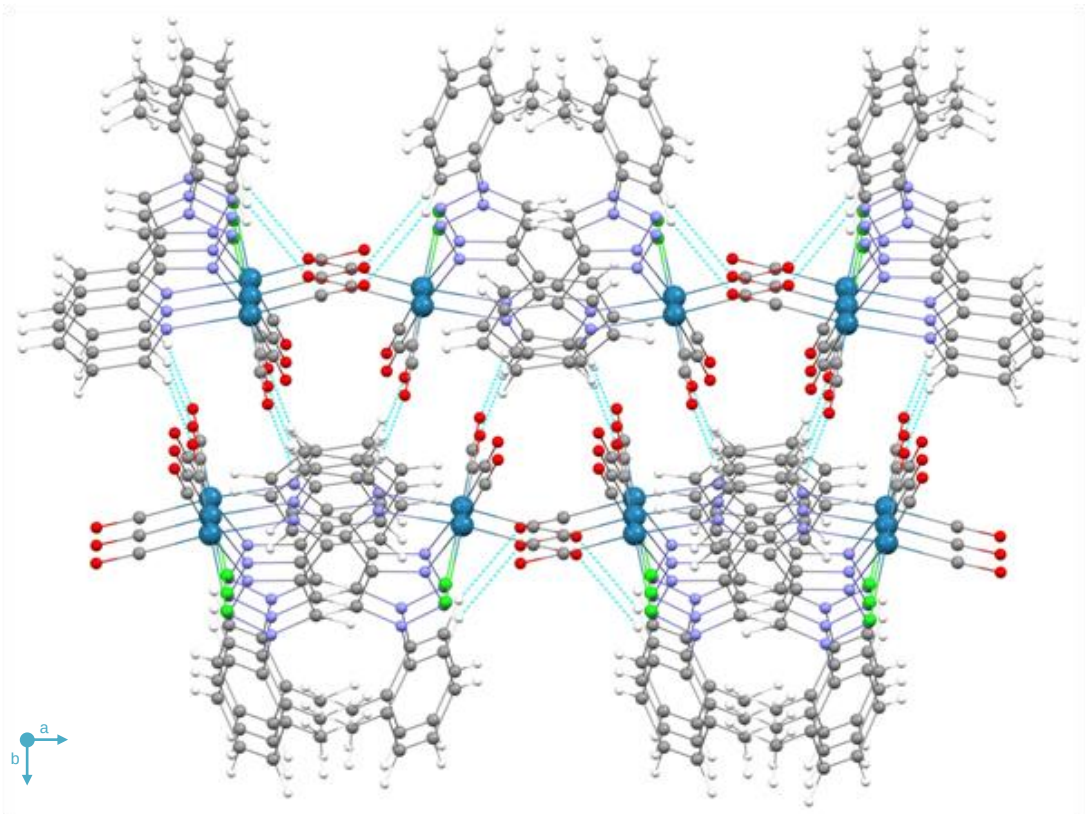

Figure S23. Two dimensional network of **Re-Tol** showing the connection of molecules through the intermolecular C–H···O interactions in the *ab* plane. The C12–H12(tol)···O2(CO) contacts involve the CH groups of the tolyl ring and the equatorial carbonyl groups, and the C10–H10(py)···O3(CO) contacts involve the CH groups of the pyridine ring and the apical carbonyl groups.

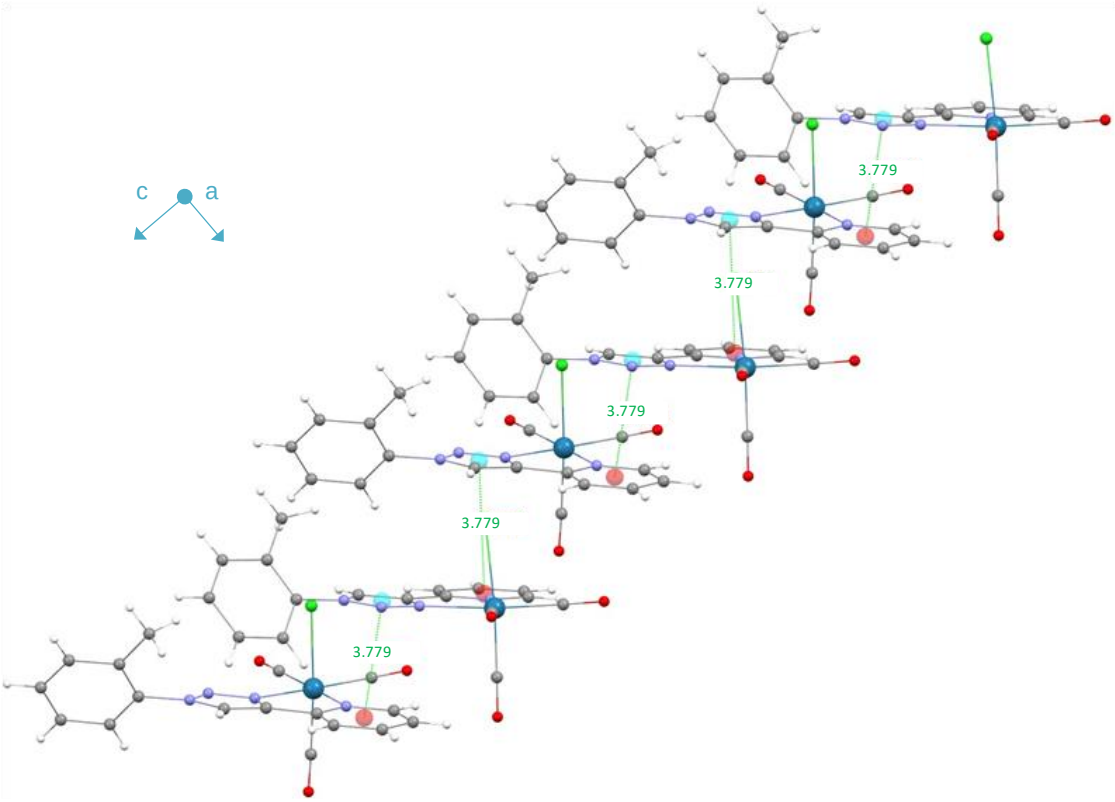

Figure S24. $\pi_{(trz)}\cdots\pi_{(py)}$ interactions in **Re-Tol** (with distances in Å) taking place between between the Cg2 centroid (N1/N2/N3/C4/C5) and the Cg3 centroid (N4/C6–C10), with Cg2⋯Cg3 distance of 3.779Å.

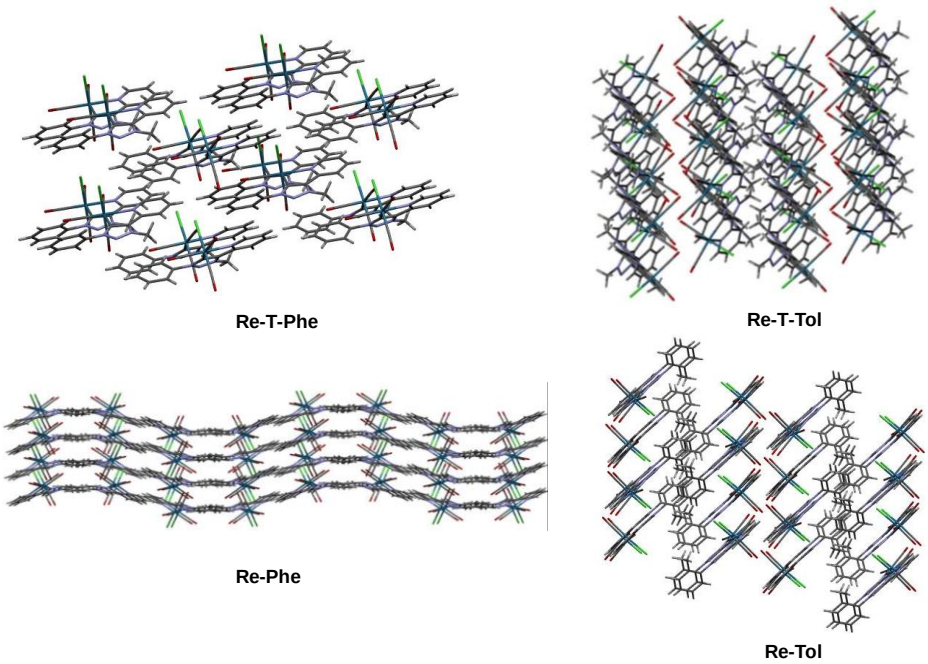

Figure S25. Crystal packing (2 × 2 × 2) of **Re-T-Phe**, **Re-T-Tol**, **Re-Phe** and **Re-Tol**, showing the presence of layers for **Re-T-Tol**, **Re-Phe** and **Re-Tol**.

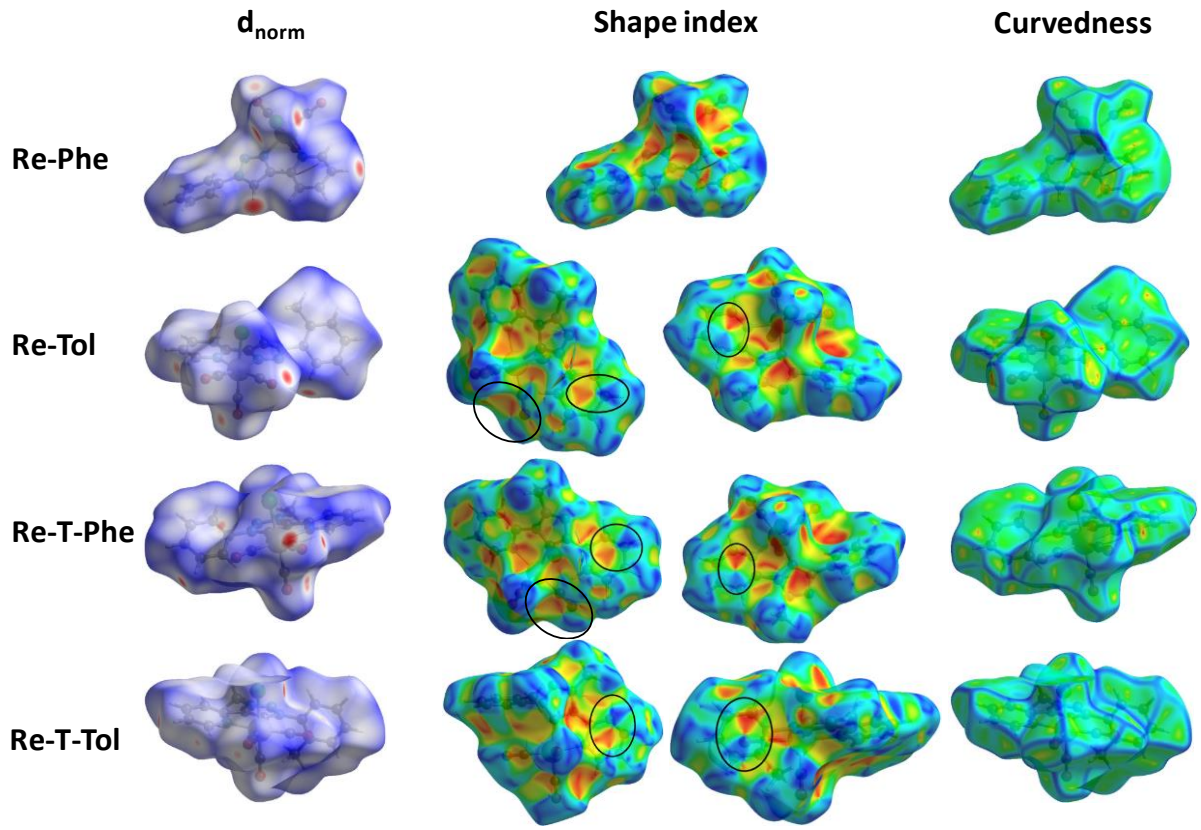

Figure S26. Hirshfeld surfaces plotted over the normalized contact distance (d_{norm}), shape index, and curvedness of **Re-Phe**, **Re-Tol**, **Re-T-Phe**, and **Re-T-Tol** (from top to bottom). The adjacent red and blue triangles that reveal $\pi\cdots\pi$ stacking interactions are highlighted by black circles.

Regarding the d_{norm} map, the intensity of the d_{norm} point provides a simple visual information about important regions of intermolecular interaction through color mapping. Intermolecular contacts shorter than the sum of the van der Waals radii ($d_{norm}<0$) of the interacting atoms are denoted as red spots on the surfaces, whereas longer than the sum of the van der Waals radii ($d_{norm}>0$) of the interacting atoms are represented by blue regions. The van der Waals contacts ($d_{norm}=0$) are coloured white.

Regarding the explanation of the colors on the shape-index map, the convex blue regions symbolize hydrogen-donor groups and the concave red regions symbolize hydrogen-acceptor groups.

For **Re-Phe**, the HS is generated between –0.3555 a.u. (red spot) and 1.1732 a.u. (blue colour); the shape index plot and curvedness plot are generated from –0.9973 to 0.9962 a.u. and –3.7269 to 0.3550 a.u., respectively
For **Re-Tol**, the colour scale on the HS ranges from –0.2502 a.u. (red spot) and 1.5401 a.u. (blue colour). The shape index and curvedness plots are mapped in the colour range between –0.9952 a.u. to 0.9972 a.u. and –3.3807 a.u. to 0.1747 a.u., respectively.
For **Re-T-Phe**, the HS was generated over a colour scale ranging from −0.1444 (red spot) to 1.0626 (blue colour). The shape index and curvedness plots are mapped in the colour range between –0.9921 a.u. to 0.9973 a.u. and –3.5133 a.u. to 0.2804 a.u., respectively.
For **Re-T-Tol**, the colour scale on the HS ranges from –0.1461 a.u. (red spot) and 1.4366 a.u. (blue colour). The shape index and curvedness plots are mapped in the colour range between –0.9954 a.u. to 0.9963 a.u. and –3.9176 a.u. to 0.2727 a.u., respectively.

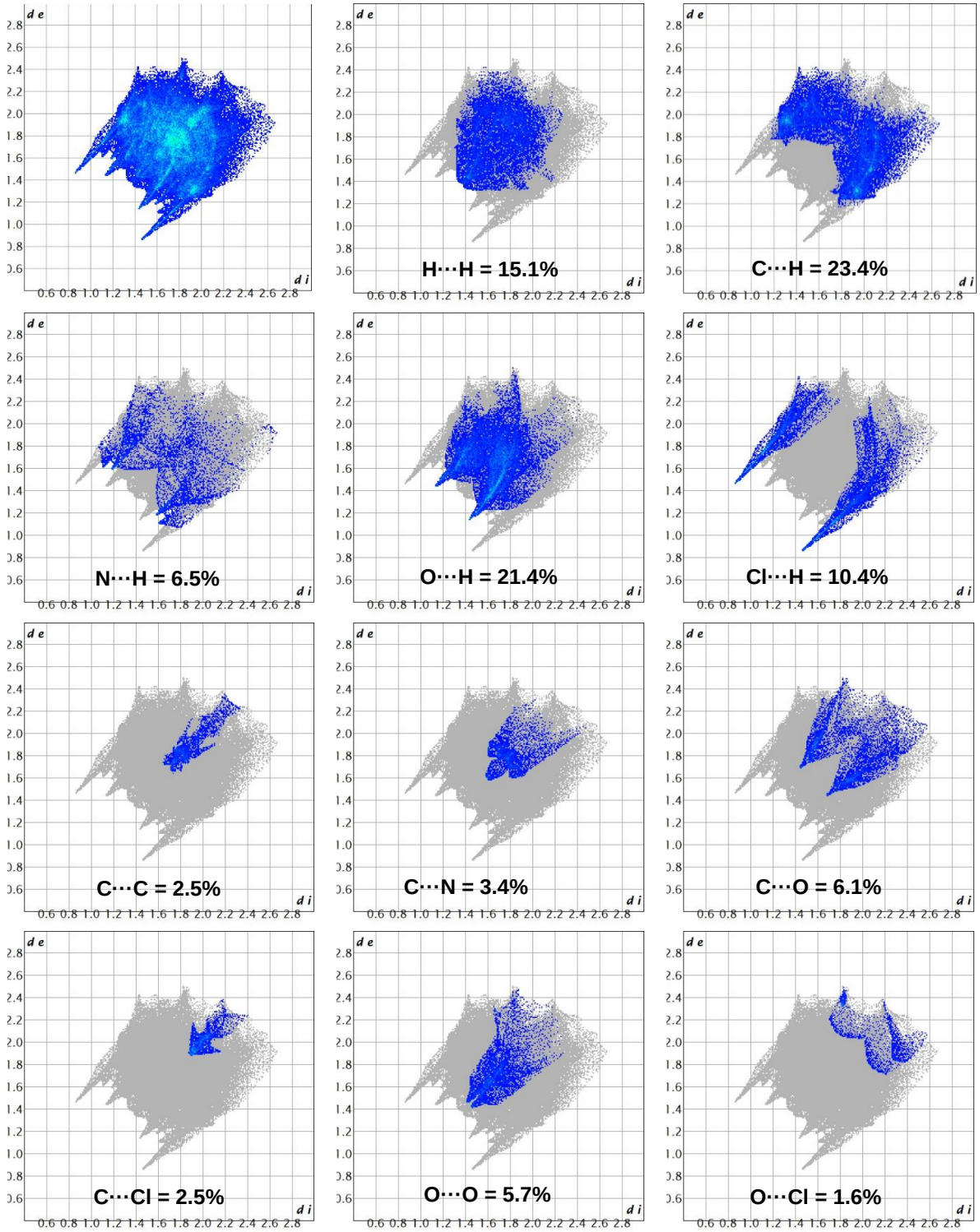

Figure S27. Two-dimensional fingerprint plots for overall interactions and individual interactions in crystal packing of **Re-Phe** (Volume = 399.78 Å^3; Area = 364.93 Å^2).

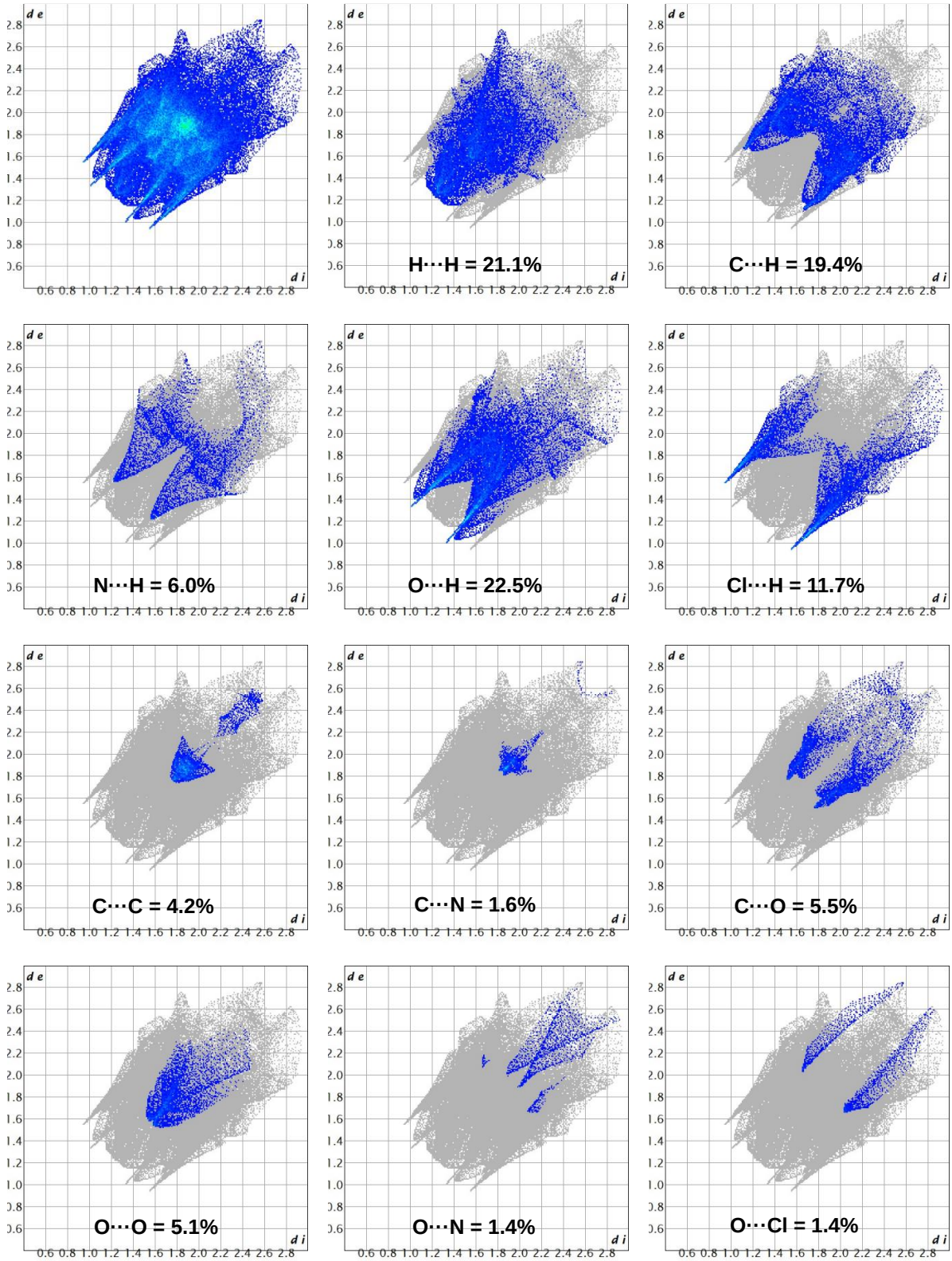

Figure S28. Two-dimensional fingerprint plots for overall interactions and individual interactions in crystal packing of **Re-Tol** (Volume = 439.11 Å^3; Area = 380.12 Å^2).

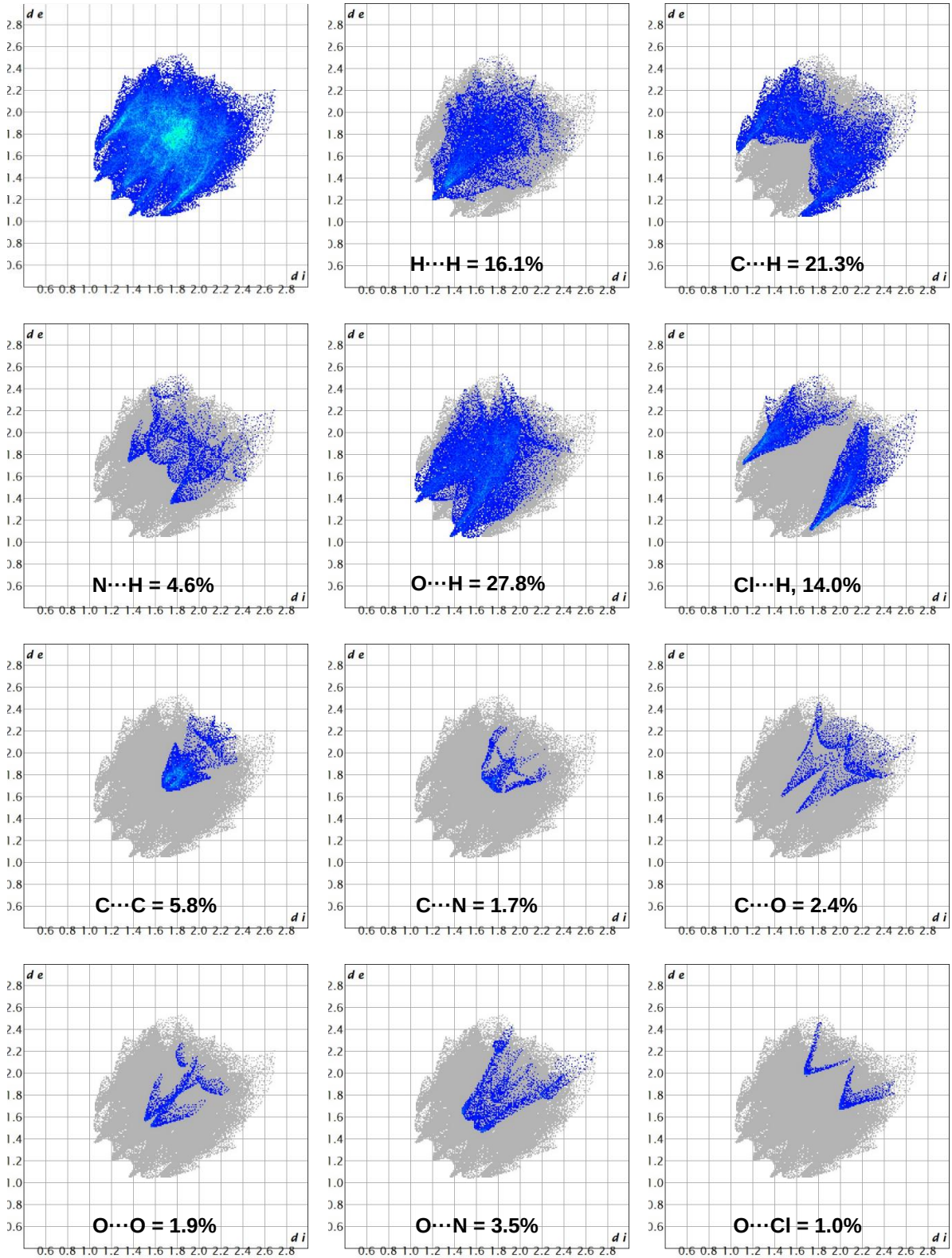

Figure S29. Two-dimensional fingerprint plots for overall interactions and individual interactions in crystal packing of **Re-T-Phe** (Volume = 420.65 Å^3; Area = 365.33 Å^2).

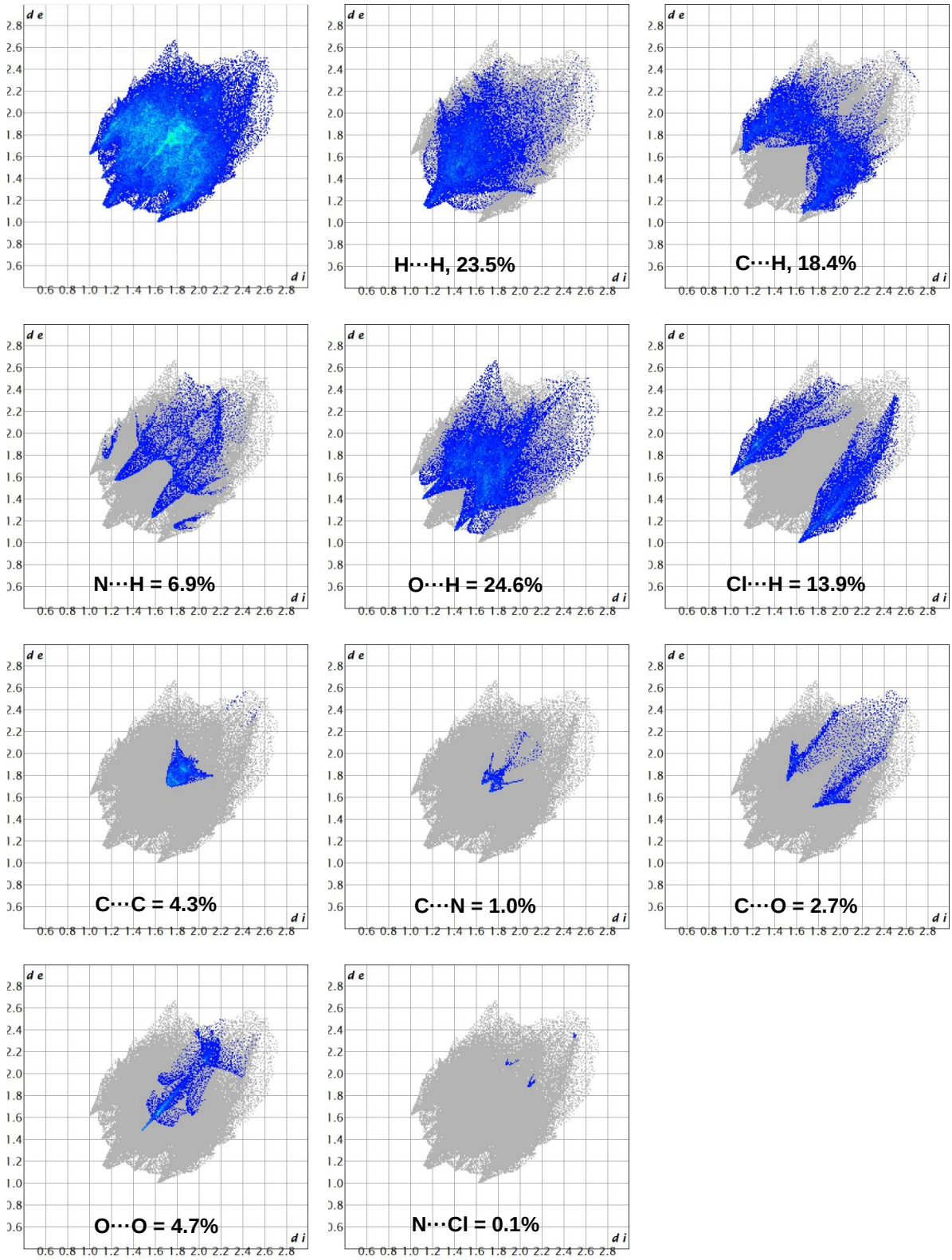

Figure S30. Two-dimensional fingerprint plots for overall interactions and individual interactions in crystal packing of **Re-T-Tol** (Volume = 450.50 Å^3; Area = 378.63 Å^2).

Calculations

Table S9. Selected calculated bond lengths [Å] and angles [°] in the ground state (S_0), first singlet excited state (S_1), and first triplet excited state (T_1) for **Re-Tol**, together with the experimental data.

Bond lengths	Exp.	Optimized					Bond angles	Exp.	Optimized				
		gas phase		dichloromethane					gas phase		dichloromethane		
		S_0	T_1	S_0	S_1	T_1			S_0	T_1	S_0	S_1	T_1
Re(1)-C(1)	1.921(3)	1.914	1.931	1.914	1.956	1.928	C(2)-Re(1)-C(1)	88.08(13)	89.79	91.84	89.56	85.25	91.17
Re(1)-C(2)	1.916(3)	1.918	1.986	1.912	1.950	1.990	C(2)-Re(1)-C(3)	88.47(13)	90.84	88.21	90.42	93.46	89.96
Re(1)-C(3)	1.932(3)	1.904	1.952	1.897	1.955	1.949	C(1)-Re(1)-C(3)	91.46(13)	91.03	90.24	90.53	90.25	88.27
Re(1)-N(1)	2.152(2)	2.154	2.129	2.153	2.105	2.130	C(2)-Re(1)-N(1)	99.97(11)	97.68	94.76	97.56	98.18	94.94
Re(1)-N(4)	2.195(2)	2.208	2.093	2.211	2.148	2.078	C(1)-Re(1)-N(1)	170.94(11)	170.13	171.27	171.60	176.43	172.10
Re(1)-Cl(1)	2.4738(8)	2.497	2.419	2.524	2.419	2.456	C(3)-Re(1)-N(1)	92.87(11)	95.29	95.67	93.86	90.53	95.22
							C(2)-Re(1)-N(4)	173.79(11)	170.94	170.57	171.27	173.99	171.16
C(1)-O(1)	1.149(4)	1.158	1.153	1.159	1.150	1.154	C(1)-Re(1)-N(4)	97.47(11)	97.55	97.16	98.13	100.30	97.36
C(2)-O(2)	1.146(4)	1.163	1.147	1.159	1.148	1.147	C(3)-Re(1)-N(4)	94.13(10)	94.32	88.94	93.62	88.84	89.41
C(3)-O(3)	1.110(4)	1.155	1.151	1.163	1.151	1.149	N(1)-Re(1)-N(4)	74.29(8)	74.45	76.58	74.46	76.24	76.78
							C(2)-Re(1)-Cl(1)	92.39(10)	92.14	87.09	92.31	91.55	87.34
							C(1)-Re(1)-Cl(1)	92.92(9)	92.24	90.39	91.91	90.54	90.77
							C(3)-Re(1)-Cl(1)	175.55(9)	175.58	175.28	176.35	174.97	175.56
							N(1)-Re(1)-Cl(1)	82.68(7)	81.08	84.26	83.35	88.38	84.53
							N(4)-Re(1)-Cl(1)	84.59(6)	82.31	95.63	83.39	86.13	94.84
							O(1)-C(1)-Re(1)	177.3(3)	178.48	179.24	179.47	178.54	179.30
							O(2)-C(2)-Re(1)	175.4(3)	178.77	178.38	178.93	179.83	178.54
							O(3)-C(3)-Re(1)	174.2(4)	179.62	178.78	179.87	179.23	179.10

Table S10. Selected calculated bond lengths [Å] and angles [°] in the ground state (S_0), first singlet excited state (S_1), and first triplet excited state (T_1) for **Re-T-Tol**, together with the experimental data.

Bond lengths	Exp.	Optimized					Bond angles	Exp.	Optimized				
		gas phase		dichloromethane					gas phase		dichloromethane		
		S_0	T_1	S_0	S_1	T_1			S_0	T_1	S_0	S_1	T_1
Re(1)-C(1)	1.897(2)	1.901	1.944	1.893	1.948	1.934	C(1)-Re(1)-C(2)	88.42(9)	89.92	90.97	90.18	91.75	90.88
Re(1)-C(2)	1.911(2)	1.912	1.929	1.907	1.934	1.922	C(1)-Re(1)-C(3)	91.76(9)	92.29	89.40	91.59	90.99	89.99
Re(1)-C(3)	1.958(2)	1.948	2.012	1.948	1.996	2.014	C(2)-Re(1)-C(3)	89.54(10)	89.57	89.66	90.14	86.10	89.35
Re(1)-C(4)	2.117(2)	2.120	2.069	2.124	2.113	2.056	C(1)-Re(1)-C(4)	91.62(8)	94.88	85.03	93.88	85.68	87.14
Re(1)-N(4)	2.2341(17)	2.238	2.199	2.240	2.177	2.198	C(2)-Re(1)-C(4)	98.69(8)	100.30	99.41	98.79	100.72	98.66
Re(1)-Cl(1)	2.5260(5)	2.519	2.425	2.546	2.420	2.475	C(3)-Re(1)-C(4)	171.19(8)	167.79	169.42	169.50	172.48	171.53
							C(1)-Re(1)-N(4)	94.35(8)	93.05	92.767	93.39	90.55	92.28
O(1)-C(1)	1.156(3)	1.165	1.154	1.166	1.150	1.154	C(2)-Re(1)-N(4)	172.88(8)	174.38	174.22	172.70	176.11	174.33
O(2)-C(2)	1.151(3)	1.158	1.153	1.161	1.154	1.156	C(3)-Re(1)-N(4)	96.92(8)	95.08	94.78	96.12	97.01	95.35
O(3)-C(3)	1.145(3)	1.157	1.147	1.159	1.149	1.147	C(4)-Re(1)-N(4)	74.71(7)	74.71	76.55	74.63	76.32	76.82
							C(1)-Re(1)-Cl(1)	176.06(6)	175.58	176.47	176.67	175.42	175.81
							C(2)-Re(1)-Cl(1)	95.39(7)	93.32	91.13	92.88	91.27	91.86
							C(3)-Re(1)-Cl(1)	89.29(7)	90.74	87.78	89.74	92.65	86.88
							C(4)-Re(1)-Cl(1)	86.81(5)	81.60	97.42	84.34	90.38	95.57
							N(4)-Re(1)-Cl(1)	81.75(4)	83.48	85.36	83.43	86.25	85.26
							O(1)-C(1)-Re(1)	179.2(2)	179.14	179.40	179.85	179.00	179.85
							O(2)-C(2)-Re(1)	178.7(2)	179.33	178.54	179.76	178.56	178.85
							O(3)-C(3)-Re(1)	178.5(2)	178.75	178.25	179.87	177.16	178.33

Table S11. Selected calculated bond lengths [Å] and angles [°] in the ground state (S_0,) first singlet excited state (S_1), and first triplet excited (T_1) state for **Re-T-BOP**.

.

Bond lengths	Optimized					Bond angles	Optimized				
	gas phase		dichloromethane				gas phase		dichloromethane		
	S_0	T_1	S_0	S_1	T_1		S_0	T_1	S_0	S_1	T_1
Re(1)-C(1)	1.900	1.942	1.893	1.948	1.936	C(1)-Re(1)-C(2)	90.97	92.32	90.81	94.08	90.55
Re(1)-C(2)	1.913	1.930	1.908	1.934	1.922	C(1)-Re(1)-C(3)	92.34	89.25	91.65	89.81	89.88
Re(1)-C(3)	1.949	2.013	1.946	1.995	2.014	C(2)-Re(1)-C(3)	89.79	90.29	89.67	86.11	88.62
Re(1)-C(4)	2.121	2.070	2.130	2.115	2.061	C(1)-Re(1)-C(4)	95.85	86.23	94.18	86.95	86.43
Re(1)-N(4)	2.231	2.197	2.236	2.175	2.197	C(2)-Re(1)-C(4)	99.50	98.52	99.57	99.79	99.87
Re(1)-Cl(1)	2.516	2.424	2.547	2.421	2.470	C(3)-Re(1)-C(4)	167.48	170.25	168.99	173.45	170.76
						C(1)-Re(1)-N(4)	95.47	94.38	94.44	90.23	91.90
O(1)-C(1)	1.166	1.154	1.166	1.150	1.153	C(2)-Re(1)-N(4)	171.83	171.54	172.52	174.17	175.69
O(2)-C(2)	1.157	1.152	1.161	1.154	1.157	C(3)-Re(1)-N(4)	94.95	94.97	95.50	97.84	94.92
O(3)-C(3)	1.156	1.147	1.159	1.149	1.147	C(4)-Re(1)-N(4)	74.88	76.79	74.76	76.50	76.75
						C(1)-Re(1)-Cl(1)	176.42	175.88	177.10	175.20	176.31
						C(2)-Re(1)-Cl(1)	91.79	89.51	91.64	90.36	91.94
						C(3)-Re(1)-Cl(1)	89.95	87.05	89.91	92.35	87.45
						C(4)-Re(1)-Cl(1)	81.44	97.15	83.89	90.48	95.83
						N(4)-Re(1)-Cl(1)	81.58	84.15	82.98	85.22	85.79
						O(1)-C(1)-Re(1)	179.14	179.27	179.74	178.86	179.75
						O(2)-C(2)-Re(1)	179.10	178.00	178.79	178.41	178.10
						O(3)-C(3)-Re(1)	178.82	178.19	179.93	177.09	178.39

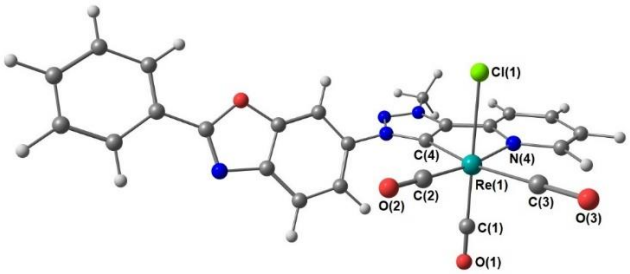

Figure S31. DFT-optimized structure of **Re-T-BOP.**

Table S12. Dihedral angle values between the triazole or triazolylidene ring and R calculated using the density functional theory (DFT) method at the PBE1PBE/LANL2DZ/6-311+G** level for the ground state S_0, the first singlet excited state S_1, and the first triplet excited state T_1 of **Re-Tol**, **Re-T-Tol** and **Re-T-BOP**, and obtained from crystallographic data.

Complex	SXRD	Gas phase		DCM		
		S_0	T_1	S_0	S_1	T_1
Re-Tol	56.25	57.20	56.95	62.15	61.97	62.83
Re-T-Tol	81.86	66.61	66.45	88.53	71.89	72.33
Re-T-BOP	–	48.38	57.71	54.76	61.15	82.66

Table S13. The frontier molecular orbital compositions (%) and energy levels for **Re-Tol** (in gas phase).

Orbital		Energy (eV)	MO Contribution (%)					Main bond type
			Re	CO	Cl	pyta	R	
100	L+5	–0.49	28	10	0	70	-6	p(Re)+π*(CO)/π*(pyta)
99	L+4	–0.80	2	3	0	42	53	π*(R)/π*(pyta)
98	L+3	–1.05	0	0	0	5	95	π*(R)
97	L+2	–1.60	0	1	0	68	29	π*(pyta)/π*(R)
96	L+1	–1.86	0	1	0	85	13	π*(pyta)
95	L	–2.36	2	2	1	93	1	π*(pyta)
HOMO–LUMO gap **(E = 3.69 eV)**								
94	H	–6.05	47	21	31	2	0	d(Re)+π(CO)/π(Cl)
93	H–1	–6.16	45	19	34	2	0	d(Re)+π(CO)/π(Cl)
92	H–2	–6.73	70	29	1	0	0	d(Re)+π(CO)
91	H–3	–7.43	18	6	51	15	9	π(Cl)/π(pyta)
90	H–4	–7.51	26	7	59	8	1	π(Cl)/d(Re)+π(CO)
89	H–5	–7.85	5	2	7	16	71	π(R)/π(pyta)
88	H–6	–7.94	2	1	3	58	37	π(pyta)/π(R)
87	H–7	–8.13	8	13	66	7	6	π(Cl)
86	H–8	–8.28	2	1	8	20	70	π(R)/π(pyta)
85	H–9	–9.57	2	2	2	93	1	π(pyta)
84	H–10	–9.62	0	4	0	94	2	π(pyta)

pyta: pyridyl-triazole; R= tolyl ring

Table S14. The frontier molecular orbital compositions (%) and energy levels for **Re-Tol** (in dichloromethane).

Orbital		Energy (eV)	MO Contribution (%)					Main bond type
			Re	CO	Cl	pyta	R	
100	L+5	–0.68	35	52	0	4	11	p(Re)+π*(CO)/π*(R)
99	L+4	–0.75	2	3	0	6	90	π*(R)
98	L+3	–0.84	33	59	0	6	4	p(Re)+π*(CO)
97	L+2	–1.37	1	4	0	82	13	π*(pyta)
96	L+1	–1.60	1	2	0	82	15	π*(pyta)
95	L	–2.21	4	5	0	90	1	π*(pyta)
HOMO–LUMO gap **(E = 4.43 eV)**								
94	H	–6.64	53	24	20	3	1	d(Re)+π(CO)/π(Cl)
93	H–1	–6.74	51	22	22	3	1	d(Re)+π(CO)/π(Cl)
92	H–2	–7.19	69	30	1	0	0	d(Re)+π(CO)
91	H–3	–7.56	0	0	2	24	73	π(R)/π(pyta)
90	H–4	–7.69	0	0	3	49	48	π(pyta)/π(R)
89	H–5	–7.90	0	0	3	32	65	π(R)/π(pyta)
88	H–6	–8.18	14	4	66	15	1	π(Cl)/π(pyta)
87	H–7	–8.24	16	5	66	7	6	π(Cl)
86	H–8	–8.87	8	14	69	10	0	π(Cl)
85	H–9	–9.44	5	3	10	81	1	π(pyta)
84	H–10	–9.46	1	1	2	95	2	π(pyta)

pyta: pyridyl-triazole; R= tolyl ring

Table S15. The frontier molecular orbital compositions (%) and energy levels for **Re-T-Tol** (in gas phase).

Orbital		Energy (eV)	MO Contribution (%)					Main bond type
			Re	CO	Cl	pytrz	R	
104	L+5	–0.48	2	4	0	21	73	π*(R)/π*(pytrz)
103	L+4	–0.56	6	5	-1	23	68	π*(R)/π*(pytrz)
102	L+3	–0.63	12	5	1	35	48	π*(R)/π*(pytrz)
101	L+2	–1.27	6	4	0	77	13	π*(pytrz)/π*(R)
100	L+1	–1.84	2	2	0	96	1	π*(pytrz)
99	L	–2.50	1	1	0	97	1	π*(pytrz)
HOMO–LUMO gap **(E = 3.37 eV)**								
98	H	–5.87	49	22	26	3	1	d(Re)+π(CO)/π(Cl)
97	H–1	–5.99	47	19	31	2	0	d(Re)+π(CO)/π(Cl)
96	H–2	–6.45	70	28	0	0	3	d(Re)+π(CO)
95	H–3	–7.07	11	5	51	32	2	π(Cl)/π(pytrz)
94	H–4	–7.36	2	0	6	1	90	π(R)
93	H–5	–7.42	22	6	58	6	9	π(Cl)/d(Re)+π(CO)
92	H–6	–7.59	0	1	0	10	89	π(R)
91	H–7	–7.92	13	9	45	31	2	π(Cl)/π(pytrz)
90	H–8	–8.14	7	8	39	42	4	π(pytrz)/π(Cl)
89	H–9	–9.15	7	14	2	75	2	π(pytrz)
88	H–10	–9.44	4	3	3	90	0	π(pytrz)

pytrz: pyridyl-triazolylidene; R= tolyl ring

Table S16. The frontier molecular orbital compositions (%) and energy levels for **Re-T-Tol** (in dichloromethane).

Orbital		Energy (eV)	MO Contribution (%)					Main bond type
			Re	CO	Cl	pytrz	R	
104	L+5	–0.54	7	9	0	5	79	π*(R)
103	L+4	–0.68	26	43	0	17	14	p(Re)+π*(CO)/π*(pytrz)
102	L+3	–0.82	1	2	0	4	93	π*(R)
101	L+2	–1.16	16	16	-1	71	0	π*(pytrz)/p(Re)+π*(CO)
100	L+1	–1.63	5	5	0	92	0	π*(pytrz)
99	L	–2.29	2	2	0	95	1	π*(pytrz)
HOMO–LUMO gap **(E = 4.12 eV)**								
98	H	–6.41	51	23	15	11	0	d(Re)+π(CO)/π(Cl)
97	H–1	–6.56	53	23	20	4	0	d(Re)+π(CO)/π(Cl)
96	H–2	–6.91	69	29	0	0	1	d(Re)+π(CO)
95	H–3	–7.45	1	1	29	65	4	π(pytrz)/π(Cl)
94	H–4	–7.47	0	0	1	3	96	π(R)
93	H–5	–7.79	0	0	1	3	96	π(R)
92	H–6	–8.06	14	3	71	12	0	π(Cl)
91	H–7	–8.16	12	7	40	41	1	π(Cl)/π(pytrz)
90	H–8	–8.74	9	12	72	6	0	π(Cl)
89	H–9	–9.16	4	8	1	86	1	π(pytrz)
88	H–10	–9.37	9	7	9	76	0	π(pytrz)

pytrz: pyridyl-triazolylidene; R= tolyl ring

Table S17. The frontier molecular orbital compositions (%) and energy levels for **Re-T-BOP** (in gas phase).

Orbital		Energy (eV)	MO Contribution (%)					Main bond type
			Re	CO	Cl	pytrz	PBO	
130	L+5	–0.59	4	0	0	12	83	π*(PBO)
129	L+4	–0.64	6	3	0	9	83	π*(PBO)
128	L+3	–1.24	7	5	0	69	21	π*(pytrz)/π*(PBO)
127	L+2	–1.76	0	1	0	74	25	π*(pytrz)/π*(PBO)
126	L+1	–2.01	1	2	0	32	64	π*(PBO)/π*(pytrz)
125	L	–2.51	1	1	0	94	4	π*(pytrz)
HOMO–LUMO gap **(E = 3.35 eV)**								
124	H	–5.86	48	21	29	1	2	d(Re)+π(CO)/π(Cl)
123	H–1	–6.00	46	19	33	2	1	d(Re)+π(CO)/π(Cl)
122	H–2	–6.47	69	28	0	0	4	d(Re)+π(CO)
121	H–3	–6.77	1	1	7	5	86	π(PBO)
120	H–4	–7.05	11	5	44	30	10	π(Cl)/π(pytrz)
119	H–5	–7.33	24	7	62	6	0	π(Cl)/d(Re)+π(CO)
118	H–6	–7.58	0	0	0	0	99	π(PBO)
117	H–7	–7.71	0	0	0	0	100	π(PBO)
116	H–8	–7.90	13	10	46	30	2	π(Cl)/π(pytrz)
115	H–9	–8.07	5	6	30	32	26	π(Cl)/π(pytrz)/π(PBO)
114	H–10	–8.28	3	2	9	17	69	π(PBO)/π(pytrz)

pytrz: pyridyl-triazolylidene; PBO = phenylbenzoxazole

Table S18. The frontier molecular orbital compositions (%) and energy levels for **Re-T-BOP** (in dichloromethane).

Orbital		Energy (eV)	MO Contribution (%)					Main bond type
			Re	CO	Cl	pytrz	PBO	
130	L+5	-0.63	12	13	0	3	72	π*(PBO)
129	L+4	-0.74	13	28	0	8	51	π*(PBO)/p(Re)+π*(CO)
128	L+3	-1.22	12	13	-1	68	9	π*(pytrz)
127	L+2	-1.63	4	4	0	78	14	π*(pytrz)
126	L+1	-2.03	1	2	0	14	83	π*(PBO)
125	L	-2.31	2	2	0	93	3	π*(pytrz)
HOMO–LUMO gap **(E = 4. 11 eV)**								
124	H	-6.42	51	23	15	9	2	d(Re)+π(CO)/π(Cl)
123	H–1	-6.58	53	23	19	4	1	d(Re)+π(CO)/π(Cl)
122	H–2	-6.86	13	5	1	3	78	π(PBO)
121	H–3	-6.94	56	24	1	0	18	d(Re)+π(CO)/π(PBO)
120	H–4	-7.46	1	1	31	67	1	π(pytrz)/π(Cl)
119	H–5	-7.64	0	0	0	0	99	π(PBO)
118	H–6	-7.73	0	0	0	0	99	π(PBO)
117	H–7	-8.05	13	4	70	12	1	π(Cl)
116	H–8	-8.12	7	4	28	27	34	π(PBO)/π(Cl)/π(pytrz)
115	H–9	-8.34	6	3	15	14	62	π(PBO)
114	H–10	-8.77	9	12	71	6	2	π(Cl)

pytrz: pyridyl-triazolylidene; PBO = phenylbenzoxazole

Table S19. The main electronic transitions for **Re-Tol**, calculated with TDDFT method at the PBE1PBE/LANL2DZ level (in gas phase).

Electronic transition	Contribution	Assignment		E_{calc} /eV	λ_{calc} /nm	*f*
$S_0 \rightarrow S_1$	H→L	d(Re)+π(CO)/π(Cl)→π*(pyta)	MLCT/LLCT	2.73	454.8	*0.0038*
$S_0 \rightarrow S_2$	H–1→L	d(Re)+π(CO)/π(Cl)→π*(pyta)	MLCT/LLCT	2.92	425.2	*0.0431*
$S_0 \rightarrow S_7$	H–1→L+2	d(Re)+π(CO)/π(Cl)→π*(pyta)/π*(R)	MLCT/LLCT	3.72	333.3	*0.0217*
$S_0 \rightarrow S_{10}$	H–4→L	π(Cl)/d(Re)+π(CO)→π*(pyta)	LLCT/MLCT	4.22	293.7	*0.0307*
$S_0 \rightarrow S_{11}$	H–2→L+2	d(Re)+π(CO)→π*(pyta)/π*(R)	MLCT/LLCT	4.24	292.5	*0.0260*
$S_0 \rightarrow S_{18}$	H–1→L+4	d(Re)+π(CO)/π(Cl)→π*(R)/π*(pyta)	MLCT/LLCT	4.67	265.8	*0.0312*
	H–6→L	π(pytrz)/π(R)→π*(pyta)	ILCT			
$S_0 \rightarrow S_{20}$	H–3→L+1	π(Cl)/π(pytrz)→π*(pyta)	LLCT/ILCT	4.75	261.1	*0.1575*
$S_0 \rightarrow S_{22}$	H–4→L+1	π(Cl)/d(Re)+π(CO)→π*(pyta)	LLCT/MLCT	4.87	254.5	*0.0752*
	H–5→L	π(R)/π(pytrz)→π*(pyta)	ILCT			
$S_0 \rightarrow S_{23}$	H–7→L	π(Cl)→π*(pyta)	LLCT	4.91	252.6	*0.0297*
$S_0 \rightarrow S_{26}$	H–3→L+2	π(Cl)/π(pyta)→π*(pyta)/π*(R)	LLCT/ILCT	4.98	248.7	*0.1056*
$S_0 \rightarrow S_{29}$	H–5→L+1	π(R)/π(pyta)→π*(pyta)	ILCT	5.10	243.0	*0.0629*
	H–5→L+2	π(R)/π(pyta)→π*(pyta)/π*(R)	ILCT			
$S_0 \rightarrow S_{30}$	H–4→L+2	π(Cl)/d(Re)+π(CO)→π*(pyta)/π*(R)	LLCT/MLCT	5.13	241.8	*0.2121*
$S_0 \rightarrow S_{35}$	H–8→L	π(R)/π(pyta)→π*(pyta)	ILCT	5.36	231.1	*0.1096*
$S_0 \rightarrow S_{37}$	H–7→L+1	π(Cl)→π*(pyta)	LLCT	5.46	227.3	*0.0214*
$S_0 \rightarrow S_{38}$	H→L+8	d(Re)+π(CO)/π(Cl)→π*(pyta)	MLCT/LLCT	5.49	226.0	*0.0212*
$S_0 \rightarrow S_{43}$	H–5→L+2	π(R)/π(pyta)→π*(pyta)/π*(R)	ILCT	5.60	221.6	*0.0217*
$S_0 \rightarrow S_{45}$	H–6→L+2	π(pyta)/π(R)→π*(pyta)/π*(R)	ILCT	5.69	218.0	*0.0442*
$S_0 \rightarrow S_{71}$	H–1→L+12	d(Re)+π(CO)/π(Cl)→p(Re)+π*(CO)/π*(R)	MLCT/LLCT	6.17	201.0	*0.0314*

MLCT: metal-to-ligand charge transfer; LMCT: ligand-to-metal charge transfer; LLCT: ligand-to-ligand charge transfer; ILCT: intraligand charge transfer. pyta: pyridyl-triazole; R= tolyl ring

Table S20. The main electronic transitions for **Re-Tol**, calculated with TDDFT method at the PBE1PBE/LANL2DZ level (in dichloromethane).

Electronic transition	Contribution	Assignment		E_{calc} /eV	λ_{calc} /nm	*f*	λ_{exp} /nm
$S_0 \rightarrow S_1$	H→L	d(Re)+π(CO)/π(Cl)→π*(pya)	MLCT/LLCT	3.43	361.7	*0.0043*	
$S_0 \rightarrow S_2$	H–1→L	d(Re)+π(CO)/π(Cl)→π*(pyta)	MLCT/LLCT	3.60	344.5	*0.0914*	344
$S_0 \rightarrow S_{11}$	H–3→L	π(R)/π(pyta)→π*(pyta)	ILCT	4.62	268.3	*0.3443*	276
$S_0 \rightarrow S_{17}$	H–5→L	π(R)/π(pyta)→π*(pyta)	ILCT	4.98	248.8	*0.0891*	
	H–6→L	π(Cl)/π(pyta)→π*(pyta)	LLCT/ILCT				
$S_0 \rightarrow S_{19}$	H–2→L+3	d(Re)+π(CO)→p(Re)+π*(CO)	MLCT/ILCT	5.08	244.2	*0.0772*	
$S_0 \rightarrow S_{22}$	H–4→L+1	π(pyta)/π(R)→π*(pyta)	ILCT	5.24	236.7	*0.2726*	240
$S_0 \rightarrow S_{26}$	H–1→L+4	d(Re)+π(CO)/π(Cl)→π*(R)	MLCT/LLCT	5.44	228.1	*0.0552*	
	H–5→L+1	π(R)/π(pyta)→ π*(pyta)	ILCT				
$S_0 \rightarrow S_{40}$	H–5→L+2	π(R)/π(pyta)→ π*(pyta)	ILCT	5.88	211.0	*0.0645*	
$S_0 \rightarrow S_{50}$	H–3→L+5	π(R)/π(pyta)→p(Re)+π*(CO)/π*(R)	LLCT/ILCT	6.15	201.8	*0.0635*	
	H–4→L+5	π(pyta)/π(R)→p(Re)+π*(CO)/π*(R)	LLCT/ILCT				

MLCT: metal-to-ligand charge transfer; LMCT: ligand-to-metal charge transfer; LLCT: ligand-to-ligand charge transfer; ILCT: intraligand charge transfer. pyta: pyridyl-triazole; R= tolyl ring.

Table S21. The main electronic transitions for **Re-T-Tol** calculated with TDDFT method at the PBE1PBE/LANL2DZ level (in gas phase).

Electronic transition	Contribution	Assignment		E_{calc} /eV	λ_{calc} /nm	*f*
$S_0 \rightarrow S_1$	H→L	d(Re)+π(CO)/π(Cl)→π*(pytrz)	MLCT/LLCT	2.46	504.0	*0.0014*
$S_0 \rightarrow S_2$	H–1→L	d(Re)+π(CO)/π(Cl)→π*(pytrz)	MLCT/LLCT	2.64	470.4	*0.0286*
$S_0 \rightarrow S_8$	H–3→L	π(Cl)/π(pytrz)→π*(pytrz)	LLCT/ILCT	3.74	331.8	*0.0488*
$S_0 \rightarrow S_{10}$	H–5→L	π(Cl)/d(Re)+π(CO)→π*(pytrz)	LLCT/MLCT	4.02	308.3	*0.0313*
$S_0 \rightarrow S_{18}$	H–7→L	π(Cl)/π(pytrz)→π*(pytrz)	LLCT/ILCT	4.60	269.8	*0.0763*
$S_0 \rightarrow S_{27}$	H–1→L+5	d(Re)+π(CO)/π(Cl)→π*(R)/π*(pytrz)	MLCT/LLCT	4.86	255.2	*0.1034*
	H–8→L	π(pytrz)/π(Cl)→π*(pytrz)	ILCT/LLCT			
$S_0 \rightarrow S_{29}$	H–3→L+2	π(Cl)/π(pytrz)→π*(pytrz)/π*(R)	LLCT/ILCT	4.92	252.1	*0.0380*
$S_0 \rightarrow S_{30}$	H–1→L+7	d(Re)+π(CO)/π(Cl)→p(Re)+π*(CO)/π*(pytrz)	MLCT/LLCT	4.95	250.7	*0.0457*
$S_0 \rightarrow S_{31}$	H–2→L+4	d(Re)+π(CO)→π*(R)/π*(pytrz)	MLCT/LLCT	5.08	243.9	*0.0411*
	H–6→L+1	π(R)→π*(pytrz)	ILCT			
$S_0 \rightarrow S_{33}$	H–5→L+2	π(Cl)/d(Re)+π(CO)→π*(pytrz)/π*(R)	LLCT/MLCT	5.20	238.7	*0.0556*
$S_0 \rightarrow S_{46}$	H–9→L	π(pytrz)→π*(pytrz)	ILCT	5.48	226.2	*0.0690*
$S_0 \rightarrow S_{55}$	H–7→L+2	π(Cl)/π(pytrz)→π*(pytrz)/π*(R)	LLCT/ILCT	5.78	214.6	*0.0304*
	H–3→L+4	π(Cl)/π(pytrz)→π*(R)/π*(pytrz)	LLCT/ILCT			
$S_0 \rightarrow S_{78}$	H–10→L	π(pytrz)→π*(pytrz)	ILCT	6.20	200.0	*0.0325*
	H–8→L+2	π(pytrz)/π(Cl)→π*(pytrz)/π*(R)	ILCT/LLCT			

MLCT: metal-to-ligand charge transfer; LMCT: ligand-to-metal charge transfer; LLCT: ligand-to-ligand charge transfer; ILCT: intraligand charge transfer. pytrz: pyridyl-triazolylidene; R= tolyl ring.

Table S22. The main electronic transitions for **Re-T-Tol** calculated with TDDFT method at the PBE1PBE/LANL2DZ level (in dichloromethane).

Electronic transition	Contribution	Assignment		E_{calc} /eV	λ_{calc} /nm	*f*	λ_{exp} /nm
$S_0 \rightarrow S_1$	H→L	d(Re)+π(CO)/π(Cl)→π*(pytrz)	MLCT/LLCT	3.19	389.2	*0.0071*	
$S_0 \rightarrow S_2$	H–1→L	d(Re)+π(CO)/π(Cl)→π*(pytrz)	MLCT/LLCT	3.39	366.2	*0.0747*	354
$S_0 \rightarrow S_9$	H–3→L	π(pytrz)/π(Cl)→π*(pytrz)	ILCT/LLCT	4.35	285.1	*0.1271*	290
$S_0 \rightarrow S_{21}$	H–2→L+4	d(Re)+π(CO)→p(Re)+π*(CO)/π*(pytrz)	MLCT/LLCT	5.06	244.9	*0.1992*	240
$S_0 \rightarrow S_{28}$	H–3→L+2	π(pytrz)/π(Cl)→π*(pytrz)/p(Re)+π*(CO)	ILCT/LLCT	5.37	231.1	*0.0446*	
	H–2→L+3	d(Re)+π(CO)→π*(R)	MLCT/LLCT				
$S_0 \rightarrow S_{48}$	H–7→L+2	π(Cl)/π(pytrz)→π*(pytrz)/p(Re)+π*(CO)	LLCT/ILCT	5.97	207.8	*0.0413*	
	H→L+18	d(Re)+π(CO)/π(Cl)→p(Re)+π*(CO)/π*(R)	MLCT/LLCT				
$S_0 \rightarrow S_{60}$	H–10→L	π(pytrz)→π*(pytrz)	ILCT	6.23	199.0	*0.0563*	
	H–7→L+2	π(Cl)/π(pytrz)→π*(pytrz)/p(Re)+π*(CO)	LLCT/ILCT				

MLCT: metal-to-ligand charge transfer; LMCT: ligand-to-metal charge transfer; LLCT: ligand-to-ligand charge transfer; ILCT: intraligand charge transfer. pytrz: pyridyl-triazolylidene; R= tolyl ring.

Table S23. The main electronic transitions for **Re-T-BOP** calculated with TDDFT method at the PBE1PBE/LANL2DZ level (in gas phase).

Electronic transition	Contribution	Assignment		E_{calc} /eV	λ_{calc} /nm	*f*
$S_0 \rightarrow S_1$	H→L	d(Re)+π(CO)/π(Cl)→π*(pytrz)	MLCT/LLCT	2.45	506.0	*0.0014*
$S_0 \rightarrow S_2$	H–1→L	d(Re)+π(CO)/π(Cl)→π*(pytrz)	MLCT/LLCT	2.64	469.1	*0.0327*
$S_0 \rightarrow S_8$	H–3→L	π(PBO)→π*(pytrz)	ILCT	3.60	344.8	*0.1891*
$S_0 \rightarrow S_{13}$	H–5→L	π(Cl)/d(Re)+π(CO)→π*(pytrz)	LLCT/MLCT	3.93	315.4	*0.0277*
$S_0 \rightarrow S_{15}$	H–3→L+1	π(PBO)→π*(PBO)/π*(pytrz)	ILCT	4.15	298.6	*0.7859*
$S_0 \rightarrow S_{17}$	H–2→L+3	d(Re)+π(CO)→π*(pytrz)/π*(PBO)	MLCT/LLCT	4.30	288.5	*0.0264*
$S_0 \rightarrow S_{20}$	H–6→L	π(PBO)→π*(pytrz)	ILCT	4.39	282.2	*0.0255*
	H–1→L+7	d(Re)+π(CO)/π(Cl)→p(Re)+π*(CO)/π*(PBO)	MLCT/LLCT			
$S_0 \rightarrow S_{23}$	H–8→L	π(Cl)/π(pytrz)→π*(pytrz)	LLCT/ILCT	4.55	272.8	*0.0265*
$S_0 \rightarrow S_{25}$	H–4→L+2	π(Cl)/π(pytrz)→π*(pytrz)/π*(PBO)	LLCT/ILCT	4.62	268.4	*0.1517*
$S_0 \rightarrow S_{31}$	H–6→L+1	π(PBO)→π*(PBO)/π*(pytrz)	ILCT	4.80	258.2	*0.0407*
$S_0 \rightarrow S_{33}$	H–5→L+2	π(Cl)/d(Re)+π(CO)→π*(pytrz)/π*(PBO)	LLCT/MLCT	4.89	253.5	*0.0523*
$S_0 \rightarrow S_{38}$	H–2→L+7	d(Re)+π(CO)→p(Re)+π*(CO)/π*(PBO)	MLCT/LLCT	4.94	250.9	*0.0347*
$S_0 \rightarrow S_{41}$	H–4→L+3	π(Cl)/π(pytrz)→π*(pytrz)/π*(PBO)	LLCT/ILCT	5.08	243.9	*0.0836*
$S_0 \rightarrow S_{55}$	H–3→L+4	π(PBO)→π*(PBO)	ILCT	5.42	228.7	*0.0271*
$S_0 \rightarrow S_{58}$	H–8→L+2	π(Cl)/π(pytrz)→π*(pytrz)/π*(PBO)	LLCT/ILCT	5.47	226.6	*0.0249*
$S_0 \rightarrow S_{69}$	H–6→L+3	π(PBO)→π*(pytrz)/π*(PBO)	ILCT	5.68	218.3	*0.0530*
$S_0 \rightarrow S_{71}$	H–6→L+3	π(PBO)→π*(pytrz)/π*(PBO)	ILCT	5.71	217.0	*0.0260*
	H–10→L+1	π(PBO)/π(pytrz)→π*(PBO)/π*(pytrz)	ILCT			
$S_0 \rightarrow S_{103}$	H–9→L+3	π(Cl)/π(pytrz)/π(PBO)→π*(pytrz)/π*(PBO)	LLCT/ILCT	6.19	200.1	*0.0298*
	H–12→L+1	π(pytrz)→π*(PBO)/π*(pytrz)	ILCT			

MLCT: metal-to-ligand charge transfer; LMCT: ligand-to-metal charge transfer; LLCT: ligand-to-ligand charge transfer; ILCT: intraligand charge transfer. pytrz: pyridyl-triazolylidene; PBO= phenylbenzoxazole.

Table S24. The main electronic transitions for **Re-T-BOP** calculated with TDDFT method at the PBE1PBE/LANL2DZ level (in dichloromethane).

Electronic transition	Contribution	Assignment		E_{calc} /eV	λ_{calc} /nm	*f*	λ_{exp} /nm
$S_0 \rightarrow S_1$	H→L	d(Re)+π(CO)/π(Cl)→ π*(pytrz)	MLCT/LLCT	3.19	389.3	*0.0095*	
$S_0 \rightarrow S_2$	H–1→L	d(Re)+π(CO)/π(Cl)→ π*(pytrz)	MLCT/LLCT	3.40	364.8	*0.0864*	360
$S_0 \rightarrow S_4$	H→L+1	d(Re)+π(CO)/π(Cl)→ π*(PBO)	MLCT/LLCT	3.70	335.2	*0.0988*	
$S_0 \rightarrow S_6$	H–2→L	π(PBO)→π*(pytrz)	ILCT	4.00	309.9	*0.1966*	302
$S_0 \rightarrow S_8$	H–2→L+1	π(PBO)→π*(PBO)	ILCT	4.11	301.4	*0.1449*	
$S_0 \rightarrow S_9$	H→L+3	d(Re)+π(CO)/π(Cl)→π*(pytrz)	MLCT/LLCT	4.16	298.2	*0.5334*	
$S_0 \rightarrow S_{10}$	H–3→L+1	d(Re)+π(CO)/π(PBO)→π*(PBO)	MLCT/LLCT/ILCT	4.17	297.5	*0.4342*	
	H→L+3	d(Re)+π(CO)/π(Cl)→π*(pytrz)	MLCT/LLCT				
$S_0 \rightarrow S_{13}$	H–4→L	π(pytrz)/π(Cl)→π*(pytrz)	LLCT/ILCT	4.36	284.1	*0.0713*	
$S_0 \rightarrow S_{19}$	H–5→L	π(PBO)→π*(pytrz)	ILCT	4.69	264.3	*0.0604*	
$S_0 \rightarrow S_{29}$	H–4→L+2	π(pytrz)/π(Cl)→π*(pytrz)	ILCT/LLCT	5.12	242.4	*0.1542*	
$S_0 \rightarrow S_{34}$	H–4→L+3	π(pytrz)/π(Cl)→π*(pytrz)	ILCT/LLCT	5.33	232.8	*0.0419*	238
$S_0 \rightarrow S_{50}$	H–7→L+2	π(Cl)→π*(pytrz)	LLCT	5.66	219.2	*0.0573*	
$S_0 \rightarrow S_{60}$	H–2→L+7	π(PBO)→π*(PBO)/p(Re)+π*(CO)	ILCT/LLCT	5.84	212.2	*0.0364*	
$S_0 \rightarrow S_{72}$	H–10→L+1	π(Cl)→π*(PBO)	LLCT	6.10	203.3	*0.0340*	
$S_0 \rightarrow S_{80}$	H–3→L+8	d(Re)+π(CO)/π(PBO)→π*(PBO)/π*(pytrz)	MLCT/LLCT/ILCT	6.20	200.1	*0.0509*	

MLCT: metal-to-ligand charge transfer; LMCT: ligand-to-metal charge transfer; LLCT: ligand-to-ligand charge transfer; ILCT: intraligand charge transfer. pytrz: pyridyl-triazolylidene; PBO= phenylbenzoxazole.

Table S25. The frontier molecular orbital compositions (%) and energy levels for complex **Re-BOP** (in dichloromethane). Selected data published in Wang *et al*., *Dalton Trans.* 2018, **47**, 8087–8099.

Orbital		Energy (eV)	MO Contribution (%)					Main bond type
			Re	CO	Cl	P_1	P_2	
126	LUMO+5	–0.74	2	2	0	3	92	π*(PBO)
125	LUMO+4	–0.83	35	59	0	5	2	p(Re) + π*(CO)
124	LUMO+3	–1.35	1	3	0	71	25	π*(pyta) + π*(PBO)
123	LUMO+2	–1.55	0	1	0	78	21	π*(pyta) + π*(PBO)
122	LUMO+1	–2.16	1	2	0	25	73	π*(PBO) + π*(pyta)
121	LUMO	–2.23	3	4	0	88	5	π*(pyta)
HOMO–LUMO gap (E = 4.38 eV)								
120	HOMO	–6.61	48	22	18	4	7	d(Re) + π(CO) + p(Cl)
119	HOMO–1	–6.71	47	20	20	4	8	d(Re) + π(CO) + p(Cl)
118	HOMO–2	–6.92	9	3	8	5	75	π(PBO)
117	HOMO–3	–7.19	69	30	1	0	0	d(Re) + π(CO)
116	HOMO–4	–7.68	0	0	0	9	90	π(PBO)
115	HOMO–5	–7.72	0	0	2	60	38	π(pyta) + π(PBO)

pyta: pyridyl-triazole; PBO = phenylbenzoxazole.

Table 26. The main electronic transitions for complex **Re-BOP**, calculated with TDDFT method at the PBE1PBE/LANL2DZ level (in dichloromethane). From Wang *et al*., *Dalton Trans.* 2018, **47**, 8087–8099.

Electronic transition	Contribution	Assignment		E_{calc} /eV	λ_{calc} /nm	*f*	λ_{exp} /nm
$S_0 \rightarrow S_2$	H – 1 → LUMO	d(Re) + π(CO) + p(Cl) → π*(pyta)	MLCT/LLCT	3.57	347.4	*0.0801*	
$S_0 \rightarrow S_3$	HOMO → L + 1	d(Re) + π(CO) + p(Cl) → π*(PBO) + π*(pyta)	MLCT/LLCT	3.82	324.4	*0.5028*	
$S_0 \rightarrow S_5$	H – 1 → L + 1	d(Re) + π(CO) + p(Cl) → π*(PBO) + π*(pyta)	MLCT/LLCT	3.92	316.4	*0.3102*	
$S_0 \rightarrow S_6$	H – 2 → L + 1	π(PBO) → π*(PBO) + π*(pyta)	ILCT/IL	4.08	304.1	*0.6416*	303
	H – 2 → LUMO	π(PBO) → π*(pyta)	ILCT				
$S_0 \rightarrow S_7$	H – 2 → LUMO	π(PBO) → π*(pyta)	ILCT	4.17	297.5	*0.0478*	
	H – 2 → L + 1	π(PBO) → π*(PBO) + π*(pyta)	ILCT/IL				
$S_0 \rightarrow S_8$	HOMO → L + 2	d(Re) + π(CO) + p(Cl) → π*(pyta) + π*(PBO)	MLCT/LLCT	4.27	290.3	*0.0177*	289
$S_0 \rightarrow S_{17}$	H – 5 → LUMO	π(pyta) + π(PBO) → π*(pyta)	ILCT/IL	4.71	263.2	*0.1093*	
$S_0 \rightarrow S_{18}$	H – 5 → L + 1	π(pyta) + π(PBO) → π*(PBO) + π*(pyta)	ILCT/IL	4.72	262.5	*0.0882*	
	H – 2 → L + 2	π(PBO) → π*(pyta) + π*(PBO)	ILCT/IL				
$S_0 \rightarrow S_{27}$	H – 2 → L + 3	π(PBO) → π*(pyta) + π*(PBO)	ILCT/IL	5.05	245.6	*0.0954*	
$S_0 \rightarrow S_{28}$	H – 3 → L + 4	d(Re) + π(CO) → p(Re) + π*(CO)	MLCT/ILCT	5.12	242.2	*0.1173*	
$S_0 \rightarrow S_{34}$	H – 4 → L + 2	π(PBO) → π*(pyta) + π*(PBO)	ILCT/IL	5.43	228.5	*0.1500*	229
	HOMO → L + 5	d(Re) + π(CO) + p(Cl) → π*(PBO)	MLCT/LLCT				
$S_0 \rightarrow S_{36}$	H – 5 → L + 2	π(pyta) + π(PBO) → π*(pyta) + π*(PBO)	ILCT/IL	5.47	226.6	*0.0761*	

MLCT: metal-to-ligand charge transfer; LMCT: ligand-to-metal charge transfer; LLCT: ligand-to-ligand charge transfer; ILCT: intraligand charge transfer. pyta: pyridyl-triazole; PBO = phenylbenzoxazole.

Table S27. Phosphorescence emission energies of **Re-Tol**, **Re-T-Tol** and **Re-T-BOP** calculated with DFT and TDDFT methods at the PBE1PBE/LANL2DZ level, in comparison with the experimental values. ΔE_{T1}–S_0 is the energy difference between the ground singlet and triplet states.

Complex	DFT					TDDFT					
	ΔE_{T1}–S_0				Character	Major contribution	Character	gas phase		DCM	
	gas phase		DCM								
	eV	nm	eV	nm				eV	nm	eV	nm
Re-Tol	2.05	604.8	2.39	518.8	MLCT	H→L	MLCT/LLCT	1.77	702.4	2.26	549.5
Re-T-Tol	1.60	774.9	2.05	604.8	MLCT	H→L	MLCT/LLCT	1.36	914.7	1.89	655.2
Re-T-BOP	1.62	765.3	2.00	619.9	MLCT	H→L	MLCT/LLCT	1.38	900.8	1.85	669.0

Table S28. Natural populations of the $5d_{xy}$, $5d_{xz}$, $5d_{yz}$, $5d_{x^2-y^2}$ and $5d_{z^2}$ orbitals of the central atom in **Re-Tol**, **Re-T-Tol** and **Re-T-BOP**.

Orbital	Complex					
	Re-Tol		**Re-T-Tol**		**Re-T-BOP**	
	Gas phase	DCM	Gas phase	DCM	Gas phase	DCM
$5d_{xy}$	1.208	1.478	1.289	1.108	1.346	1.134
$5d_{xz}$	1.397	1.539	1.287	1.548	1.444	1.531
$5d_{yz}$	1.467	1.480	1.494	1.537	1.205	1.439
$5d_{x^2-y^2}$	1.416	1.074	1.406	1.510	1.371	1.504
$5d_{z^2}$	1.223	1.117	1.320	1.070	1.432	1.165

The population of 5*d* orbitals ($5d_{xy}$, $5d_{xz}$, $5d_{yz}$, $5d_{x^2-y^2}$ and $5d_{z^2}$) of the central atoms shows that in free Re (+1) state, the population of $5d_{xy}$, $5d_{xz}$ and $5d_{yz}$ orbitals are 2.0, 2.0 and 2.0 (e) and the other two ($5d_{x^2-y^2}$ and $5d_{z^2}$) orbitals remain vacant. On complex formation, some decrease in populations for the $5d_{xy}$, $5d_{xz}$ and $5d_{yz}$ orbital and some increase in the populations of $5d_{x^2-y^2}$ and $5d_{z^2}$ orbital can be observed in comparison to free Re (+1) state.

Table S29. Atomic charges from the Natural Population Analysis (NPA) for **Re-Tol**, **Re-BOP**, **Re-T-Tol** and **Re-T-BOP**.

Atom	Complex						
	Re-Tol		**Re-BOP** [a]	**Re-T-Tol**		**Re-T-BOP**	
	Gas phase	DCM	DCM	Gas phase	DCM	Gas phase	DCM
Re(1)	–1.03	–0.99	–1.00	–1.21	–1.17	–1.22	–1.17
C(1)	+0.76	+0.76	+0.74	+0.74	+0.75	+0.73	+0.75
C(2)	+0.78	+0.77	+0.78	+0.79	+0.78	+0.79	+0.78
C(3)	+0.73	+0.75	+0.76	+0.76	+0.76	+0.76	+0.76
N(1) / C(4)	–0.17	–0.19	–0.18	+0.14	+0.12	+0.13	+0.11
N(4)	–0.38	–0.40	–0.40	–0.36	–0.38	–0.36	–0.38
Cl(1)	–0.40	–0.46	–0.46	–0.40	–0.47	–0.39	–0.47
O(1)	–0.47	–0.48	–0.50	–0.49	–0.51	–0.50	–0.51
O(2)	–0.46	–0.48	–0.48	–0.47	–0.50	–0.47	–0.50
O(3)	–0.48	–0.50	–0.48	–0.47	–0.48	–0.47	–0.48

a From Wang *et al*., *Dalton Trans.* 2018, **47**, 8087–8099.

Table S30. Absolute electronegativity (χ), absolute hardness (η), electrophilicity index (ω), absolute softness (σ) and dipole moment (μ) of complexes **Re-Tol**, **Re-BOP, Re-T-Tol** and **Re-T-BOP**.

Parameters [a]	Complex							
	Re-Tol		**Re-BOP**[b]		**Re-T-Tol**		**Re-T-BOP**	
	gas phase	DCM	gas phase	DCM	gas phase	DCM	gas phase	DCM
Total Energy (Hartree)	–1192.5966	–1192.6241	–1551.4356	–1551.4654	–1231.8280	–1231.8577	–1590.6660	–1590.6993
E_{HOMO} (eV)	–6.05	–6.64	–6.02	–6.61	–5.87	–6.41	–5.86	–6.42
E_{LUMO} (eV)	–2.36	–2.21	–2.44	–2.23	–2.50	–2.21	–2.51	–2.31
Energy gap ΔE (eV)	3.69	4.43	3.58	4.38	3.37	4.12	3.35	4.11
Ionization Potential I	6.05	6.64	6.02	6.61	5.87	6.41	5.86	6.42
Electron Affinity A	2.36	2.21	2.21	2.23	2.50	2.21	2.51	2.31
Electronegativity χ (eV)	4.21	4.43	4.23	4.42	4.19	4.31	4.19	4.37
Hardness η (eV)	1.85	2.22	1.79	2.19	1.69	2.10	1.68	2.10
Electrophilicity ω	4.78	4.42	5.00	4.46	5.20	4.42	5.23	4.55
Softness σ (eV)	0.27	0.23	0.56	0.46	0.30	0.24	0.30	0.24
Dipole moment μ (D)	12.36	17.36	11.73	15.25	11.84	16.17	11.59	16.08

[a] The frontier molecular orbital descriptors such as ionization potential (IP = $-E_{HOMO}$), electron affinity (EA = $-E_{LUMO}$), hardness (η = (I – A)/2), electronegativity (χ = (I + A)/2), chemical potential ($\mu = -\chi$), softness ($\sigma = 1/\eta$), electrophilicity index ($\omega = \mu^2/2\eta$) calculated according to Koopmans theorem [T. Koopmans, *Physica*, 1933, **1**, 104–113], and dipole moment calculated using the equation: $\mu = 2.54 \times (x^2 + y^2 + z^2)^{1/2}$.

[b] From Wang *et al*., *Dalton Trans.* 2018, **47**, 8087–8099.

Occupied orbitals		Unoccupied orbitals	
HOMO / 94 (–6.05 eV)	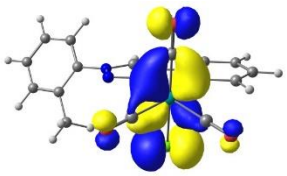	**LUMO / 95** (–2.36 eV)	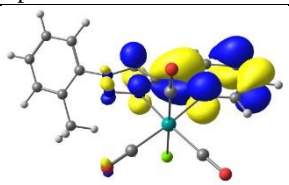
HOMO–1 / 93 (–6.16 eV)	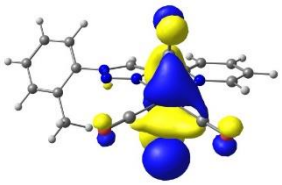	**LUMO+1 / 96** (–1.86 eV)	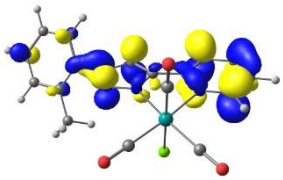
HOMO–2 / 92 (–6.73 eV)	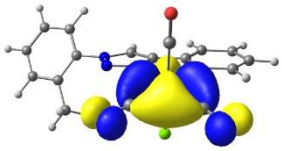	**LUMO+2 / 97** (–1.60 eV)	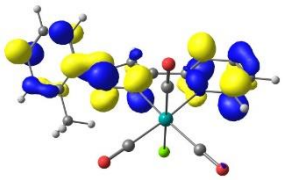
HOMO–3 / 91 (–7.43 eV)	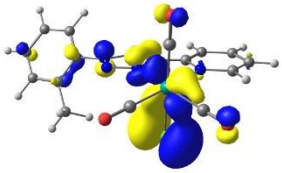	**LUMO+3 / 98** (–1.05 eV)	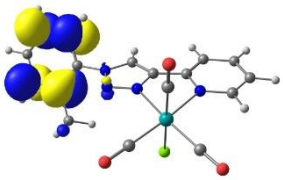
HOMO–4 / 90 (–7.51 eV)	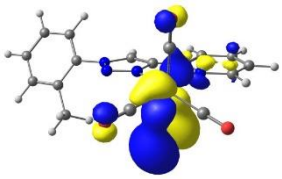	**LUMO+4 / 99** (–0.80 eV)	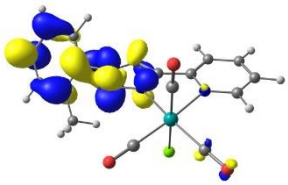
HOMO–5 / 89 (–7.85 eV)	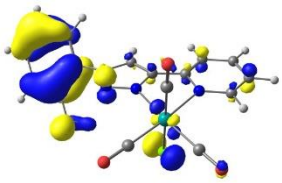	**LUMO+5 / 100** (–0.49 eV)	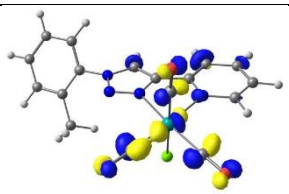

Figure S32. The isodensity plots of the frontier molecular orbitals of **Re-Tol** (in gas phase).

Occupied orbitals		Unoccupied orbitals	
HOMO / 94 (–6.64 eV)	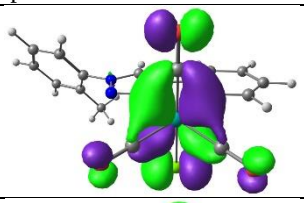	**LUMO / 95** (–2.21 eV)	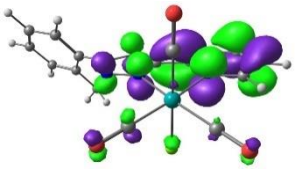
HOMO–1 / 93 (–6.74 eV)	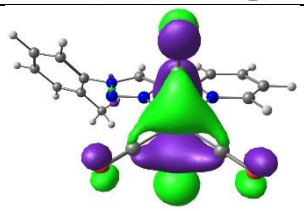	**LUMO+1 / 96** (–1.60 eV)	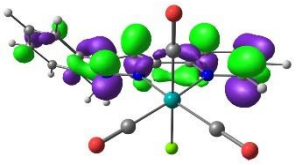
HOMO–2 / 92 (–7.19 eV)	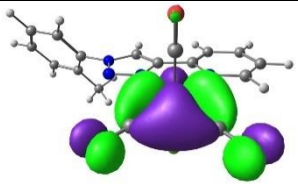	**LUMO+2 / 97** (–1.37 eV)	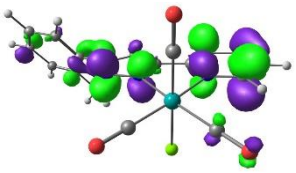
HOMO–3 / 91 (–7.56 eV)	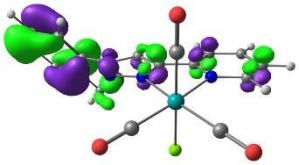	**LUMO+3 / 98** (–0.84 eV)	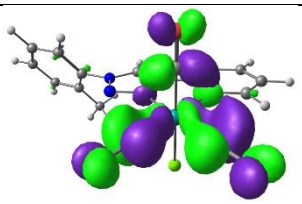
HOMO–4 / 90 (–7.69 eV)	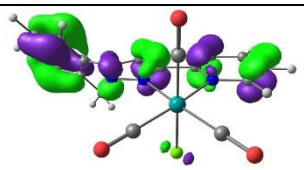	**LUMO+4 / 99** (–0.75 eV)	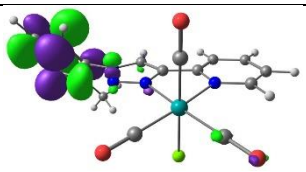
HOMO–5 / 89 (–7.90eV)	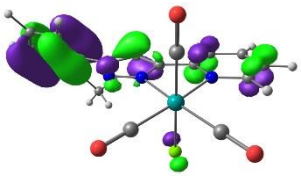	**LUMO+5 / 100** (–0.68 eV)	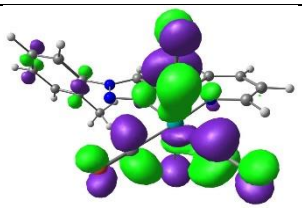

Figure S33. The isodensity plots of the frontier molecular orbitals of **Re-Tol** (in dichloromethane).

Occupied orbitals		Unoccupied orbitals	
HOMO / 98 (–5.87 eV)	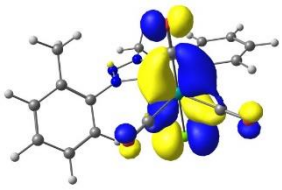	**LUMO / 99** (–2.50 eV)	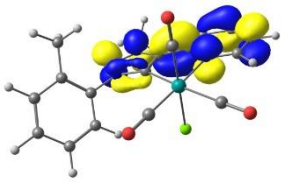
HOMO–1 / 97 (–5.99 eV)	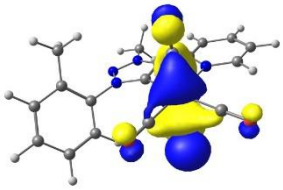	**LUMO+1 / 100** (–1.84 eV)	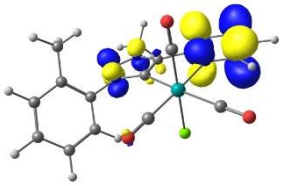
HOMO–2 / 96 (–6.45 eV)	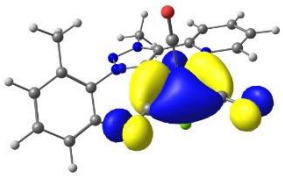	**LUMO+2 / 101** (–1.27 eV)	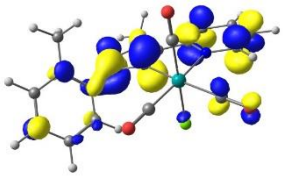
HOMO–3 / 95 (–7.07 eV)	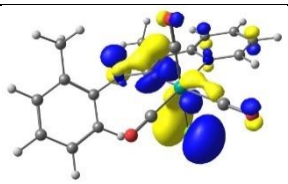	**LUMO+3 / 102** (–0.63 eV)	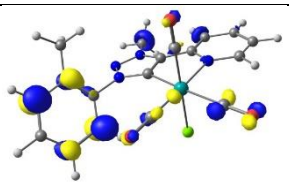
HOMO–4 / 94 (–7.36 eV)	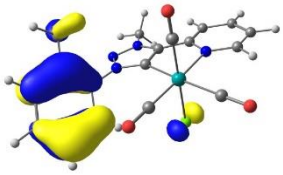	**LUMO+4 / 103** (–0.56 eV)	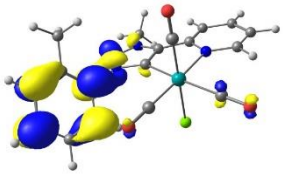
HOMO–5 / 93 (–7.42 eV)	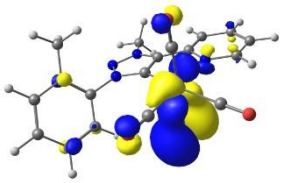	**LUMO+5 / 104** (–0.48 eV)	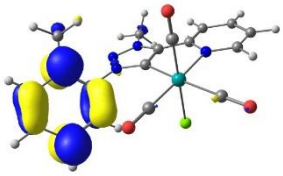

Figure S34. The isodensity plots of the frontier molecular orbitals of **Re-T-Tol** (in gas phase).

Occupied orbitals		Unoccupied orbitals	
HOMO / 98 (–6.41 eV)	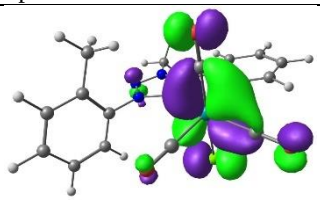	**LUMO / 99** (–2.29 eV)	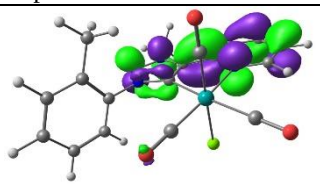
HOMO–1 / 97 (–6.56 eV)	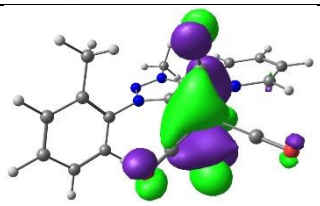	**LUMO+1 / 100** (–1.63 eV)	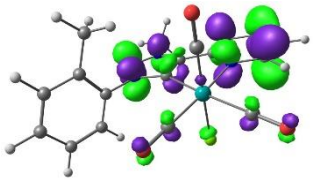
HOMO–2 / 96 (–6.91 eV)	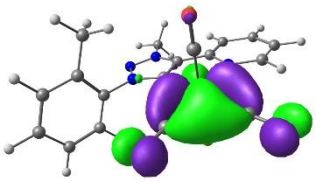	**LUMO+2 / 101** (–1.16 eV)	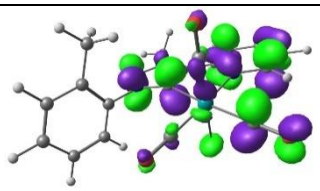
HOMO–3 / 95 (–7.45 eV)	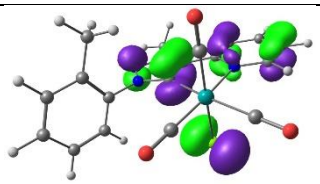	**LUMO+3 / 102** (–0.82 eV)	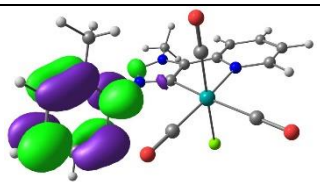
HOMO–4 / 94 (–7.47 eV)	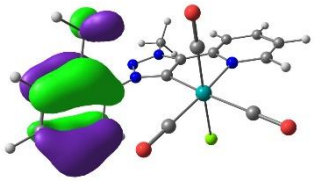	**LUMO+4 / 103** (–0.68 eV)	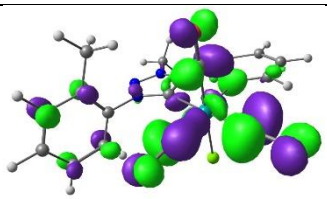
HOMO–5 / 93 (–7.79 eV)	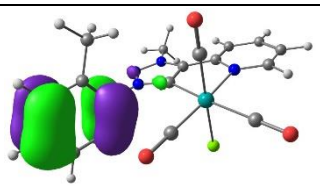	**LUMO+5 / 104** (–0.54 eV)	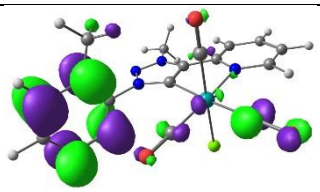

Figure S35. The isodensity plots of the frontier molecular orbitals of **Re-T-Tol** (in dichloromethane).

Occupied orbitals		Unoccupied orbitals	
HOMO / 124 (–5.86 eV)	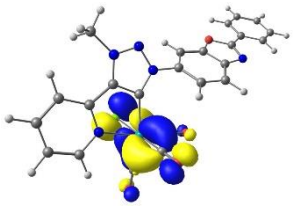	**LUMO / 125** (–2.51 eV)	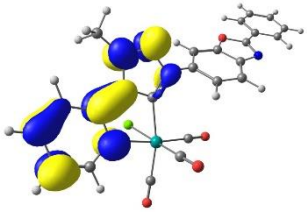
HOMO–1 / 123 (–6.00 eV)	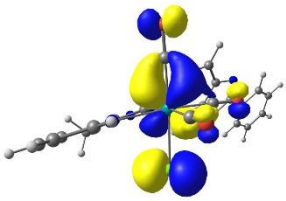	**LUMO+1 / 126** (–2.01 eV)	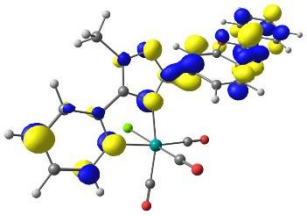
HOMO–2 / 122 (–6.47 eV)	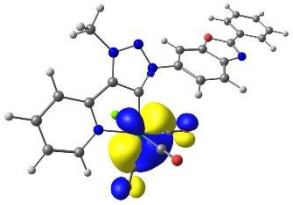	**LUMO+2 / 127** (–1.76 eV)	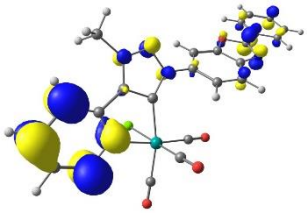
HOMO–3 / 121 (–6.77 eV)	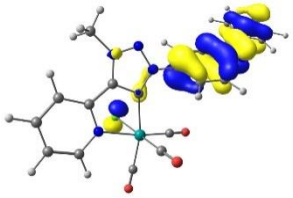	**LUMO+3 / 128** (–1.24 eV)	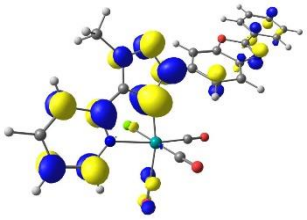
HOMO–4 / 120 (–7.05 eV)	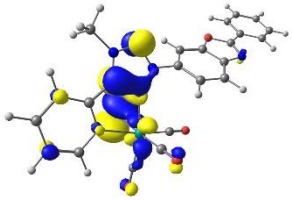	**LUMO+4 / 129** (–0.64 eV)	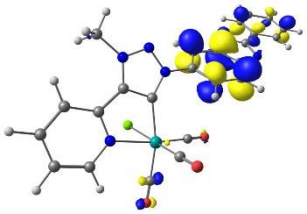
HOMO–5 / 119 (–7.33 eV)	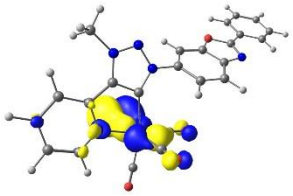	**LUMO+5 / 130** (–0.59 eV)	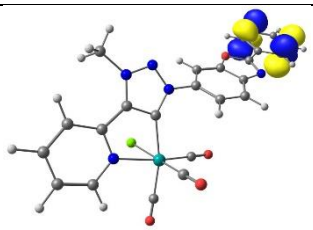

Figure S36. The isodensity plots of the frontier molecular orbitals of **Re-T-BOP** (in gas phase).

Occupied orbitals		Unoccupied orbitals	
HOMO / 124 (–6.42 eV)	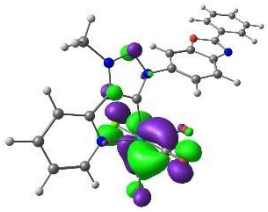	**LUMO / 125** (–2.31 eV)	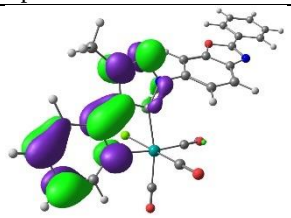
HOMO–1 / 123 (–6.58 eV)	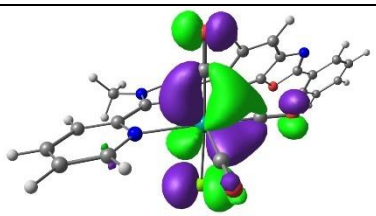	**LUMO+1 / 126** (–2.03 eV)	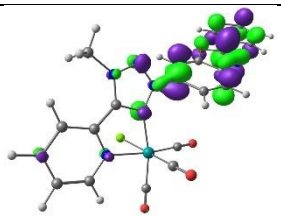
HOMO–2 / 122 (–6.86 eV)	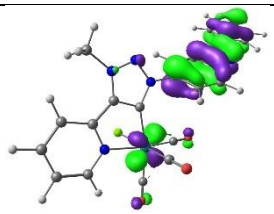	**LUMO+2 / 127** (–1.63 eV)	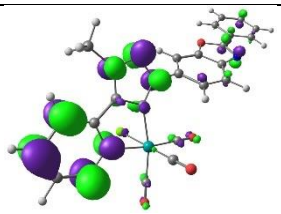
HOMO–3 / 121 (–6.94 eV)	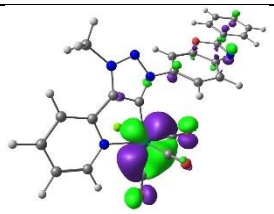	**LUMO+3 / 128** (–1.22 eV)	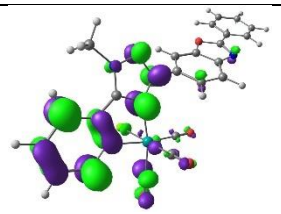
HOMO–4 / 120 (–7.46 eV)	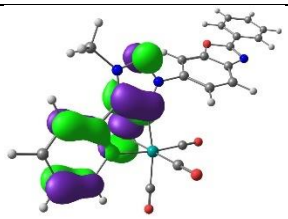	**LUMO+4 / 129** (–0.74 eV)	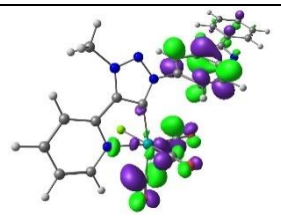
HOMO–5 / 119 (–7.64 eV)	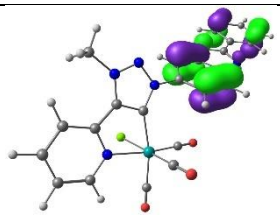	**LUMO+5 / 130** (–0.63 eV)	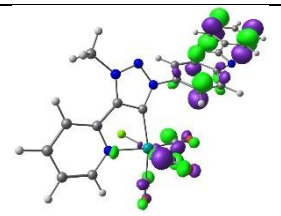

Figure S37. The isodensity plots of the frontier molecular orbitals of **Re-T-BOP** (in dichloromethane).

Occupied orbitals		Unoccupied orbitals	
HOMO (–6.61 eV)	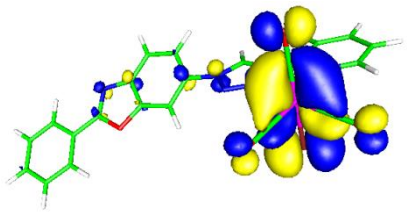	**LUMO** (–2.23 eV)	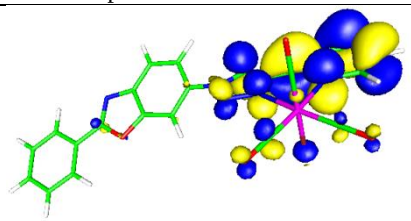
HOMO–1 (–6.71 eV)	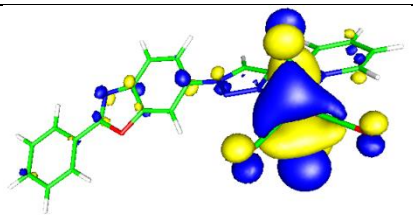	**LUMO+1** (–2.16 eV)	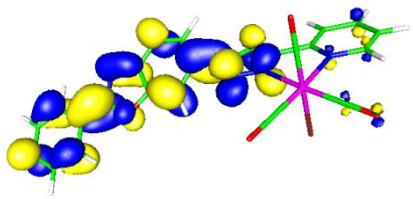
HOMO–2 (–6.92 eV)	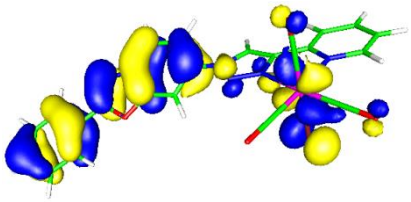	**LUMO+2** (–1.55 eV)	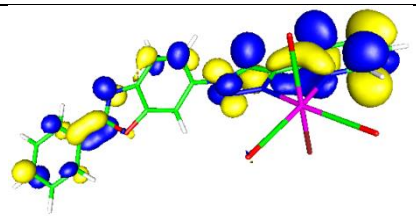
HOMO–3 (–7.19 eV)	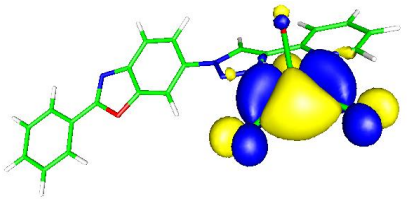	**LUMO+3** (–1.35 eV)	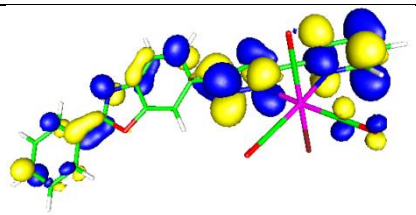
HOMO–4 (–7.68 eV)	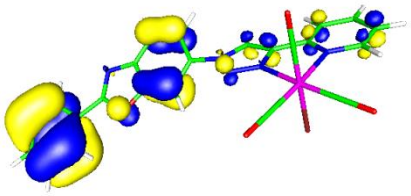	**LUMO+4** (–0.83 eV)	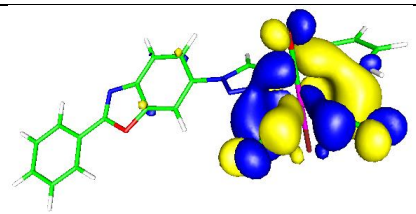
HOMO–5 (– 7.72 eV)	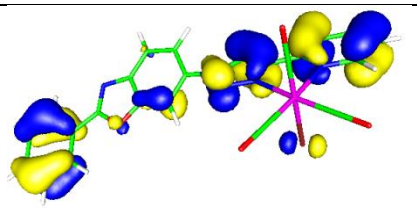	**LUMO+5** (–0.74 eV)	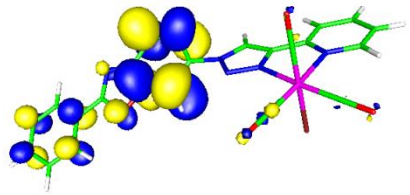

Figure S38. The isodensity plots of the frontier molecular orbitals of complex **Re-BOP** (in dichloromethane).

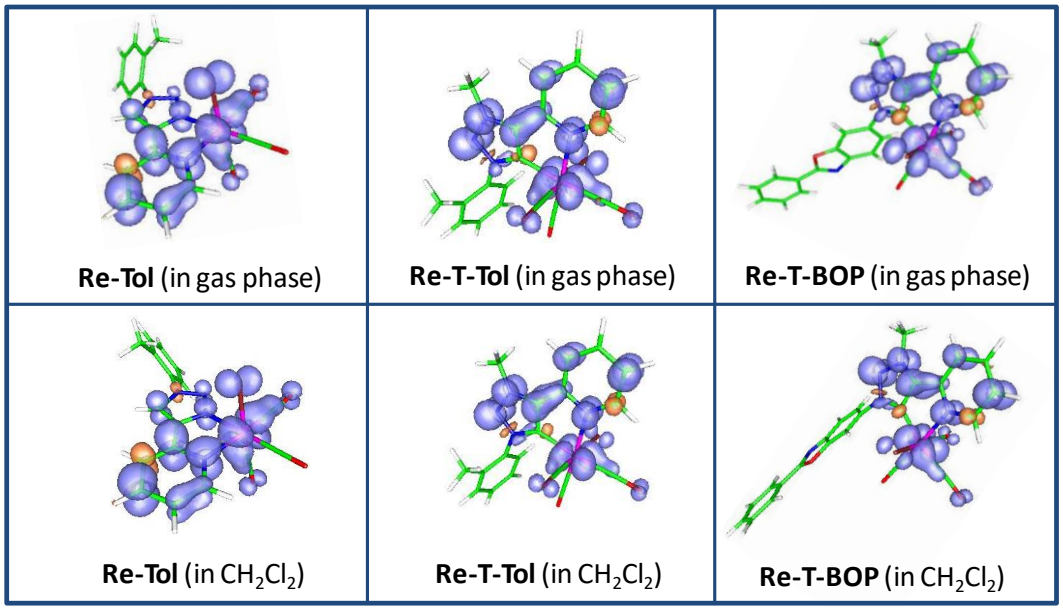

Figure S39. Spin density distribution for the lowest triplet state T_1 of **Re-Tol**, **Re-T-Tol** and **Re-T-BOP** in gas phase and in dichloromethane, calculated based on the optimized triplet state with DFT method at the PBE1PBE/LanL2DZ level.

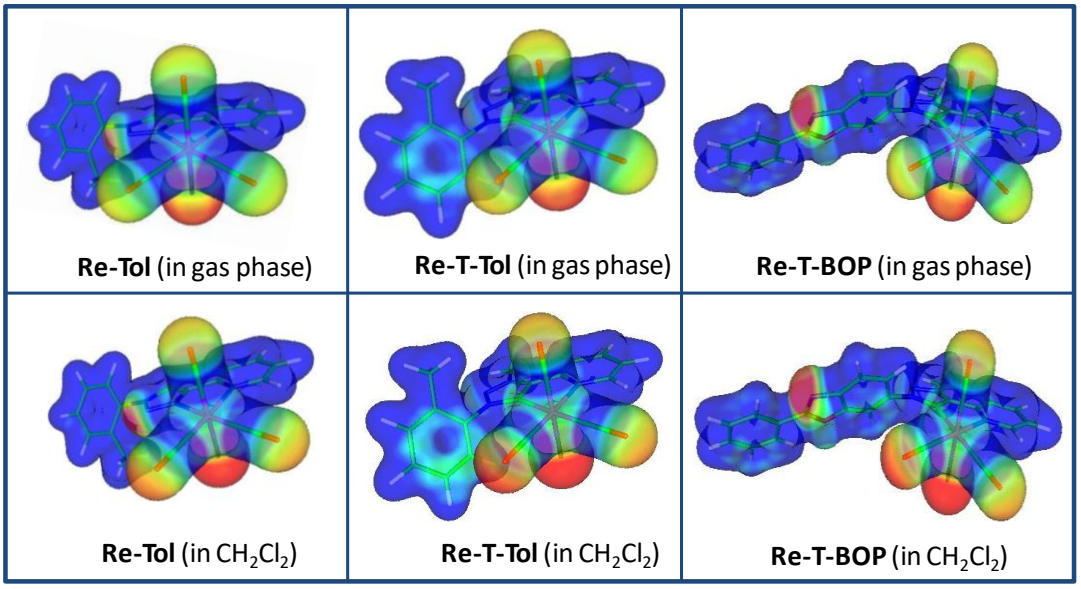

Figure S40. Molecular Electrostatic Potential (MEP) of **Re-Tol**, **Re-T-Tol** and **Re-T-BOP** on the ρ(r) = 0.02 au isodensity surface, calculated based on the optimized ground state geometry with DFT method at the PBE1PBE/LanL2DZ level. Mapping colours range from red –0.05 au to blue +0.05 au.

MEP surface plot helps to understand visually the relative polarity of the molecule, as shown in Figure 9. It is also useful to explain quantitatively hydrogen bonding, reactivity and structure–activity relationship of molecules including the biomolecules and drugs. MEP helps to find the sites for electrophilic and nucleophilic attacks as well as hydrogen bonding interactions. The MEP surfaces of **Re-Tol**, **Re-T-Tol** and **Re-T-BOP** studied by PBE1PBE/LanL2DZ were generated by mapping electrostatic potential onto the molecular electron density surface. In the MEP surface map, regions are represented by different colors which corresponds to different values of the electrostatic potential. The maximum negative region which preferred site for electrophilic attack is indicated as red color, whereas the maximum positive region which preferred site for nucleophilic attack is indicated as blue color. Potential increases in the order red < orange < yellow < green < cyan < blue, where red shows the strongest repulsion and blue shows the strongest attraction. Regions having the negative potential are over the electronegative atoms while the regions having the positive potential are over the electropositive atoms.

Negative electrostatic potential regions (red colour) of complexes **Re-Tol**, **Re-T-Tol** and **Re-T-BOP** are mainly localized around the chlorine Cl, the nitrogens N of the ligand as well as carbonyl oxygens. The positive electrostatic potential regions (blue colour) are around the hydrogen atoms.

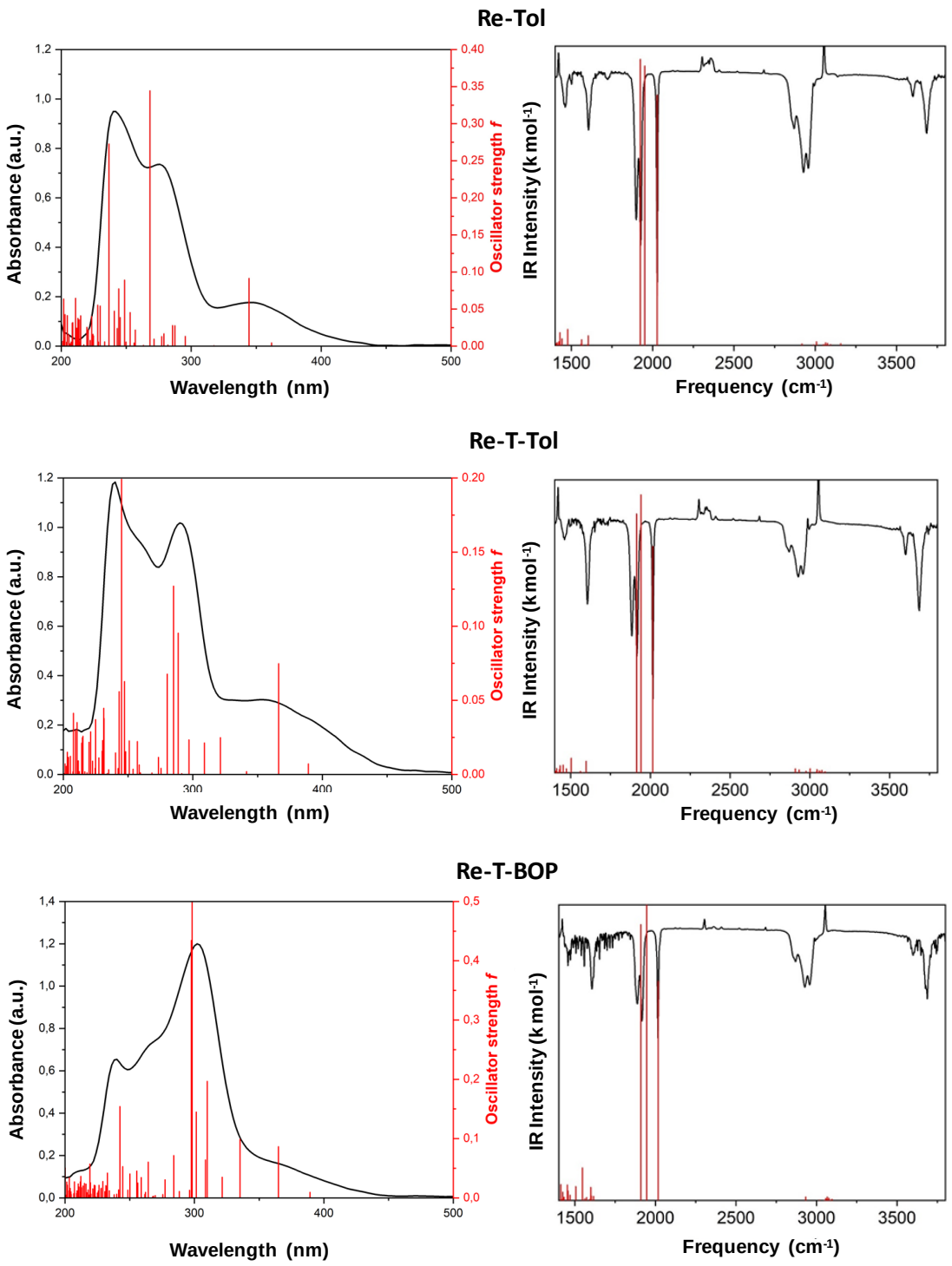

Figure S41. Left: The experimental (black) and simulated (red) UV-vis absorption spectra of **Re-Tol**, **Re-T-Tol**, and **Re-T-BOP (**from top to bottom) in DCM. Right: The experimental (black) FT-IR spectra recorded on powders (ATR) and simulated (red) FT-IR spectra of these complexes in gas phase.

Electrochemistry

Table S31. Experimental electrochemical data used, and calculated values of the energy gaps (*Eg*) for the indicated compounds

Compound	$E_{onset\ ox}$ (V)	$E_{onset\ red}$ (V)	E_{HOMO} (eV)	E_{LUMO} (eV)	E_g^{el} (eV)	E_{calc} * (eV)
Re-Tol	1.41	–1.54	–6.15	–3.20	2.95	3.03
Re-BOP	1.40	–1.45	–6.14	–3.29	2.85	3.01[a]
Re-T-Tol	1.22	–1.48	–5.96	–3.26	2.70	2.76
Re-T-BOP	1.22	–1.43	–5.96	–3.31	2.65	2.78

[a] From Wang *et al*., *Dalton Trans.* 2018, **47**, 8087–8099.
*Values obtained from theoretical study.
E_g^{el} = electrochemical energy gap; E_{calc}^* = calculated energy gap at the geometrically-optimized first excited singlet state S_1.

Evaluation of the energy gap values (E_g^{el}) for the Re complexes.

The onset oxidation and reduction potentials (*E*onset ox, *E*onset red) were measured by cyclic voltammetry in volt *versus* SCE. The CVs were carried out at a potential scan rate of 200 mV s^{-1} at room temperature.

The HOMO and LUMO energy levels (E_{HOMO} and E_{LUMO}) in electron volt (eV) were calculated according to the empirical equations (1) and (2): [1]
E_{HOMO} (eV) = -e (*E*onset ox (V vs. SCE) + 4.74 V) *Eq(1)*
E_{LUMO} (eV) = -e (*E*onset red (V vs. SCE) + 4.74 V) *Eq(2)*,
and the energy gap value was obtained as follows: $Eg^{el} = (E_{LUMO} - E_{HOMO})$

The differences observed for the estimation of the energy gaps using experimental methods or theoretical calculations are well known. See for example: R. Stowasser, R. Hoffmann, *J. Am. Chem. Soc.* **1999**, *121*, 3414-3420.
[1] a) Y. Zhou, J. W. Kim, R. Nandhakumar, M. J. Kim, E. Cho, Y. S. Kim, Y. H. Jang, C. Lee, S. Han, K. M. Kim, J.-J. Kim and J. Yoon, *Chem. Commun.* **2010**, *46*, 6512-6514 and references therein; b) G. V. Loukova, *Chem. Phys. Lett.* **2002**, *353*, 244–252.

Electrochemical selected curves

OSWV study was performed on a Pt working electrode in CH_2Cl_2 + 0.1 M [*n*Bu_4N][BF_4] at room temperature in the presence of ferrocene used as internal reference. Frequency 20 Hz, amplitude 20 mV, step potential 5 mV. Cyclic voltammograms of the indicated compounds were performed on a Pt working electrode in CH_2Cl_2 + 0.1 M [*n*Bu_4N][BF_4] at room temperature at a scan rate of 0.2 Vs^{-1} or at other mentioned scan rates.

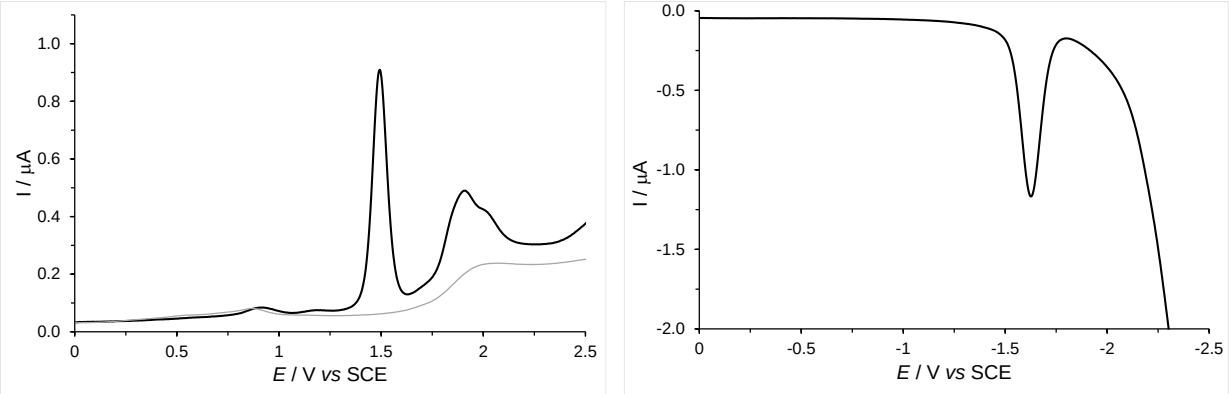

Figure S42. OSWVs: anodic (left) and cathodic (right) scans of complex **Re-Tol**.

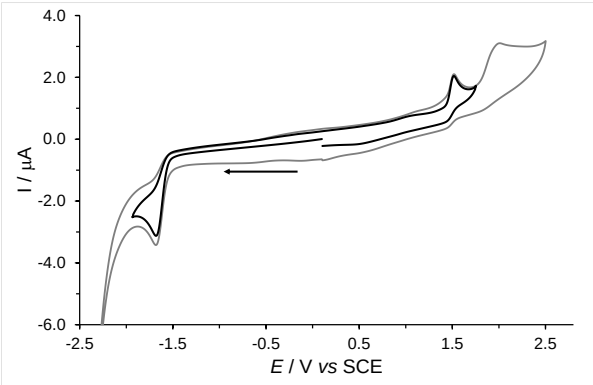

Figure S43. Cyclic voltammograms of complex **Re-Tol** (gray), and of its first oxidation and reduction processes (black) at 0.2 V/s.

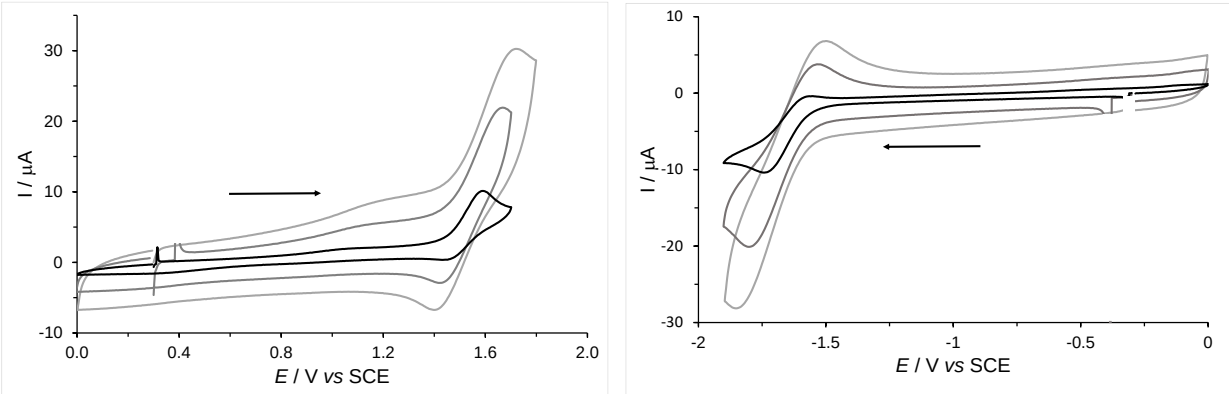

Figure S44. Cyclic voltammograms of the first oxidation process of complex **Re-Tol** at 10, 50, and100 V/s from bottom-black line to top-light gray line (left), and of its first reduction process at 10, 50, and 100 V/s from bottom-black line to top-gray line (right).

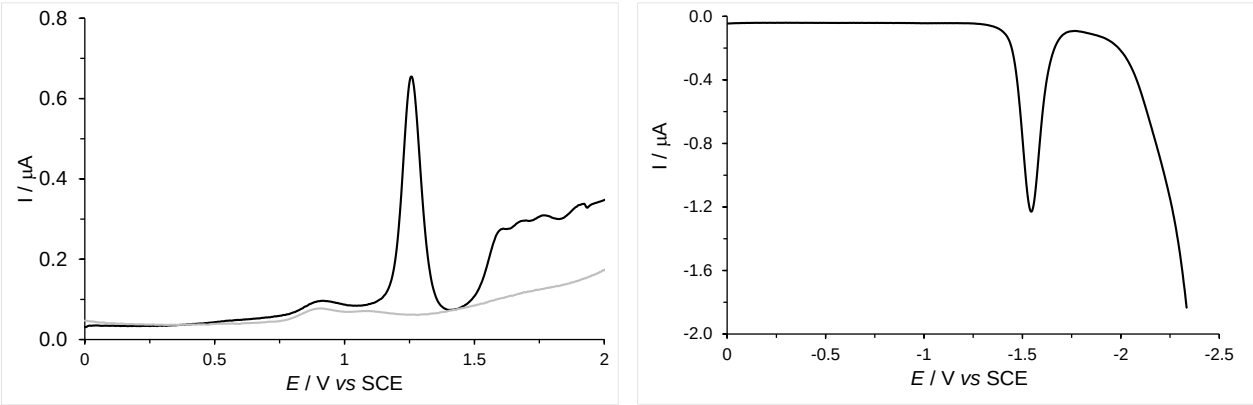

Figure S45. OSWVs: anodic (left) and cathodic (right) scans of complex **Re-T-Tol**.

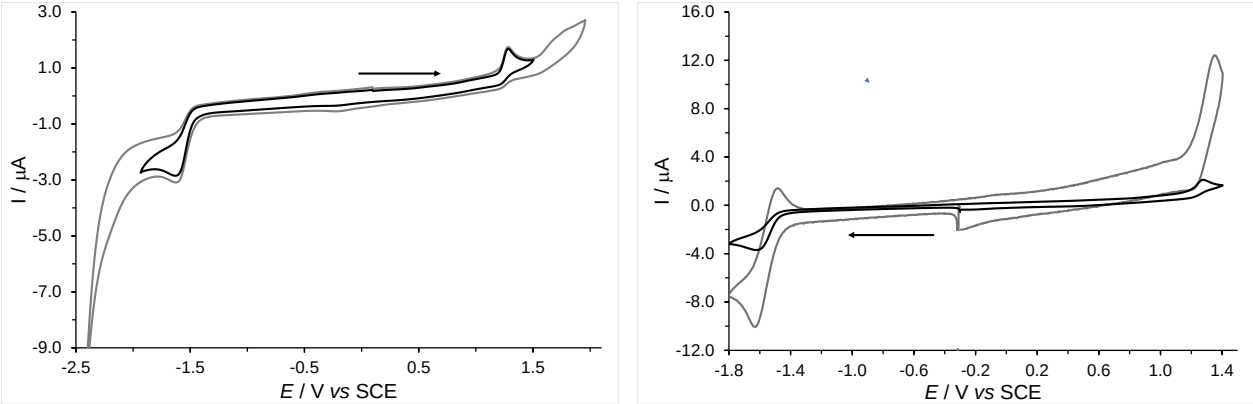

Figure S46. Cyclic voltammograms of complex **Re-T-Tol** (gray), and of its first oxidation and reduction processes (black) at 0.2 V/s (left); and cyclic voltammograms of its first oxidation process and reduction process at 0.2 (black) and 10 V/s (gray), right.

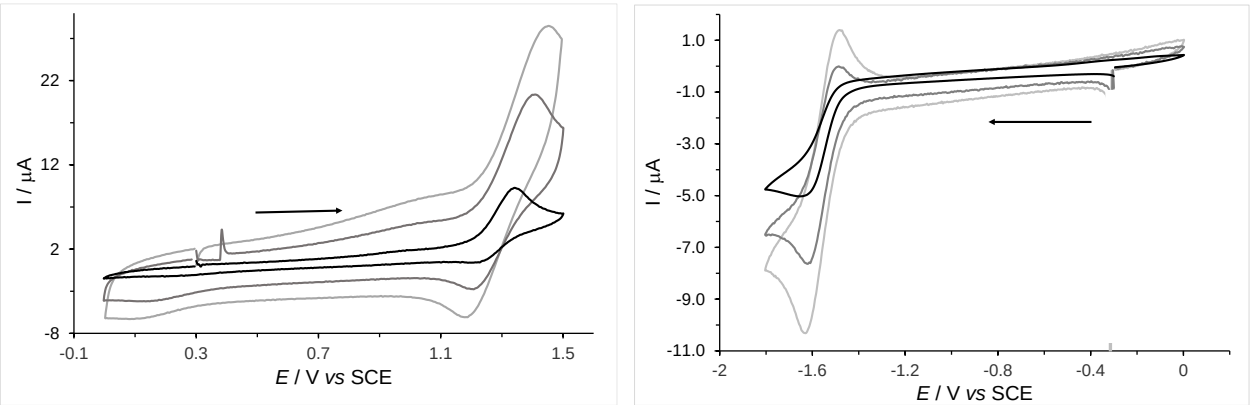

Figure S47. Cyclic voltammograms of the first oxidation process of complex **Re-T-Tol** at 10, 50, and 100 V/s from bottom-black line to top-light gray line (left), and of its first reduction process at 1, 5, and 10 V/s from bottom-black line to top-gray line (right).

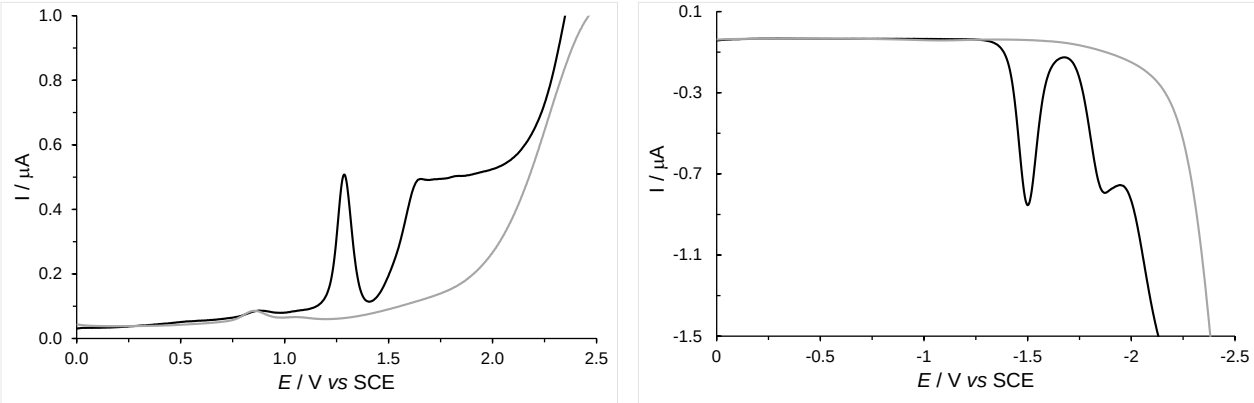

Figure S48. OSWVs: anodic (left) and cathodic (right) scans of complex **Re-T-BOP**.

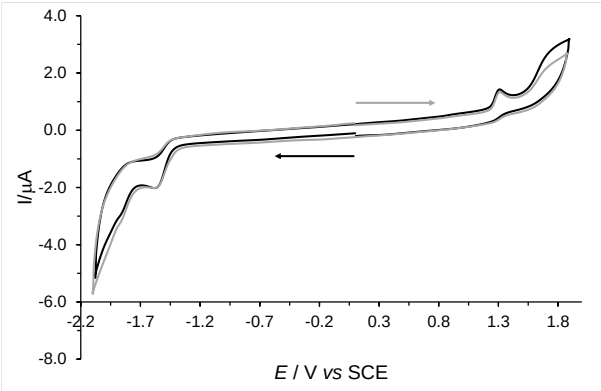

Figure S49. Cyclic voltammograms of complex **Re-T-BOP**.

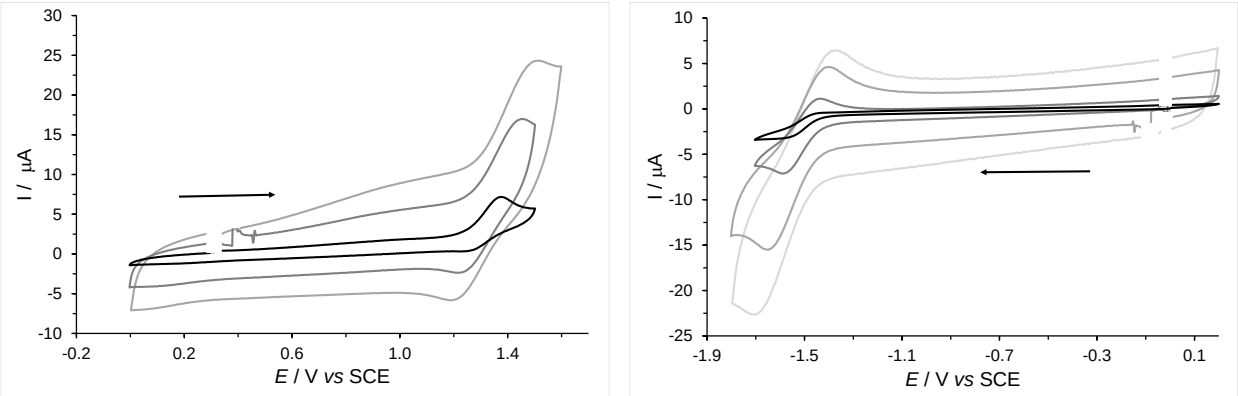

Figure S50. Cyclic voltammograms of the first oxidation process of complex **Re-T-BOP** at 10, 50, and 100 V/s from bottom-black line to top-light gray line (left), and of its first reduction process at 1, 10, 50, and 100 V/s from bottom-black line to top-gray line (right).

Spectroscopy

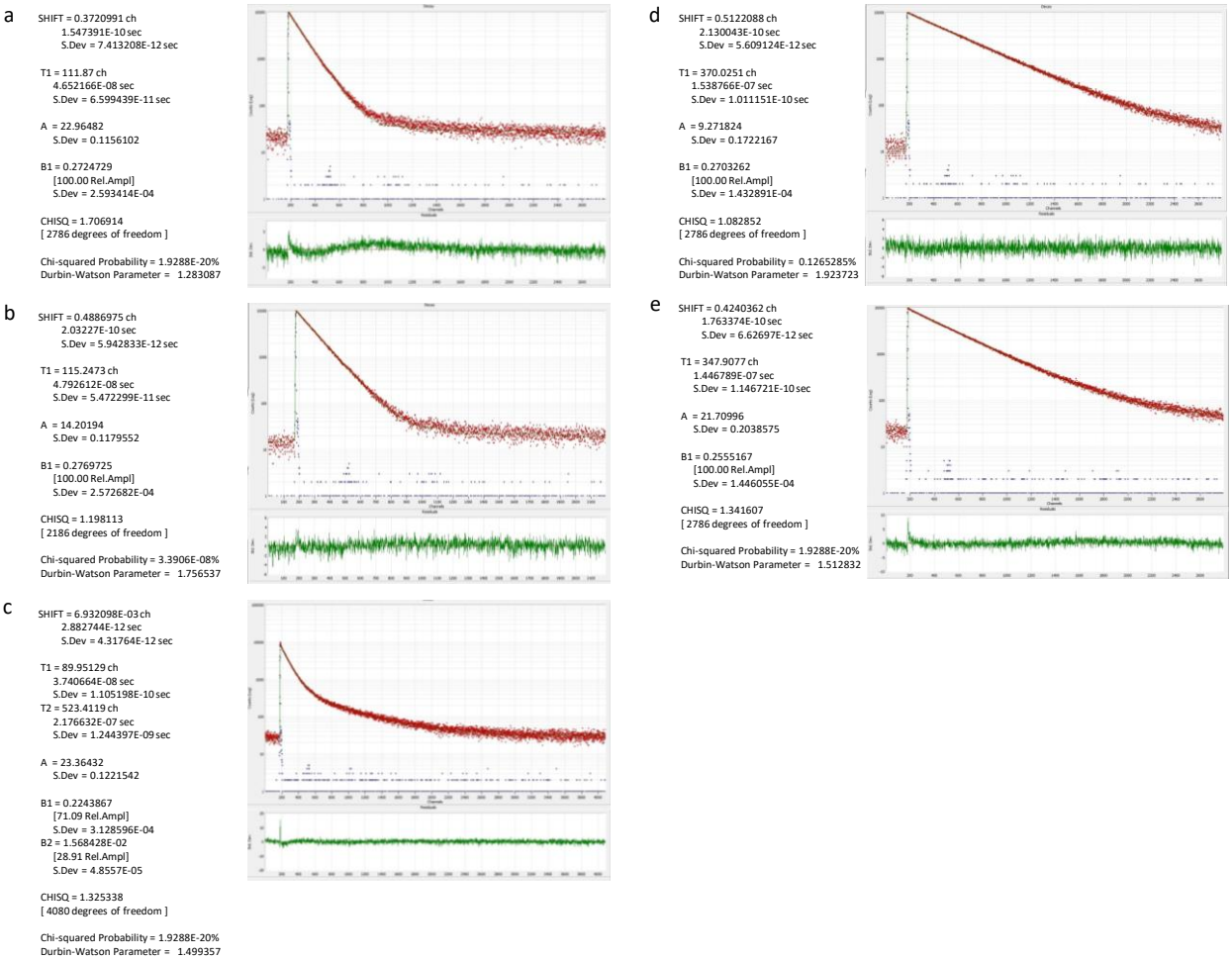

Figure S51. Emission decays of **Re-T-Phe** (a), **Re-T-Tol** (b), **Re-T-BOP** (c), **Re-Phe** (d), and **Re-Tol** (e) at ~ 1.2×10^{-5} M in dichloromethane solutions.

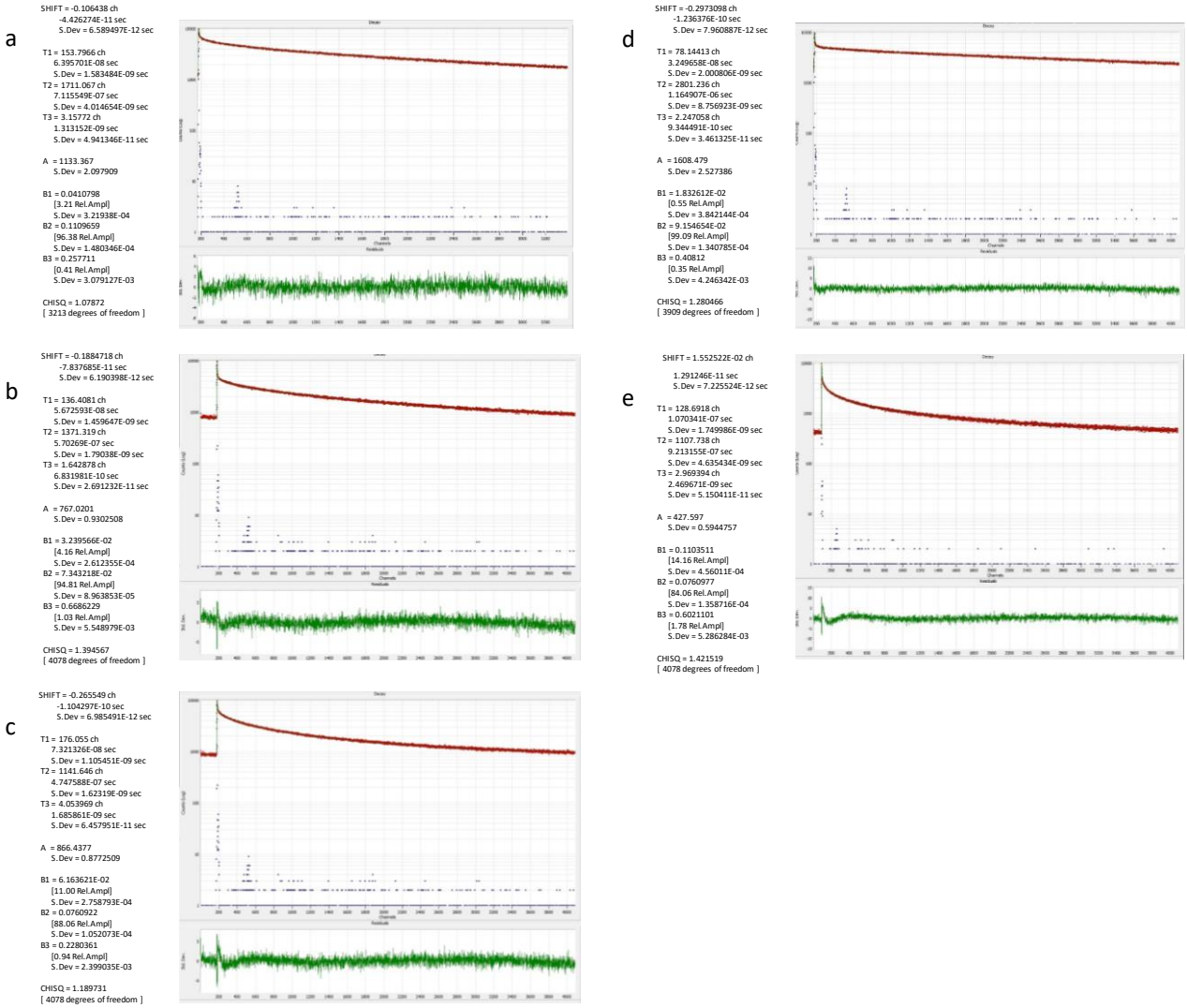

Figure S52. Photoluminescence decays of **Re-T-Phe** (a), **Re-T-Tol** (b), **Re-T-BOP** (c), **Re-Phe** (d), and **Re-Tol** (e) in the solid state (pristine microcrystalline powders, except for **Re-Tol** (ground powder)).

Table S32. Minimum inhibitory concentration (MIC) of the complexes towards antibiotic-susceptible (S) and multidrug-resistant (R) bacteria, with irradiation by UV light. Comparison with conventional antibiotics.

Compound	**MIC (μM) Irradiated samples**							
	S. aureus		***P. aeroginosa***		***E. coli***		***A. baumannii***	
	(S) ATCC 35923	(R) ATCC 43300	(S) ATCC 27853	(R) ATCC BAA-2108	(S) ATCC 25922	(R) ATCC BAA-196	(S) ATCC 19606	(R) ATCC BAA-1797
Re-T-Phe	32	32	>128	>128	>128	>128	>128	>128
Re-T-Tol	64	>128	>128	>128	>128	>128	>128	>128
Re-T-BOP	4	4	>128	>128	>128	>128	>128	>128
Re-Phe	>128	>128	>128	>128	>128	>128	>128	>128
Re-Tol	32	32	>128	>128	>128	>128	>128	>128
Re-BOP	8	>128	>128	>128	>128	>128	>128	>128
Re-[*1,2,4*]-Phe	>128	>128	>128	>128	>128	>128	>128	>128
Re-[*1,2,4*]-BOP	>128	>128	>128	>128	>128	>128	>128	>128
Gentamicin sulfate	1	128	0.5	8	0.125	>128	0.5	>128
Ampicillin	0.25	32	>128	>128	16	>128	>128	>128

Table S33. Cartesian coordinates of **Re-Tol** in S_0 (in gas phase).

6	12.895328000	11.568135000	10.472812000
6	11.343046000	12.790025000	8.625608000
6	13.871585000	12.023899000	7.971038000
6	11.295760000	8.662028000	5.442009000
1	11.198344000	7.732482000	4.903664000
6	11.976854000	9.029869000	6.579022000
6	12.848847000	8.359783000	7.527251000
6	13.276388000	7.041120000	7.390141000
1	12.954696000	6.453376000	6.536723000
6	14.108573000	6.499037000	8.359788000
1	14.451593000	5.472277000	8.277871000
6	14.491150000	7.294359000	9.436315000
1	15.136308000	6.914869000	10.220960000
6	14.026907000	8.600872000	9.503128000
1	14.295358000	9.251596000	10.327685000
6	9.745299000	9.942339000	3.962451000
6	10.237141000	9.655911000	2.690780000
1	11.276518000	9.362965000	2.571726000
6	9.397696000	9.772716000	1.588813000
1	9.773543000	9.555255000	0.594023000
6	8.080406000	10.184871000	1.777262000
1	7.414634000	10.284901000	0.924993000
6	7.609805000	10.468921000	3.056418000
1	6.577862000	10.781908000	3.191357000
6	8.423579000	10.352634000	4.188666000
6	7.888464000	10.651993000	5.558730000
1	8.227864000	9.927335000	6.305077000
1	6.796030000	10.646986000	5.546398000
1	8.222437000	11.634620000	5.906425000
17	10.356531000	9.869514000	9.501862000
7	11.674001000	10.338557000	6.809124000
7	10.870670000	10.796186000	5.903854000
7	10.631525000	9.782664000	5.070726000
7	13.224989000	9.133368000	8.571707000
8	13.239650000	11.790026000	11.555915000
8	10.727148000	13.765829000	8.571774000
8	14.810281000	12.549279000	7.530048000
75	12.338723000	11.152442000	8.689074000

Table S34. Cartesian coordinates of **Re-Tol** in T_1 (in gas phase).

6	12.860462000	11.534788000	10.505170000
6	11.397814000	12.843258000	8.488171000
6	13.905994000	11.860078000	7.980879000
6	11.297612000	8.655711000	5.425523000
1	11.254327000	7.756325000	4.833414000
6	11.957756000	8.992916000	6.601875000
6	12.835807000	8.370333000	7.525862000
6	13.321313000	7.060672000	7.427546000
1	13.006609000	6.450607000	6.584982000
6	14.186256000	6.557318000	8.373838000
1	14.567090000	5.544776000	8.298351000
6	14.577624000	7.411351000	9.458628000
1	15.265031000	7.067954000	10.223321000
6	14.070304000	8.674064000	9.533955000
1	14.343059000	9.333839000	10.350670000
6	9.720051000	9.935350000	3.978980000
6	10.265134000	9.730607000	2.713212000
1	11.319338000	9.485733000	2.620074000
6	9.459184000	9.862043000	1.587893000
1	9.878550000	9.707266000	0.598671000
6	8.118496000	10.205455000	1.745881000
1	7.478041000	10.314884000	0.875498000
6	7.592235000	10.405714000	3.019276000
1	6.542189000	10.662930000	3.131558000
6	8.372723000	10.271662000	4.172575000
6	7.776396000	10.473712000	5.535252000
1	8.122407000	9.720285000	6.249248000
1	6.686124000	10.423514000	5.481950000
1	8.056182000	11.447211000	5.949356000
17	10.168674000	10.280535000	9.597724000
7	11.569391000	10.282143000	6.879343000
7	10.744144000	10.744499000	5.979834000
7	10.577570000	9.764211000	5.106928000
7	13.185166000	9.194917000	8.625603000
8	13.202866000	11.794136000	11.575124000
8	10.890395000	13.858392000	8.320964000
8	14.865364000	12.337789000	7.562089000
75	12.277852000	11.077970000	8.721998000

Table S35. Cartesian coordinates of **Re-Tol** in S_0 (in dichloromethane).

6	13.618023000	12.009640000	10.070423000
6	12.122261000	13.209652000	8.176046000
6	14.295154000	11.768919000	7.460093000
6	10.988294000	8.752435000	5.695705000
1	10.763264000	7.795208000	5.252435000
6	11.755014000	9.130477000	6.774360000
6	12.557832000	8.439089000	7.768206000
6	12.711805000	7.056313000	7.811690000
1	12.212095000	6.431714000	7.079491000
6	13.509607000	6.500587000	8.803686000
1	13.644523000	5.425256000	8.859335000
6	14.129810000	7.344577000	9.720494000
1	14.761413000	6.957167000	10.511834000
6	13.928966000	8.714025000	9.614278000
1	14.394199000	9.401660000	10.310793000
6	9.686149000	10.113308000	4.045486000
6	10.213391000	10.852912000	2.989042000
1	11.223297000	11.244121000	3.062171000
6	9.435912000	11.073143000	1.857635000
1	9.836419000	11.647995000	1.028705000
6	8.146265000	10.546435000	1.800262000
1	7.530290000	10.710800000	0.921030000
6	7.636847000	9.816125000	2.871075000
1	6.624042000	9.425365000	2.821977000
6	8.389273000	9.583334000	4.028127000
6	7.808877000	8.815437000	5.181458000
1	8.141607000	7.771234000	5.179983000
1	6.718518000	8.808798000	5.117980000
1	8.091183000	9.250234000	6.144774000
17	10.644340000	10.817761000	9.761214000
7	11.695523000	10.488504000	6.838527000
7	10.950368000	10.967636000	5.891289000
7	10.517644000	9.916471000	5.194056000
7	13.160909000	9.260750000	8.660643000
8	14.149164000	12.357900000	11.040393000
8	11.736773000	14.284521000	7.980718000
8	15.254200000	11.982975000	6.837709000
75	12.732280000	11.422470000	8.478095000

Table S36. Cartesian coordinates of **Re-Tol** in S_1 (in dichloromethane).

6	13.651215000	12.102651000	10.018805000
6	12.114538000	13.216684000	8.175918000
6	14.273961000	11.549407000	7.375477000
6	10.981647000	8.757137000	5.680613000
1	10.775087000	7.818477000	5.193019000
6	11.746107000	9.099786000	6.792597000
6	12.538229000	8.430808000	7.756578000
6	12.760615000	7.040656000	7.807000000
1	12.301467000	6.409179000	7.051656000
6	13.544491000	6.497086000	8.795764000
1	13.718808000	5.427325000	8.839248000
6	14.123893000	7.371448000	9.765284000
1	14.745169000	6.993238000	10.568847000
6	13.881797000	8.718920000	9.674917000
1	14.307731000	9.403928000	10.401179000
6	9.670809000	10.137049000	4.066225000
6	10.190479000	10.920412000	3.037711000
1	11.186560000	11.339499000	3.139683000
6	9.426003000	11.147548000	1.898802000
1	9.822635000	11.756076000	1.092206000
6	8.154195000	10.584103000	1.804847000
1	7.547789000	10.753370000	0.919841000
6	7.650745000	9.810299000	2.847476000
1	6.651032000	9.390877000	2.771402000
6	8.391417000	9.568669000	4.010506000
6	7.813247000	8.753325000	5.131948000
1	8.161504000	7.714918000	5.096430000
1	6.723334000	8.734640000	5.059846000
1	8.084878000	9.157028000	6.111470000
17	10.747393000	10.954263000	9.885635000
7	11.640557000	10.473036000	6.891191000
7	10.882170000	10.972979000	5.935610000
7	10.492996000	9.932294000	5.219353000
7	13.113020000	9.283800000	8.711396000
8	14.221375000	12.557270000	10.908342000
8	11.785807000	14.303801000	7.989907000
8	15.217045000	11.637800000	6.727483000
75	12.675787000	11.375160000	8.487009000

Table S37. Cartesian coordinates of **Re-Tol** in T_1 (in dichloromethane).

6	13.521591000	11.918363000	10.146552000
6	12.160233000	13.201678000	8.064156000
6	14.347095000	11.627197000	7.549222000
6	10.982596000	8.740804000	5.666268000
1	10.778062000	7.799211000	5.182941000
6	11.748451000	9.091797000	6.770798000
6	12.541772000	8.429341000	7.746158000
6	12.724578000	7.047466000	7.840493000
1	12.213225000	6.404975000	7.129130000
6	13.547085000	6.510390000	8.810791000
1	13.695590000	5.438975000	8.886022000
6	14.217181000	7.412337000	9.707997000
1	14.891253000	7.041908000	10.472423000
6	14.003564000	8.752491000	9.602141000
1	14.495564000	9.449349000	10.271586000
6	9.664345000	10.124491000	4.055235000
6	10.186078000	10.887955000	3.013073000
1	11.191234000	11.288985000	3.097907000
6	9.411470000	11.118603000	1.881441000
1	9.809110000	11.712018000	1.064171000
6	8.128711000	10.577339000	1.808294000
1	7.514937000	10.748951000	0.928844000
6	7.623952000	9.822088000	2.864059000
1	6.616500000	9.419116000	2.803234000
6	8.374375000	9.578465000	4.020293000
6	7.798527000	8.782967000	5.157049000
1	8.146847000	7.744146000	5.139403000
1	6.708484000	8.763191000	5.088546000
1	8.072952000	9.204445000	6.128447000
17	10.517655000	11.131406000	9.662361000
7	11.654172000	10.457112000	6.865298000
7	10.897753000	10.954182000	5.921485000
7	10.493986000	9.915135000	5.202129000
7	13.153178000	9.317098000	8.676821000
8	14.013713000	12.266931000	11.130741000
8	11.854222000	14.269663000	7.778144000
8	15.336596000	11.810917000	6.993981000
75	12.678894000	11.333460000	8.513584000

Table S38. Cartesian coordinates of **Re-T-Tol** in S_0 (in gas phase).

75	8.774905000	3.287469000	6.249532000
17	10.934294000	2.184629000	5.566787000
8	6.286507000	4.808547000	7.191852000
8	7.485324000	2.891832000	3.491882000
8	7.629047000	0.551772000	7.166335000
7	10.280172000	5.898992000	4.905773000
7	11.207000000	6.784656000	5.253673000
7	11.467924000	6.507011000	6.506663000
7	9.872840000	3.672771000	8.161490000
6	7.225865000	4.221677000	6.832479000
6	7.977921000	3.045561000	4.528523000
6	8.046672000	1.570695000	6.811957000
6	9.918005000	5.037436000	5.895138000
6	12.480063000	7.300987000	7.176793000
1	12.853036000	8.027045000	6.455542000
1	13.297713000	6.654563000	7.503520000
1	12.042340000	7.821063000	8.031892000
6	10.725007000	5.458744000	6.952528000
6	10.714695000	4.739226000	8.209763000
6	11.449980000	5.039408000	9.356981000
1	12.108516000	5.898736000	9.382567000
6	11.330603000	4.220698000	10.473203000
1	11.897935000	4.437922000	11.373077000
6	10.478929000	3.124015000	10.415125000
1	10.357120000	2.452050000	11.257386000
6	9.771839000	2.891222000	9.241592000
1	9.098393000	2.046222000	9.154692000
6	9.852049000	5.876419000	3.535884000
6	9.118859000	6.949812000	3.018452000
6	8.748308000	6.860122000	1.673860000
1	8.170656000	7.670165000	1.235974000
6	9.088327000	5.755023000	0.896685000
1	8.776934000	5.714517000	-0.143206000
6	9.807525000	4.698981000	1.450472000
1	10.056975000	3.826615000	0.854976000
6	10.195220000	4.757059000	2.784795000
1	10.735734000	3.940928000	3.259707000
6	8.730381000	8.132652000	3.858560000
1	8.294544000	7.818606000	4.813060000
1	7.990655000	8.744188000	3.336562000
1	9.595214000	8.765686000	4.084214000

Table S39. Cartesian coordinates of **Re-T-Tol** in T_1 (in gas phase).

75	8.854317000	3.317334000	6.235429000
17	10.546760000	1.657663000	5.726218000
8	6.650238000	5.341994000	7.031812000
8	7.576518000	2.950941000	3.455107000
8	7.022022000	0.986453000	7.324348000
7	10.271168000	5.902035000	4.914229000
7	11.111042000	6.895519000	5.274490000
7	11.337737000	6.654090000	6.609470000
7	9.948402000	3.594392000	8.122363000
6	7.470894000	4.584937000	6.742115000
6	8.063882000	3.102589000	4.488964000
6	7.704321000	1.818385000	6.926856000
6	10.010265000	4.995889000	5.879387000
6	12.403200000	7.396196000	7.230037000
1	12.638616000	8.236860000	6.576450000
1	13.303600000	6.780936000	7.355555000
1	12.085740000	7.785936000	8.201211000
6	10.738388000	5.471412000	7.000305000
6	10.741609000	4.732926000	8.197761000
6	11.461583000	5.017443000	9.385422000
1	12.066500000	5.914135000	9.446375000
6	11.400917000	4.147183000	10.448738000
1	11.954615000	4.359847000	11.358445000
6	10.624920000	2.977555000	10.342399000
1	10.562391000	2.256368000	11.148627000
6	9.926266000	2.759145000	9.164139000
1	9.319386000	1.867629000	9.044384000
6	9.867811000	5.849211000	3.544895000
6	9.056218000	6.862908000	3.018519000
6	8.708193000	6.754549000	1.669163000
1	8.072157000	7.519844000	1.231367000
6	9.145091000	5.689219000	0.884778000
1	8.850459000	5.633701000	-0.159300000
6	9.947743000	4.694822000	1.437613000
1	10.284456000	3.856838000	0.835325000
6	10.314876000	4.777582000	2.776411000
1	10.935222000	4.014809000	3.238489000
6	8.568640000	8.007755000	3.858354000
1	8.156596000	7.657559000	4.810714000
1	7.787474000	8.562672000	3.332953000
1	9.383792000	8.698460000	4.096824000

Table S40. Cartesian coordinates of **Re-T-Tol** in S_0 (in dichloromethane).

75	8.755899000	3.376530000	6.241211000
17	10.792157000	1.930095000	5.748778000
8	6.405664000	5.197047000	6.960350000
8	7.606127000	2.985589000	3.423619000
8	7.224411000	0.858226000	7.221671000
7	10.476785000	5.812646000	4.827762000
7	11.443166000	6.658264000	5.166122000
7	11.684380000	6.395699000	6.424479000
7	9.825367000	3.774503000	8.168707000
6	7.300575000	4.501468000	6.686321000
6	8.040002000	3.132994000	4.490853000
6	7.795389000	1.798675000	6.858787000
6	10.069007000	4.995437000	5.832490000
6	12.717186000	7.166746000	7.098905000
1	13.122854000	7.870542000	6.374386000
1	13.506817000	6.497759000	7.444719000
1	12.279212000	7.711052000	7.937139000
6	10.884957000	5.397605000	6.886287000
6	10.777410000	4.747206000	8.179034000
6	11.518013000	5.033624000	9.324036000
1	12.272184000	5.809741000	9.315738000
6	11.278795000	4.307270000	10.485187000
1	11.847824000	4.517609000	11.385036000
6	10.305421000	3.315573000	10.472481000
1	10.082987000	2.723826000	11.353102000
6	9.606026000	3.084089000	9.294177000
1	8.840237000	2.318881000	9.245946000
6	9.992798000	5.844649000	3.475616000
6	8.939478000	6.707793000	3.152451000
6	8.502266000	6.691564000	1.824007000
1	7.685111000	7.346738000	1.534081000
6	9.090194000	5.857883000	0.874185000
1	8.725625000	5.869623000	-0.148909000
6	10.138928000	5.011792000	1.230333000
1	10.597992000	4.359927000	0.493787000
6	10.594470000	5.003996000	2.545476000
1	11.404292000	4.351362000	2.857022000
6	8.309730000	7.604531000	4.178083000
1	7.876358000	7.025434000	5.000375000
1	7.513837000	8.201837000	3.728364000
1	9.044090000	8.289897000	4.614548000

Table S41. Cartesian coordinates of **Re-T-Tol** in S_1 (in dichloromethane).

75	8.888163000	3.275707000	6.226599000
17	10.743200000	1.820798000	5.679127000
8	6.693447000	5.318310000	7.007223000
8	7.604389000	2.802672000	3.458049000
8	7.058458000	0.897371000	7.163551000
7	10.404838000	5.837594000	4.860198000
7	11.281852000	6.773473000	5.201617000
7	11.544782000	6.509709000	6.491581000
7	9.907537000	3.626965000	8.118115000
6	7.499279000	4.551050000	6.716897000
6	8.095485000	2.991665000	4.485295000
6	7.754123000	1.752297000	6.840393000
6	10.086664000	4.972231000	5.840961000
6	12.482696000	7.356781000	7.188562000
1	12.825181000	8.118664000	6.489262000
1	13.339511000	6.771453000	7.533592000
1	11.997434000	7.840121000	8.041076000
6	10.843312000	5.416574000	6.939684000
6	10.777053000	4.728866000	8.173463000
6	11.471611000	5.025880000	9.369587000
1	12.137598000	5.880760000	9.403130000
6	11.308587000	4.238033000	10.482381000
1	11.843290000	4.466220000	11.398705000
6	10.431271000	3.120227000	10.412964000
1	10.273653000	2.465589000	11.262014000
6	9.773209000	2.874379000	9.229854000
1	9.099254000	2.027628000	9.148196000
6	9.925821000	5.832787000	3.508847000
6	9.033022000	6.826927000	3.090141000
6	8.604475000	6.764178000	1.759838000
1	7.905276000	7.514723000	1.400433000
6	9.047026000	5.763449000	0.896485000
1	8.692214000	5.744138000	-0.129978000
6	9.934923000	4.787999000	1.346119000
1	10.279227000	4.003719000	0.679259000
6	10.378360000	4.823426000	2.664671000
1	11.066424000	4.075993000	3.048269000
6	8.552765000	7.908561000	4.013823000
1	8.262805000	7.505309000	4.989335000
1	7.688975000	8.421707000	3.585047000
1	9.336831000	8.651788000	4.192380000

Table S42. Cartesian coordinates of **Re-T-Tol** in T_1 (in dichloromethane).

75	8.843212000	3.348455000	6.235535000
17	10.574252000	1.649765000	5.741706000
8	6.641786000	5.358045000	7.041987000
8	7.581041000	3.017877000	3.447354000
8	7.017050000	0.976297000	7.250375000
7	10.339546000	5.852341000	4.881045000
7	11.215753000	6.820434000	5.228729000
7	11.452088000	6.585591000	6.560614000
7	9.918677000	3.628454000	8.131342000
6	7.465325000	4.607163000	6.742244000
6	8.063761000	3.152558000	4.489463000
6	7.696079000	1.828745000	6.893004000
6	10.044538000	4.973253000	5.857514000
6	12.471708000	7.371447000	7.209284000
1	12.727897000	8.193519000	6.540885000
1	13.371328000	6.776139000	7.402366000
1	12.094531000	7.788411000	8.146567000
6	10.801978000	5.442431000	6.976757000
6	10.769936000	4.731520000	8.184566000
6	11.499610000	5.013475000	9.369756000
1	12.153231000	5.876270000	9.407682000
6	11.380029000	4.183650000	10.459331000
1	11.938193000	4.392271000	11.366764000
6	10.531846000	3.060765000	10.383607000
1	10.413241000	2.376915000	11.215720000
6	9.831763000	2.838652000	9.204838000
1	9.168987000	1.984320000	9.117153000
6	9.906407000	5.823978000	3.517901000
6	9.012820000	6.800108000	3.057166000
6	8.635505000	6.723813000	1.712332000
1	7.937384000	7.460188000	1.322637000
6	9.127508000	5.726689000	0.871448000
1	8.812062000	5.696300000	-0.167546000
6	10.016322000	4.770578000	1.359269000
1	10.400846000	3.990423000	0.709667000
6	10.410039000	4.821724000	2.692994000
1	11.099997000	4.090764000	3.104122000
6	8.479660000	7.876322000	3.957521000
1	8.108942000	7.462400000	4.900802000
1	7.659848000	8.410822000	3.472411000
1	9.259298000	8.602850000	4.209825000

Table S43. Cartesian coordinates of **Re-T-BOP** in S_0 (in gas phase).

6	5.251086000	-0.745637000	16.927207000
6	3.576671000	-0.172089000	14.862907000
6	4.412179000	1.861993000	16.473624000
6	7.649094000	2.161191000	16.707102000
1	6.824093000	2.517915000	17.313227000
6	8.923572000	2.696714000	16.847354000
1	9.099111000	3.481427000	17.574784000
6	9.943300000	2.209671000	16.038191000
1	10.951662000	2.604689000	16.115239000
6	9.654547000	1.204639000	15.123538000
1	10.436358000	0.810578000	14.486295000
6	8.350831000	0.715455000	15.037693000
6	7.868363000	-0.335160000	14.164349000
7	7.642733000	-1.896175000	12.618394000
7	7.356360000	1.194559000	15.831043000
6	6.537343000	-0.748239000	14.229666000
7	6.496232000	-1.708805000	13.264713000
7	8.469950000	-1.045555000	13.174459000
8	5.234548000	-1.492996000	17.821327000
8	2.542488000	-0.537008000	14.493031000
8	3.914580000	2.709126000	17.083340000
17	5.486803000	2.005208000	13.482812000
75	5.286583000	0.451707000	15.452272000
6	5.075719000	-2.618039000	11.523155000
6	3.993000000	-3.427503000	11.242318000
6	3.236104000	-4.094587000	12.213705000
6	3.563061000	-3.961547000	13.563178000
6	4.651197000	-3.160728000	13.884437000
6	5.378999000	-2.509342000	12.878904000
8	3.455175000	-3.724012000	10.029064000
6	2.403779000	-4.554626000	10.318654000
7	2.233274000	-4.804295000	11.580860000
1	5.640650000	-2.090827000	10.763602000
1	2.986424000	-4.463580000	14.332178000
1	4.946434000	-3.021465000	14.919016000
6	1.615072000	-5.052759000	9.201726000
6	1.917543000	-4.690993000	7.883021000
6	0.535658000	-5.907924000	9.462145000
6	1.144970000	-5.183021000	6.836060000
6	-0.230257000	-6.394643000	8.410518000
6	0.071882000	-6.034288000	7.096226000
1	2.752144000	-4.026248000	7.684629000
1	0.313937000	-6.175979000	10.490384000
1	1.380470000	-4.899781000	5.814358000
1	-1.066889000	-7.056318000	8.615024000
1	-0.529835000	-6.415830000	6.276177000
6	9.822315000	-0.982642000	12.654220000
1	10.535981000	-1.261388000	13.432816000
1	9.885891000	-1.690298000	11.828636000
1	10.029515000	0.026887000	12.292010000

Table S44. Cartesian coordinates of **Re-T-BOP** in T_1 (in gas phase).

6	5.434461000	-0.864095000	16.693846000
6	3.615848000	-0.250241000	14.665491000
6	4.329006000	1.681208000	16.555792000
6	7.532140000	2.406028000	16.411156000
1	6.671639000	2.861913000	16.889631000
6	8.795828000	2.951085000	16.581505000
1	8.924678000	3.832520000	17.198325000
6	9.880410000	2.331717000	15.932421000
1	10.886472000	2.725275000	16.043116000
6	9.655363000	1.224109000	15.148633000
1	10.478040000	0.740796000	14.635409000
6	8.340927000	0.714203000	15.006628000
6	7.932341000	-0.389592000	14.234364000
7	7.738121000	-2.163386000	12.832120000
7	7.283586000	1.322697000	15.670122000
6	6.567115000	-0.762769000	14.196944000
7	6.545462000	-1.835324000	13.375360000
7	8.606288000	-1.266880000	13.407059000
8	5.506528000	-1.661781000	17.524855000
8	2.602767000	-0.640824000	14.279253000
8	3.770956000	2.347481000	17.304158000
17	5.123134000	2.240694000	13.643309000
75	5.299720000	0.462603000	15.281876000
6	5.101383000	-2.667825000	11.619448000
6	4.007177000	-3.452685000	11.314657000
6	3.251078000	-4.152658000	12.263615000
6	3.597126000	-4.086451000	13.612747000
6	4.698140000	-3.310511000	13.954531000
6	5.419742000	-2.610218000	12.975942000
8	3.455877000	-3.694437000	10.094466000
6	2.398499000	-4.525447000	10.358454000
7	2.235315000	-4.825672000	11.610545000
1	5.675293000	-2.125802000	10.877020000
1	3.030768000	-4.627006000	14.363364000
1	5.019855000	-3.244098000	14.988474000
6	1.595132000	-4.967782000	9.228301000
6	1.892257000	-4.555222000	7.923351000
6	0.507473000	-5.820491000	9.461002000
6	1.106043000	-4.993863000	6.862838000
6	-0.272074000	-6.253772000	8.396069000
6	0.024492000	-5.842321000	7.095546000
1	2.734175000	-3.893697000	7.746268000
1	0.290663000	-6.129392000	10.478785000
1	1.338062000	-4.671565000	5.851955000
1	-1.114755000	-6.914051000	8.579313000
1	-0.587603000	-6.182428000	6.265004000
6	9.927517000	-1.178440000	12.844727000
1	10.691128000	-1.277159000	13.622253000
1	10.037599000	-2.004898000	12.141820000
1	10.069508000	-0.232118000	12.307725000

Table S45. Cartesian coordinates of **Re-T-BOP** in S_0 (in dichloromethane).

6	5.336195000	-0.728296000	16.894316000
6	3.568830000	-0.222218000	14.908183000
6	4.374657000	1.822253000	16.505794000
6	7.617251000	2.257179000	16.609360000
1	6.790315000	2.637635000	17.197376000
6	8.892893000	2.789679000	16.750221000
1	9.063102000	3.594184000	17.456572000
6	9.920580000	2.271169000	15.971701000
1	10.929973000	2.661984000	16.049930000
6	9.640891000	1.236769000	15.085822000
1	10.430208000	0.819619000	14.474333000
6	8.338090000	0.749707000	15.000333000
6	7.865220000	-0.329570000	14.153036000
7	7.669607000	-1.967019000	12.690973000
7	7.332492000	1.262905000	15.759603000
6	6.530112000	-0.722579000	14.195471000
7	6.502586000	-1.727880000	13.279426000
7	8.491809000	-1.104778000	13.228793000
8	5.377297000	-1.470095000	17.792856000
8	2.529966000	-0.622398000	14.578552000
8	3.841588000	2.627937000	17.145249000
17	5.304932000	2.072805000	13.451838000
75	5.268208000	0.469461000	15.430033000
6	5.062381000	-2.606713000	11.538958000
6	3.987503000	-3.426053000	11.254107000
6	3.261161000	-4.136252000	12.217741000
6	3.614137000	-4.044526000	13.564655000
6	4.694911000	-3.233783000	13.889631000
6	5.389215000	-2.535253000	12.891978000
8	3.431850000	-3.695686000	10.042551000
6	2.402070000	-4.552433000	10.320710000
7	2.258047000	-4.843593000	11.579549000
1	5.607606000	-2.053305000	10.783097000
1	3.070478000	-4.588617000	14.329452000
1	5.016505000	-3.135107000	14.920875000
6	1.605091000	-5.028042000	9.199445000
6	1.888390000	-4.619014000	7.889257000
6	0.540628000	-5.908064000	9.442211000
6	1.111559000	-5.088340000	6.834347000
6	-0.230114000	-6.371885000	8.382876000
6	0.052984000	-5.963783000	7.077553000
1	2.711640000	-3.937587000	7.700459000
1	0.329304000	-6.218504000	10.460594000
1	1.333287000	-4.769382000	5.820296000
1	-1.053953000	-7.053059000	8.574136000
1	-0.551305000	-6.327875000	6.251673000
6	9.875742000	-1.110686000	12.780839000
1	10.531757000	-1.344175000	13.620855000
1	9.966769000	-1.881304000	12.017529000
1	10.126258000	-0.138001000	12.354444000

Table S46. Cartesian coordinates of **Re-T-BOP** in S_1 (in dichloromethane).

6	5.519428000	-0.752902000	16.752121000
6	3.576141000	-0.267788000	14.737101000
6	4.224136000	1.692361000	16.450462000
6	7.495861000	2.393466000	16.441318000
1	6.634369000	2.821926000	16.943491000
6	8.746715000	2.935168000	16.631114000
1	8.868929000	3.791108000	17.284308000
6	9.849665000	2.348559000	15.951611000
1	10.851605000	2.746486000	16.075945000
6	9.630128000	1.266421000	15.135063000
1	10.460284000	0.803451000	14.613699000
6	8.324977000	0.745248000	14.972489000
6	7.925657000	-0.359752000	14.184675000
7	7.754931000	-2.107764000	12.779032000
7	7.243500000	1.335215000	15.644338000
6	6.580274000	-0.767344000	14.163253000
7	6.574649000	-1.812981000	13.314639000
7	8.582963000	-1.195124000	13.313485000
8	5.684133000	-1.482579000	17.625600000
8	2.549891000	-0.685905000	14.415613000
8	3.582661000	2.343427000	17.146122000
17	5.180921000	2.044126000	13.417725000
75	5.278728000	0.482789000	15.265479000
6	5.097454000	-2.635570000	11.580422000
6	4.014541000	-3.442239000	11.289918000
6	3.311545000	-4.190696000	12.242294000
6	3.699553000	-4.154924000	13.581795000
6	4.789476000	-3.356945000	13.910719000
6	5.457675000	-2.614568000	12.926623000
8	3.428421000	-3.664041000	10.082655000
6	2.405565000	-4.531859000	10.352314000
7	2.292591000	-4.872880000	11.601632000
1	5.627594000	-2.053620000	10.835382000
1	3.177356000	-4.733121000	14.336511000
1	5.143373000	-3.310632000	14.935196000
6	1.581316000	-4.964067000	9.233180000
6	1.828779000	-4.499820000	7.934261000
6	0.526986000	-5.858546000	9.466708000
6	1.026415000	-4.928778000	6.881344000
6	-0.269280000	-6.281954000	8.409431000
6	-0.021974000	-5.818739000	7.115342000
1	2.644282000	-3.807161000	7.752864000
1	0.344079000	-6.211668000	10.476637000
1	1.220273000	-4.567061000	5.875949000
1	-1.085127000	-6.974643000	8.593552000
1	-0.646126000	-6.151358000	6.290942000
6	9.972852000	-1.220378000	12.925828000
1	10.607529000	-1.435850000	13.790019000
1	10.095877000	-2.007983000	12.183304000
1	10.259132000	-0.261082000	12.486081000

Table S47. Cartesian coordinates of **Re-T-BOP** in T_1 (in dichloromethane).

6	5.174033000	-0.464622000	16.358441000
6	3.622783000	-0.656411000	14.106798000
6	3.941070000	1.802193000	15.296595000
6	7.091491000	2.750364000	15.424442000
1	6.149649000	3.284311000	15.490559000
6	8.284388000	3.397283000	15.720346000
1	8.271196000	4.439258000	16.017415000
6	9.482904000	2.666837000	15.627882000
1	10.433892000	3.136971000	15.858286000
6	9.442708000	1.348273000	15.234911000
1	10.357644000	0.776058000	15.146556000
6	8.197203000	0.743547000	14.929195000
6	7.976367000	-0.565021000	14.467159000
7	8.111567000	-2.673057000	13.654059000
7	7.018586000	1.470466000	15.049774000
6	6.655667000	-0.977461000	14.112824000
7	6.829299000	-2.233082000	13.647563000
7	8.806094000	-1.648551000	14.256459000
8	5.172721000	-0.962280000	17.398833000
8	2.668574000	-1.244257000	13.821383000
8	3.222964000	2.598222000	15.703047000
17	5.185120000	1.563478000	12.448959000
75	5.171666000	0.364538000	14.608932000
6	5.043385000	-2.598657000	12.056893000
6	4.128797000	-3.504680000	11.556062000
6	4.013891000	-4.830587000	11.988351000
6	4.854996000	-5.309263000	12.995115000
6	5.777224000	-4.421587000	13.535033000
6	5.856282000	-3.096083000	13.075432000
8	3.203778000	-3.312788000	10.577146000
6	2.571435000	-4.520111000	10.460758000
7	3.007539000	-5.444867000	11.264133000
1	5.133629000	-1.580015000	11.695247000
1	4.785811000	-6.332386000	13.349194000
1	6.447408000	-4.739442000	14.326758000
6	1.506654000	-4.626024000	9.473862000
6	1.141523000	-3.524948000	8.687274000
6	0.839775000	-5.849411000	9.315003000
6	0.118755000	-3.650682000	7.751891000
6	-0.180386000	-5.966274000	8.378450000
6	-0.543633000	-4.868387000	7.595289000
1	1.656267000	-2.577437000	8.809798000
1	1.129670000	-6.696268000	9.928991000
1	-0.161883000	-2.795348000	7.144485000
1	-0.694544000	-6.915256000	8.258120000
1	-1.341662000	-4.962673000	6.864458000
6	10.245898000	-1.726955000	14.224852000
1	10.661477000	-1.438740000	15.193017000
1	10.513548000	-2.765543000	14.029496000
1	10.667480000	-1.095216000	13.434066000